République Algérienne Démocratique et Populaire
People's Democratic Republic of Algeria
Ministère de l'Enseignement Supérieur et de la Recherche Scientifique
Ministry of Higher Education and Scientific Research

Mohamed Khider University – Biskra
Faculty of Science and Technology
Department: Industrial Chemistry

Université Mohamed Khider – Biskra
Faculté des sciences et technologies
Département : Chimie Industrielle

Thesis presented with a view to

obtaining the Diploma of

**Doctorat LMD**

**Option: chemical engineering**

# Synthesis of activated carbons from plant waste and their environmental applications

Presented by :

**Azri Naima**

Publicly supported on 16/ 11/2023

## Before the jury composed of:

| | | | |
|---|---|---|---|
| **MERZOUGUI Abdelkrim** | **Professor** | **U. of Biskra** | **President** |
| **FADEL Amar** | **Professor** | **U. of Biskra** | **Rapporteur** |
| **CHEBBI Rachid** | **Lecturer** | **U. of Biskra** | **Co-rapporteur** |
| **CHIBANE Lemnouer** | **Professeur** | **U. of Sétif** | **Examiner** |
| **CHAFAI Nadjib** | **Lecturer** | **U. of Sétif** | **Examiner** |
| **REHALI Hanane** | **Lectur** | **U. of Biskra** | **Examiner** |
| **OUAKOUAK Abdelkader** | **Lecturer** | **U. El oued** | **invite** |

**Dedicate**

I thank God Almighty for his full success

I dedicate my humble work to the dearest and most precious thing I have in life, my father and mother, who had it not been for them and had it not been for their prayers in secret before publicly, in my absence before my presence, I would not have been successful in my work. Near or far, especially my friend and companion, Abdelrahmani Safa, for her support throughout my journey

## Remerciment

First of all, I thank Al Mighty God who gave me the determination and the strength to carry out this work.

I would like to extend my sincere thanks and gratitude to **Pr. Amar Fadel**, a professor at the Department of Industrial Chemistry at the University of Biskra, for being able to supervise me during the preparation of my doctoral dissertation, and for his continuous support and valuable advice for the good course. I am very grateful for the trust he placed in me.

**Pr. MERZOUGUI Abdelkrim,** Professor at the University of Biskra, for the honor that he gave me to preside over this jury, and I thank him for his continuous support and encouragement and extend my gratitude to him for his great efforts

I would also like to express my sincere thanks to **Dr. Chebbi Rachid**, Doctor at University Mohamed Kheider -Biskra, Department of Industrial Chemistry, for their help when I was in need and their support which has given me the necessary means to proceed effectively in my research work.

I would like to express my deep gratitude to **Dr. Abdelkader Ouakouak**, a doctor at El Oued University and a member of the (LARYHSS) laboratory, for his help, hard work, and keenness to work accurately and qualitatively. Also, for his valuable advice and great efforts in obtaining works of a distinctive nature, I extend to him my full gratitude and appreciation.

I thank **Pr. Chibane Lemnouer**, a professor at the University of Setif, for his presence and for accepting the discussion of my work, and I extend my sincere thanks and gratitude to him

I would also like to thank **Dr. Chafai Nadjib**, Doctor of the University of Setif, who honored me with his presence by accepting the judgment on this modest work

I also address my sincere thanks to **Dr. Rehali Hanane** lecturer A at Biskra University for agreeing to judge this thesis.

The (LARGHYDE) laboratory, the Department of Civil Engineering and Hydraulics, University of Biskra, Algeria, and the Directorate General of Scientific Research and Technology Development, Ministry of Higher Education and Scientific Research, Algeria supported this work.

I extend my sincere thanks and gratitude to the Director of the Scientific and Technical Research Center for Arid Zones (CRSTRA) **Mr. Kechbar Mohamed**, University of Biskra, Algeria for his cooperation and reception at the center level. In addition, I especially

thank the laboratory officials, **Mrs. Ben Aoun Saliha**, the water laboratory official who accompanied me throughout my work at the laboratory level, and also the soil laboratory official, **Mr. Tariq Othman**, for his support, and **Mr. Amir Djellouli**

My thanks go to **Pr. Hafiane Amor**, director of the "Water, membrane and environmental biotechnology" laboratory, Technopole de Borj- Cédria, Tunisia as well as **Dr. Chemingui Hajer** for her effort to succeed in this internship. To **Dr. Abdedayem Asma** for her warm welcome and her help. So all the members of LEMBE. I would also like to thank the entire Geo-resource Laboratory team who helped me access the various laboratory techniques and all those who contributed to the realization of this thesis.

# Summary

**Chapter IV: Adsorption of Diclofenac and Paracetamol in the binary system**

## List of Symbole

| Symbols | Meaning | Unit |
|---|---|---|
| $C_0$ | Initial adsorbate solute concentration | [mg/l] |
| $C_e$ | Adsorbate concentration at adsorption equilibrium | [mg/l] |
| K1 | first-order adsorption reaction rate constant | [min-1] |
| $K_2$ | adsorption second-order reaction rate constant | [mg/g.min] |
| **PF**O | Pseudo-first order | / |
| PSO | Pseudo-second order | / |
| $q_{max}$ | Adsorption capacity at saturation | [mg/g] |
| $q_t$ | Capacity adsorbed at time t | [mg/g] |
| R | Yield | [%] |
| $R^2$ | Correlation coefficient | [Sans unité] |
| DRX | . X-ray diffraction | / |
| UV | Ultraviolet | / |
| MEB | Scanning Electron Microscopy | / |
| IR | Infrared | / |
| IRTF | Infrared spectra by Fourier Transform | / |
| PHpzc | hydrogen potential at the point of zero charge. | / |
| $S_{BET}$ | surface BET | ($m^2$/g) |
| $S_{Lang}$ | Langmuir area | ($m^2$/g) |
| $S_{Micr}$ | microporous surface | ($m^2$/g) |
| $V_{total}$ | total pore volume | ($cm^3$/g) |
| $V_{non\text{-}micro}$ | non-microporous volume | ($cm^3$/g) |

## List of Table

## List of Table

# Abstract

# Résumé

# الملخص

**Abstract**

In this work, we prepared biochar from the organic residues of pepper stems from the Biskra region and studied its morphological and structural properties. Then, we tested its efficiency in the elimination of pharmaceutical residues in aqueous solutions; several parametric conditions were studied, including pH, contact time, initial concentration, and temperature to obtain optimal conditions. PS-biochar was a carbonaceous mesoporous adsorbent with well-developed textural properties ($S_{BET}$ = 727.5 $m^2/g$ and $V_{Total}$ = 0.36 $cm^3/g$). The adsorption mechanism contributes to π-π interaction, pore filling, and hydrogen bonding. FTIR analysis showed both qualitative and quantitative decreases in the functional groups of the raw material after adsorption. The results obtained in this study demonstrate that PS-biochar is a very effective adsorbent for Diclofenac and Paracetamol adsorbates and has a high adsorption capacity for these contaminants in the single system. Moreover, a relatively higher capacity for Paracetamol and Diclofenac than for in the binary system. The nonlinear isothermal Temkin and Langmuir models adequately described the equilibrium adsorption data. Although the adsorption kinetics followed the pseudo-second-order model, the thermodynamic study revealed that the adsorption process was spontaneous and exothermic. The adsorption values for polluants indicated that the adsorption mechanism was physical in nature.

**Keywords:** Biochar, adsorption, isotherms, Binary system, single system, mechanism, pharmaceutical products.

**Résumé**

Dans ce travail, nous avons préparé du biochar à partir des résidus organiques de tiges de poivre de la région de Biskra et on a étudié ses propriétés morphologiques et structurales. Ensuite, nous avons testé son efficacité dans l'élimination des résidus pharmaceutiques dans les solutions aqueuses, plusieurs conditions paramétriques ont été étudié, notamment pH, temps de contact, concentration initiale et la température pour obtenir des conditions optimales. Le PS-biochar était un adsorbant mésoporeux carboné avec des propriétés texturales bien développées ($S_{BET}$ = 727,5 $m^2/g$ et $V_{Total}$ = 0,36 $cm^3/g$). L'interaction π-π, le remplissage des pores et la liaison hydrogène sont contribué au mécanisme d'adsorption. L'analyse FTIR a présenté une diminution à la fois qualitative et quantitative des groupes fonctionnels de la matière première après adsorption. Les résultats obtenus dans cette étude démontrent que le PS-biochar est un adsorbant très efficace pour les adsorbats Diclofénac et Paracétamol et a une

capacité d'adsorption élevée pour ces contaminants dans le système unique. Et aussi une capacité relativement plus élevée pour le Diclofenac que pour le Paracétamol dans le système binaire. Les modèles isothermes non linéaires de Temkin et de Langmuir ont décrit de manière adéquate les données d'adsorption à l'équilibre. Bien que la cinétique d'adsorption suit le model pseudo second ordre, l'étude thermodynamique a révélé que le processus d'adsorption était spontané et exothermique. Les valeurs d'adsorption pour les pollluants indiquaient que le mécanisme d'adsorption était de nature physique.

**Mots clés** : Biochar, adsorption, isothermes, système binaire, système unique, mécanisme, produits pharmaceutiques.

**الملخص**

في هذا العمل قمنا بتحضير الفحم النباتي من المخلفات العضوية (سيقان الفلفل) من منطقة بسكرة ودرسنا خصائصه المورفولوجية والتركيبية. بعد ذلك، قمنا باختبار كفاءته في التخلص من المخلفات الصيدلانية في المحاليل المائية، وتمت دراسة العديد من الظروف المعيارية، بما في ذلك الرقم الهيدروجيني ووقت التلامس والتركيز الأولي ودرجة الحرارة للحصول على الظروف المثلى. الفحم النباتي عبارة عن مادة ماصة كربونية مسامية ذات خصائص تركيبية متطورة ( $S_{BET}$ = 727,5 $m^2/g$ et $V_{Total}$ = 0,36 $cm^3/g$). يساهم التفاعل π-π وملء المسام والارتباط الهيدروجيني في آلية الامتزاز. أظهر تحليل FTIR انخفاضًا نوعيًا وكميًا في المجموعات الوظيفية للمادة الخام بعد الامتزاز. تظهر النتائج التي تم الحصول عليها في هذه الدراسة أن PS-biochar هو مادة ماصة فعالة للغاية للديكلوفيناك والباراسيتامول ولديه قدرة امتصاص عالية لهذه الملوثات في النظام الفردي، وأيضًا سعة أكبر نسبيًا للديكلوفيناك مقارنة بالباراسيتامول في النظام الثنائي. وصفت نماذج Temkin وLangmuir متساوي الحرارة اللا خطية بيانات امتصاص التوازن بشكل كافٍ. اتبعت حركية الامتزاز نموذج الدرجة الثانية الزائف كما كشفت الدراسة الديناميكية الحرارية أن عملية الامتزاز كانت تلقائية وطاردة للحرارة. أشارت قيم الامتزاز لكل من الملوثات إلى أن آلية الامتزاز كانت فيزيائية بطبيعتها

**الكلمات المفتاحية:** الفحم الحيوي، امتزاز، متساوي الحرارة، نظام ثنائي، نظام واحد، آلية، منتجات صيدلانية.

# General Introduction

# General Introduction

Human and industrial activity increases every year, by the use of chemical substances for daily production, the waste of its rejected substances react in the atmosphere to have polluting components. Also the presence of a large number of these chemical compounds in the environment called "emerging pollutants" is highlighted in the different matrices (air, water and soil) (Mboula, V. M., 2012).

The major pollutants, linked to human made, which relate to industrial waste (metals, dyes, and chemicals), phytosanitary products (surfactants, agricultural treatment products) and pharmaceutical products (veterinary products and therapeutic molecules such as antibiotics, cancer drugs and synthetic hormones). The level use of medicinal substances for human and veterinary uses generates as source of environmental pollution, especially in wastewater, which is becoming increasingly worrying for scientists and politicians.

Since the 1980s, a number of studies have been conducted on the analysis of drug residues in wastewater. The study showed the presence of traces of several organic and inorganic compounds. Thus, the presence of drug residues and heavy metals has been observed in wastewater (Thomas, T., 2015).

For the elimination of pharmaceutical residues and medicals products in wastewater and natural resources, different methods and technologies used for the treatment of wastewater such as: Ultra filtration, biological treatments, advanced oxidation processes and adsorption. Adsorption has become one of the processes used, because of its efficiency and its ability to eliminate these pharmaceutical pollutants present in wastewater at low concentration via different adsorbents.

Adsorption efficiency depends on the quality of the adsorbent, which is related to the physico-chemical properties, for this reason, our objective of this work is to fabricate a new adsorbent (biochar) from pepper stems, that harvested from the region of Biskra, and the application on two polluting ibuprofen and paracetamol.

The thesis composes in four chapters.

**First Chapter**: Consist of literature review concerning water, air and soil contamination, with pharmaceutical residues pollutants. Also, removing methods for pollutants, especially biochar by adsorption technology. On the other hand, the biochar (adsobent) parameters affecting on the adsorption capacities.

# General Introduction

**Second Chapter:** This chapter concerns the fabrication of biochar as activated carbon from pepper stalk (PS) waste as adsorbent for the removal of IBP from aqueous media. Then biochar prepared passé characterization techniques analysis such as: FTIR, BET analyzer, XRD, SEM-Eds, and pH $_{PZC}$ method), which are used to characterize the physical properties of the adsorbent. In addition, the kinetics, equilibrium isotherms and adsorption behavior (capacity and mechanism) of IBP on PS700 sorbents were analyzed and discussed here to investigate thermodynamic behavior and regeneration of the sorbent.

**Third Chapter:** This chapter, consiste of removing DIC and PARA by PS700 from aqueous media in a single system, parameters affecting on the isotherm, kinetics, and thermodynamic systems. finally, use the Langmuir, Freundlich, Redlich-Peterson, and Temkin models to describe the equilibrium data of DIC adsorption on adsorbent.

**Fourth Chapter: IV** of this manuscript describes the adsorption properties of tissues. PS700 was used to remove DIC and PARA from aqueous media in binary system adsorption. Parameters effecting on the adsorption on the Kinetic, isotherm, thermodynamics analysis, and desorption regeneration analysis.

**Finally,** conclusions of this manuscript highlighting the most important results, especially the effect of different adsorption parameters.

# **Chapter I:** *Bibliographic research*

## I. Introduction

Pollution refers to the deterioration of species introduction, primarily human, chemical, or organisms, genes or radiation (radioactivity, artificial light), change operation more or less ecosystem. Geological phenomena such as eruptions Vulcans, which are Storm, can also cause damage. Water in nature, especially water used for industrial purposes Domestic production is by no means pure because of the impurities it may contain in its three states. A solid, liquid, or gas characterized by a possible size aqueous medium. Water pollution by various substances such as organics, dyes, pharmaceuticals and other toxic substances is a global problem and a real danger.

### I. 1. Water pollution

Pharmaceutical compounds are important for the treatment of diverse illnesses and infections. However, there's developing issue approximately the presence of those compounds with inside the aquatic environment. Residual concentrations of pharmaceutical molecules had been detected in wastewater from the pharmaceutical industry, hospitals, veterinary remedy and home facilities (Spessato L. et al. 2019).

Contamination from pharmaceutical production facilities is another major cause of pharmaceutical release into the environment (Larsson, 2014). Several studies illustrate major pollution vectors in these industries, using the example of very large factories in India whose wastewater pollutes downstream lakes. These lakes located downstream of the mills produce antibiotic concentrations of several mg. $L^{-1}$ (Fick et al., 2009).

It has been mentioned that the human frame is not able to completely metabolize those bioactive compounds and greater than 50% of the dose is excreted unchanged in wastewater (A. Mohseni- Bandpei et al. 2020). (Pena-Guzm ˜ ´ an et al. 2019) mentioned ninety-eight pharmaceutical compounds in Latin American wastewater; amongst them are acetaminophen, ibuprofen and ketoprofen.

Due to their non-stop use and simplicity of bioaccumulation, those compounds were detected at concentrations starting from ng/L to mg/L (Spessato, L et al., 2019, Pena-Guzm ˜ ´ an et al., 2019). Although at low concentrations, their

prolonged exposure and toxicity can have adverse effects on aquatic ecosystems and living organisms. (Li, Z., Gomez-Avil, A et al., 2019 ; Zur, J et al. 2018). Furthermore, the degradation of pharmaceutical molecules can generate new compounds which might be surprisingly poisonous and carcinogenic, result in mutagenic consequences in human cells. (Zur, J et al., 2018).

### I. 1. 1. Wastewater source

#### I. 1. 1. a- Urbain

The main source of urban wastewater is the living population Produces 3/4 of the wastewater. This sewage is a mixture of water and fertilizer People like toilet water and flush water (gray water). Sewage Industrial effluents may also be included, but are usually the latter must be pretreated to achieve comparable properties to those of domestic wastewater to enable joint treatment.

#### I. 1. 1. b- Industrial Source

Factory smoke contains toxic acid gases and is washed away by rain (Example: $SO_2$). Then we talk about harmful acid rain, plants and living things. Dust and gas are generated from the exhaust system in the atmosphere of the manufacturing process. These gases are water, soil, plants (see....). The chemical composition of water also depends on human activity, which is generally due to the contribution of 'pollutants' such as pesticides from pharmaceutical, industrial, agricultural or domestic practices (Douez, O et al., 2011).

#### I. 1. 1. c- Pharmaceutical products

The presence of natural micro pollutants with inside the environment is frequently related to populace growth. Human activities. Urban water aid healing Facility is a main supply of pollutants because of trace natural pollution in the aquatic environment. three hundred million heaps of trace pollution input herbal waters every 12 months via wastewater discharge, such as artificial commercial chemicals, pharmaceuticals, flame retardants, synthetic sweeteners and hormones. Concerned due to the fact they produce organic and ecological influences Trace pollution do now no longer always motive acute toxicity. Instead, they're concept to

have a long-time period impact on long-time period frame publicity to those compounds 7, 8 (Tong, Y et al., 2019).

### c. 1. Pharmaceuticals and personal care products

Pharmaceutical and private care products (PPCPs) are a big magnificence of natural contaminants utilized in clinical and private take care of people and animals. with an increasing number of research reporting the presence of PPSP in water and wastewater at low concentrations (ng/L to lg/L). PPCPs are identified as rising pollution because of their capability unfavorable results on human health and aquatic ecosystems, even at small concentrations (Yang, Ok et al. 2017).

Treated wastewater from wastewater remedy plants (WWTP) in city regions wherein the bulk of wastewater is amassed for remedy is thought to be the primary supply of PPSP with inside the aquatic environment (Luo, Y et al., 2014; Yang, Ok et al., 2017). Widespread distribution of PPCPs with inside the environment will increase human publicity via meals and water intake and doubtlessly will increase environmental and human health risks. Previous research has proven that veterinary diclofenac (DCF) could have a bad effect at the populations and variety of birds, which include steppe eagles and vultures in South Africa and India (Cuthbert, R. J et al., 2016; Galligan, T. H et al., 2014; Sharma, A. K et al., 2014).

Therefore, new methods, technology and method to do away with PPCP from water and wastewater also are crucial to save you similarly accumulation of PPCP withinside the herbal aquatic environment and decrease the unfavorable consequences of PPCP on human fitness and ecosystem. Periodic tracking is also had to apprehend the presence, destiny and elimination of PPCPs and their relevance to human health and the environment. Elimination of PPCP in water and wastewater remedy processes the physical and chemical properties of man or woman PPCP compound range widely. Therefore, the elimination of PPCP from water calls for a extensive variety of remedy technologies, consisting of bodily, chemical and organic processes. It has been proven that adsorption and AOP have extremely good capacity to successfully eliminate PPCP (Xu, Y et al, 2017).

### c. 2. Pharmaceutical contaminant

Pharmaceuticals are extensively used for the prevention and treatment of human and veterinary diseases. These bioactive chemical substances are taken into consideration rising pollution because of their long-time period staying power and ability to harm aquatic ecosystems. These refractory rising contaminants (RECs) (analgesic, anti-inflammatory, antiepileptic and antibiotic) especially belong to the elegance of endocrine disruptors, constantly getting into the aquatic environment at excessive concentrations. Low degree they continue to be energetic even at low concentrations and degrade water quality, and have bad influences on ecosystems and human health.

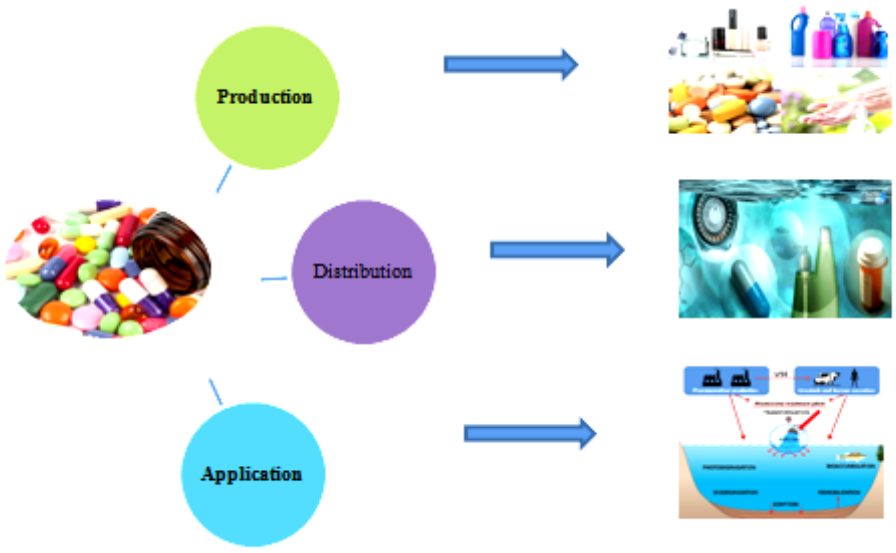


**Figure I. 1 :** The fundamental source Pharmaceutical contaminant

### I. 1. 2. Characteristics and toxicological effect of pharmaceuticals

Pharmaceuticals are chemical substances used to diagnose, treat, modify, and save you disease. This definition is prolonged to veterinary services and might additionally practice to illicit drugs (Daughton, C. G. and Ternes, T. A., 1999). Pharmaceuticals are chemical contaminants because of the subsequent characteristics:

1- They may be fashioned from a large number of molecular complexes that vary in molecular mass, structure, characteristic and shape;

2- They have the capacity to penetrate cell membranes, so they're exceptionally stable;
3- They are polar molecules with many expenses and their degree of ionization, amongst different characteristics, depends at the pH of the medium;
4- They are lipophilic and a few are reasonably soluble in water;
5- Drugs together with erythromycin, naproxen and sulfamethoxazole can persist with inside the environment for greater than a year; others, including clofibric acid, can persist for numerous years and are bioactive through accumulation;
6- After administration, the molecules are absorbed with inside the human body, dispensed and subjected to metabolic reactions that could alternate their chemical structure (Thomas. K.V., Langford. K., 2007):

The solution for removal toxical substances as pharmaceticals products from aqueous souces is Adsorption processes (Rocha, L. S et al., 2020; Quesada, H. B et al., 2019, Ahmed, M. J., Hameed, B. H., 2018). Several Scientific studies on the adsorption of Paracetamol have been reported (Spessato, L et al., 2019; Lung, I et al., 2021 ; Chauhan, M et al., 2020 ; Afolabi, I. C et al., 2020) in a single system. But so far nothing has happened Discussion of Multiple Drug Adsorption: Diclofenac Paracetamol on ZnO nanoparticles (Dhiman, N., Sharma, N., 2019). Ofloxacin hydrochloride and paracetamol in rice husk ash (Thakur, A., Sharma N., Mann, A., 2020). Paracetamol, Diclofenac and tetracycline on organosepiolite (GómezAvilés, A., et al., 2021). Naproxen and Diclofenac on an aluminum-based organometallic framework (Karami, A., Sabouni, R., Ghommem, M., 2020)

### I. 1. 3. Naturales substances

### I. 1. 3. a) Non-steroidal anti-inflammatory drugs (NSAIDs)

Non-steroidal anti-inflammatory drugs (ibuprofen or diclofenac) and lipid regulator (bezafibrate) is widely used as an over-the-counter drug estimated annual consumption of Hundreds of tons of developed countries Due to its clean operation and occasional cost, the adsorption technique is a promising treatment method for IBP elimination from water. According to literature, a lot of adsorbents has been synthesized and used to examine the IBP elimination, mainly activated carbons. But

additionally mesoporous silica's or metal natural frameworks amongst others (Li, Z et al., 2019)

### I. 1. 3. b) Analgesics

Paracetamol is an analgesic and an antipyretic. It appears to inhibit cyclo-oxygenase with inside the crucial worried device without peripheral action, that's why it lacks anti-inflammatory effects.

### I. 1. 3. c) Antibiotics

Antibiotics are recognized as a new class of environmental pollutants receiving significant research attention Because of potential ecotoxicity and harm to humans (Nakayama, T et al., 2017; Zhang, W et al., 2016).

**Table I. 1:** Physicochemical properties of Pharmaceuticals

| NSAIDs | Formula | Molecular weight (g mol−1) | PKa | Ref |
|---|---|---|---|---|
| **Paracetamol** | $C_8H_9NO_2$ | 151.16 | 9.38 | (García-Mateos, F. J et al., 2015) |
| **Diclofenac** | $C_{14}H_{11}Cl_2NO_2$ | 296.1 | 4.15 | (Bagheri, A et al., 2020) |
| **Ibuprofen** | $C_{13}H_{18}O_2$ | 206.28 | 4.91 | (Chakraborty, P et al., 2018) |
| **Naproxen** | $C_{14}H_{14}O_3$ | 230.26 | 4.19 | (Mondal, S et al., 2020) |
| **Piroxicam** | $C_{15}H_{13}N_3O_4S$ | 331.37 | 6.3 | (Calisto, V et al., 2015) |
| **ketoprofen** | $C_{16}H_{14}O_3$ | 254.28 | 4.45 | (Frohlich, A. C et al., 2019) |

### c. 1. Ibuprofen

Ibuprofen, a non-steroidal anti-inflammatory drug crafted from propionic acid, is one of the maximum usually used over the counter pills in all age groups. Ibuprofen concentrations starting from ng/L to µg/L had been determined in diverse water bodies (Xu, M. J et al., 2019).

**Table I. 2:** Adsorption capacity of IBP by various adsorbents.

| Adsorbent | $Q^0_{max}$ (mg/g) | pH | T (°C) | Method of determination | Reference |
|---|---|---|---|---|---|
| | | | **Activated carbons** | | |
| **Microporous AC** | 495.0 | 3.0 | 13 | Experimental | (Guedidi et al., 2020) |
| **AC cloth** | 492.0 | 3.0 | 25 | Experimental | (Guedidi et al., 2014) |
| **Physically activated coal** | 430.4 | 4.5 | 30 | Langmuir | (Mestre et al., 2009) |
| **Chemical + steam AC** | 416.7 | 2.0 | 25 | Langmuir | (Mestre et al., 2007) |
| **AC** | 268.2 | 4.3 | 25 | Langmuir | (Mansouri et al., 2014) |
| **Chemical AC** | 153.2 | 2-4 | 25 | Langmuir | (Mestre et al., 2007) |
| **Commercial AC** | 139 | 6.0 | 25 | Experimental | (Slomkiewicz et al., 2019) |
| | | | **Biochars** | | |
| **Oxygen pyrolyzed biochar** | 311 | 7.0 | 25 | Langmuir | (Jung et al., 2015) |
| **Activated biochar** | 172 | 4.0 | 20 | Experimental | (Du et al., 2020) |
| **Steam activated biochar** | 62.5 | 2.0 | 20 | Langmuir | (Mondal et al., 2016) |
| **Biochar pyrolyzed at 550°C** | 16.6 | 7.0 | 25 | Langmuir | (Ocampo-Perez et al., 2019) |
| **Acid activated biochar** | 12.2 | 2.0 | 15 | Langmuir | (Chakraborty et al., 2018) |

### c. 2. Paracetamol

4-Acetaminophen, commonly known as paracetamol, is currently one of the most commonly used analgesics and antipyretics available worldwide without a prescription. Despite its lack of anti-inflammatory properties, paracetamol is usually classified as one. Non-steroidal anti-inflammatory drugs (NSAIDs). Versatile and easy to use Accumulation, 4-acetaminophen is one of the most commonly seen drugs various environmental matrices B Sediment groundwater or potable water. It was recently detected in the River Tyne (UK) at levels above 65 µg $L^{-1}$(Żur, J et al., 2018).

### c. 3. Diclofenac

DCF Is one of the Most typically used anti-inflammatory drugs to be had without a prescription and is consumed international for ache relief, arthritis and rheumatism ache relief. CA is an energetic metabolite of the lipid modulators clofibrate, etofibrate, and etofylline clofibrate, and is also taken into consideration a ability endocrine disruptor as it interferes with cholesterol synthesis (Lu, X et al., 2016)

Diclofenac is characterized by a weak acidity (pKa around 4) and its solubility depends on the pH of the medium. It is sparingly soluble in hydrochloric acid (pH 1.1), sparingly soluble in water, sparingly soluble in phosphate buffer (pH 6.8), sparingly soluble in alcohol, sparingly soluble in acetone, and practically insoluble in ether. At about 280 °C, its maximum wavelength of absorption in the visible and ultraviolet range is about 276 ± 2 nm. 2007).

## I. 1. 4. pharmaceutical removal Processes from wastewater

### 1. 1. 4. a) Adsorption

Several techniques are used to remove micro-pollutants in wastewater. Specifically, chemical methods include the removal of micro-pollutants by oxidation with ozone, the removal of micro-pollutants by adsorption on powdered activated carbon (PAC) or particles (GAC), advanced oxidation processes

### I. 1. 4. b) Physical and physicochemical processes

The physicochemical processes include membrane technology (Göbel, et al., 2007), adsorption techniques (Bui, T. X. & Choi, 2009; Braschi, et al., 2010) and especially adsorption on activated carbons (Snyder, et al., 2007), reverse osmosis (Watkinson, A. J., Murby, E. J., & Costanzo, 2007) and flocculation (Xing, Z. P., Sun, & D. Z., 2009) and flocculation (Suarez, S., Lema, J. M., Omil, & F., 2009). The principle of these techniques is to separate and concentrate pollutants, and then remove them by burning or land filling.

### 1. 1. 4. a) Adsorption

In adsorption, treated wastewater comes into contact with a substance that retains compounds on its surface. The main adsorbent used in water treatment is activated carbon due to its structure, high retention capacity and good affinity for a wide range of compounds (Dominique, W et al., 2011).

**Table I. 3:** Isotherm and Kinetics model of others studies

| Pharmaceuticals | Biomass residues | Isotherm model | Kinetics model | Ref. |
|---|---|---|---|---|
| **Diclofenac** | Moringa seed | Sips model | PSO | (Bagheri. A et al., 2020) |
| | Pine chips | Langmuir | PSO | (Tang. et al., 2015) |
| | Anthriscus sylvestris- | Langmuir | PSO | (Shirani, Z et al., 2020) |
| | palm kernel shells | Langmuir | PSO | (Velma. B. K.Y et al., 2021) |
| | orange peels (OP) | langmuir | PSO | (Tomul, F et al., 2019) |
| **Ibuprofen** | Fruit shell | Langmuir | PSO | (Chakraborty, P et al., 2018) |
| | Pine chips | Langmuir | PSO | (Tang et al., 2015) |
| | Alternanthera philoxeroides | Freundlich | PSO | (Yuan-da, D et al., 2020) |
| | Tamarind seeds | Langmuir | PSO | (Sumona, S et al., 2020) |
| **Paracetamol** | GS ; YB ; CB | Langmuir | PSO | (Yusoff, N. A et al., 2017) |
| | pomelo peel wastes | Redlich–Peterson | Elovich | (Tran, H. N et al., 2020) |
| | ASK | Langmuir | PSO | (Benjedim, S. et al., 2020) |

### I. 1. 5. Origin of water micro-pollution by pharmaceutical products

Numerous studies have shown that most of the surface waters studied are contaminated by pharmaceuticals. Likewise, the presence of these products has been observed in surface water, groundwater and wastewater, sludge from treatment plants used in agricultural spread and even in domestic water drink. The main sources of water pollution by pharmaceutical products can be distinguished into two categories: Diffusion sources are mainly due to human and animal excretion, and

represent the vast majority of drugs released into the environment, and point sources are much more concentrated but geographically limited emission sources.

We find, among the diffuse sources:

- ✓ improper storage and disposal of expired or unused medications,
- ✓ Metabolic excretion, via the urinary or digestive tract, of drugs consumed by humans and animals.
- ✓ the direct discharge of drugs into waste water from the pharmaceutical and fine chemical industries,
- ✓ The direct or indirect elimination of pharmaceutical agents used in healthcare establishments (laboratories, hospitals, etc.),
- ✓ the direct dispersion of veterinary medicinal products in the environment in aquaculture or during the treatment of farmed animals, or the indirect dispersion in the event of the spreading of slurry and sewage in soils intended for agriculture,
- ✓ the direct dispersion of therapeutic molecules in the form of food supplements poured directly into fish farming ponds.

### I. 1. 6. Effect of biochar surface Properties in adsorption of organic matter trace contaminants

Adsorption of organic trace contaminants to solid adsorbents is strongly influenced by compound properties – e.g. B. Polar versus non-polar and neutral molecules versus dissociated ions - and surface properties of adsorbents. For example, adsorbents with smaller mesopores may increase steric hindrance as molecules diffuse to adsorption sites deep within the pores (Pignatello, J. J et al., 2017). Understand accordingly Adsorption kinetics and mechanisms require knowledge of: The sorbent itself this section describes the surface properties of the biochar. Depend on the surface properties of the biochar properties of the starting biomass, the pyrolysis process, and handling/treatment of biochar after pyrolysis. (Liu, Z et al., 2018)

**Figure I. 2:** present activated carbon poudre

### I. 1. 6. a) Structural shape and pore size distribution

Biochar can contain different types of adsorption the distribution of site types is usually heterogeneous. The carbon framework structure of biochar often exhibits slit-like pores or a honeycomb structure. (Keiluweit, M et al., 2010, Sun, H., et al., 2010) Biochar pores the size can range from sub-nanometers to tens of micrometers, (Brewer, C et al., 2014), but the majority of biochar pores are microspores. These results indicate this steric hindrance affects the diffusion of triazines into deep tunnels. Free energy A combination of triazine and benzene on the same biochar has also been proposed Triazine adsorption is suppressed by about 6.2 kJ $mol^{-1}$ compared to benzene due to steric effects.

### I. 1. 6. b) Surface charge

Surface charge can be measured with ions. Exchanged power or zeta potential/isoelectric point. Biochar's ion exchange capacity is a term used from soil properties by which cation exchange capacity (CEC) is measured. The negative charge of biochar retains cations and anion exchange capacity (AEC) is the opposite. Is the zeta potential more commonly used for surface charge quantification? The zeta potential is the potential at the hydrodynamic shear plane of a particle and can be used to predict Coulomb value interactions between the ions (repulsion or attraction) of particles.

### I. 1. 7. Fate of drug residues in the environment

The study of the behavior and fate of drugs in the environment, as well as the understanding of the mechanisms behind them, are areas where knowledge is still limited. You need to develop: Research on drug degradation in environments where data are limited since it seems difficult to measure and perform systematic tests for the degradation of pharmaceutical substances, the development of suitable predictive models, as for other types of pollutants, is a way to be explored Study of drug absorption (absorption) in suspended solids and sediments, where the development of models is an alternative for systematic measurement (Sumper et al., 2005).

## I. 2. General information on adsorption

Some pollutants in their decomposition produce carcinogens and toxic products for water. As a result, their disposal does not depend solely on biodegradation. In the field of polluted water treatment, current research focuses mainly on two trends: a very low cost process and the wastewater is of international standard quality (Agustiono, T et al, 2006).

Adsorption has been reported as a promising technique for the removal of pharmaceutical compounds from water due to its high efficiency, simple operation, low investment and low maintenance costs; in addition to not producing by-products that may be more toxic than the parent product. The report on acetaminophen absorption on commercial activated carbon was oxidized by $HNO_3$ by the supplier (Nguyen et al. 2020).

comparing single and binary adsorption of acetaminophen on activated carbon with different particle sizes (Pauletto, et al. 2021). Absorption of ibuprofen on functional microporous carbon P was assessed by (Pap et al. 2021). Evaluation of the absorption of acetaminophen, ibuprofen and ketoprofen using sludge-derived activated charcoal (Meanwhile, Streit et al). Good results have been reported by (Tran et al. 2020) when synthesizing biochar to remove acetaminophen.

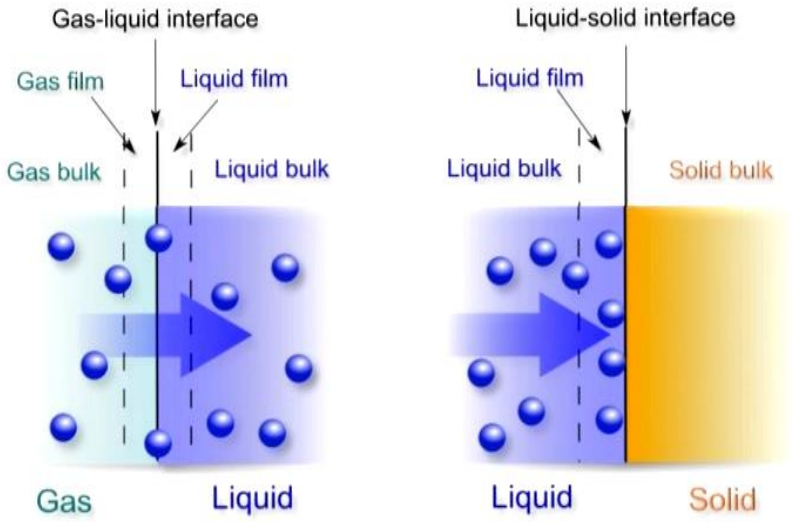


**Figure I. 3:** Schematic representation of the adsorption phenomenon (Hamdoudi, N and S. F; 2016)

### I. 2. 1. Definition of adsorption

Adsorption is a treatment process that removes a lot of harmful compounds from our environment. It is mainly used for water and air treatment. In this process, molecules of the liquid (gas or liquid), called adsorbent, attach themselves to the surface of the solid, known as adsorbent (Alaerts, L et al., 2008; Keskin, S et al., 2010; Liu, Y et al., 2007). This process determines the property of some materials to immobilize molecules on their surface (gas, metal ions, organic molecules, etc.) in a more or less reversible manner. Therefore, during this process, there will be a material transfer from the water or gas phase to the solid surface (Mechati, F et al., 2015).

### I. 2. 2. Types of adsorption

Adsorption is a surface phenomenon whereby atoms or molecules attach to the solid surface of a substrate through various processes. There are two types of adsorption, depending on the mechanisms involved:

#### I. 2. 2. a) Physical adsorption (physical adsorption)

Physisorption is the most common type of adsorption and there are most individual adsorption processes based on physisorption. Physisorption is a reversible phenomenon resulting from the attractive forces between atoms or groups of solids

and adsorbed substances (i.e., adsorbed molecules are easily desorbed by reducing pressure or increasing temperature). These attractive forces are of a physical nature, including the so-called van der Waals forces (Cenens, J and Schoonheydt, R. A., 1988). Which correspond to low energies on the order of (2–10 K cal/mol). This phenomenon essentially consists in the condensation of molecules on the surface of solids and is consequently facilitated by a decrease in temperature.

### I. 2. 2. b) Chemical adsorption (chemical adsorption)

Chemisorption or chemisorption, irreversible, slow and highly specific, resulting in modification of the adsorbed molecule. The latter cannot accumulate in multiple monolayers, and only directly bound molecules are subject to adsorption to this type of solid (Mohd, R et al., 2010) due to their strong covalent chemical bonds, which make them robust to activation energies. Change is involved. Adsorption energies are between 40 and 200 KJ/mol, stronger than physisorption. (Md. T. Uddin et al., 2009). This type of adsorption is involved in the mechanism of heterogeneous catalysis (Cenens, J and Schoonheydt, R. A., 1988).

### I. 2. 3. Modeling of adsorption kinetics

We will present the four most important kinetic models to interpret the experimental data on the adsorption results obtained from activated carbon. These models are:

### I. 2. 3. a) Pseudo-first order (PFO) model

The expression given by Lagergren: (Calvet. R, 2003 ; Allen. S. J, et al., 1989).

$$\frac{dq_t}{dt} = K_1(q_e - q_t) \qquad \text{(I. 1)}$$

Where:

$k_1$ : is the rate constant of the first order adsorption reaction.

$q_e$: amount adsorbed at equilibrium in (mg/g).

$q_t$: amount adsorbed at time t in (mg/g).

t: contact time in (minutes).

After integrating with the initial conditions $q_t$=0 to t=0, the equation becomes:

$$q_t = q_e(1 - e^{-k_1 t}) \qquad \text{(I. 2)}$$

Linearize the previous equation for:

$$ln(q_e - q_t) = lnq_e - k_1 t \qquad \text{(I. 3)}$$

We draw ln ($q_e$-$q_t$) = f(t), we get a straight line for k1 and qe.

Equations can be written in nonlinear form:

$$q_e = q_e(1 - exp(-k_t * t)) \qquad \text{(I. 4)}$$

**I. 2. 3. b) Pseudo-second order (PSO) model**

In order to get as close as possible to the real reaction mechanism, Pseudo-quadratic was developed by (Ho, Y. S and Mckay, G., 2000). The second pseudo-model (PSO) is given by the following expression:

$$\frac{dq_t}{dt} = k_2(q_e - q_t)^2 \qquad \text{(I. 5)}$$

Or:

$k_2$: rate constant of second order adsorption in (mg/g.min).

$q_e$: amount adsorbed at equilibrium in (mg/g),

$q_t$: amount adsorbed at time t in (mg/g).

t: contact time in (minutes).

After the integration we get:

$$\frac{1}{q_t} = \frac{1}{k_2 q_{e2}} + \left(\frac{1}{q_e}\right) t \qquad \text{(I. 6)}$$

**I. 2. 3. c) Elovich's model**

It can be expressed by:

$$\frac{dq_t}{d_t} * q_t = \alpha e^{-\beta q_t} \qquad \text{(I.7)}$$

Or :α initial adsorption rate (mg. $g^{-1}$.$min^{-1}$);

β : Desorption constant (g. $mg^{-1}$).

To simplify the Elovich equation, we assume that βα t=1 and $q_t$=0 at t=0, thus we get:

$$q_t = \beta ln(\alpha\beta) + \beta lnt \qquad \text{(I. 8)}$$

We plot the graph: qt= f(ln t) to determine the values of α and β.

### I. 2. 3. d) Intraparticle diffusion

If the adsorption is not limited by the reaction between the solute and the active sites, but rather by diffusion of the solute within the material (Weber. W. J, et al., 1963), the amount of solute adsorbed varies as the square root of time (t). The Weber-Morris model is inspired by previous work, in particular his Weber-Morris equations (Weber. J.W., 1972).

$$q(t) = k_d * t^{1/2} + c \qquad \text{(I. 9)}$$

$K_d$: (mg/(g.$h^{1/2}$)) is the intraparticle diffusion constant, which depends on the following factors: Diffusion of species considered, and size and number of borrowed pores inside the adsorbent.

C: in (mg/g) Constant representing the diffusion boundary layer thickness. More The Higher C is, the more important the boundary layer effect is (Sarkara, M et al., 2003). When intraparticle diffusion occurs.

$q_t$: as a function of $t^{1/2}$ is a straight line through the frame origin. In this case the process is limited only by internal diffusion. While on the right This indicates that internal diffusion is not the only limiting factor. Sorption kinetics. In this case, other mechanisms are involved (Fujiwara, K et al., 2007).

### I. 2. 4. Adsorption mechanism

Adsorption kinetics are of considerable practical interest to perform an optimal adsorbent during adsorption. It allows to highlight the physicochemical interactions between the solute and the adsorbent, to obtain the initial adsorption rate, to calculate the mass transfer coefficient and the diffusion coefficient of the adsorption mechanism.

Adsorption mainly occurs in four steps Figure I. 4 shows a material (adsorbent) with different regions in which organic or inorganic molecules capable of interacting with the solid are found.

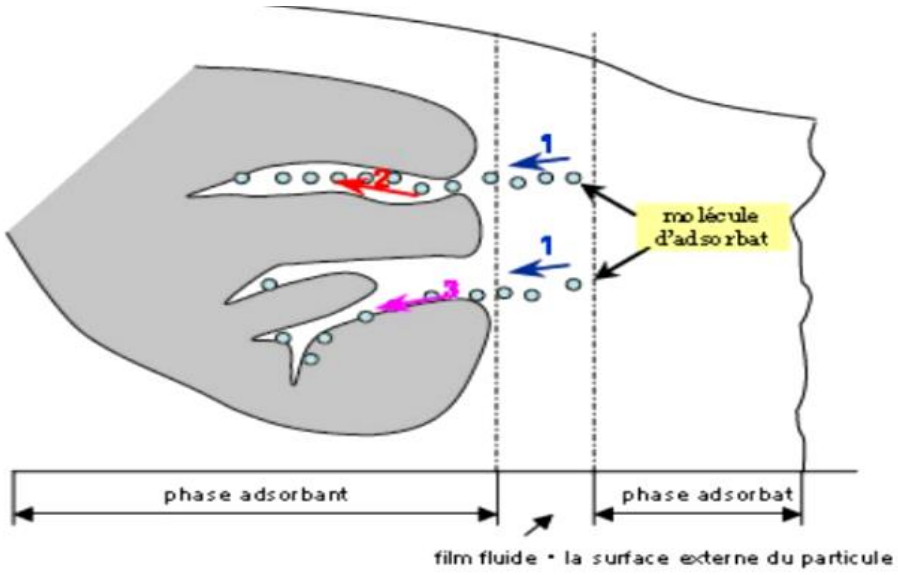


**Figure I. 4:** Diffusion mechanism from adsorbent to adsorbent (Cherraye. R, 2012)

1- Diffusion of the adsorbent from the outer liquid phase towards the near surface of the adsorbent.

2- diffusion of extra-particle material (transfer of the solute across the liquid film towards the surface of the particle).

3- transport matter in the porous structure of the outer surface of the particle to active sites).

4- The adsorption reaction is in contact with the active site, and when it is adsorbed, the molecules are considered to be immobile.

The figure (Manceau et al., 2002) illustrates the main interactions between an atom (or a molecule) and a solid.

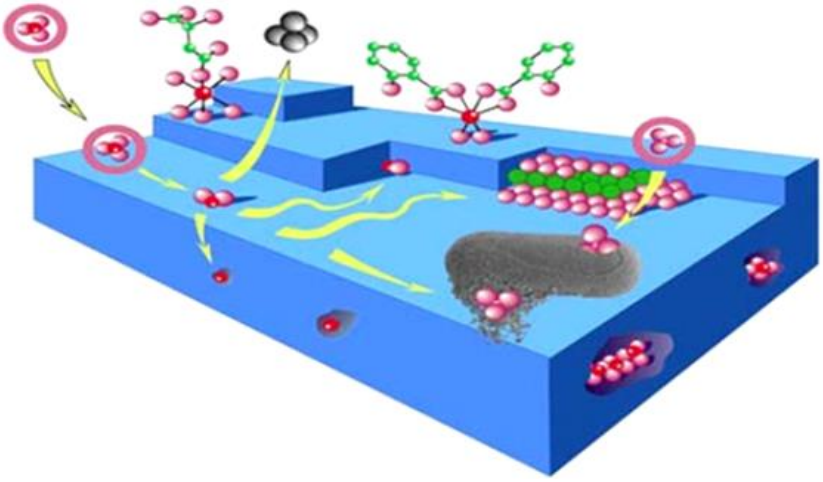

**Figure I. 5:** Major interactions between atoms or molecules and solids at the solid/liquid interface

### I. 2. 5. Thermodynamic analysis

The thermodynamic parameters, namely the change in free energy (ΔG), enthalpy (ΔH) and entropy (ΔS), which indicate the practical feasibility of adsorption structural changes of the adsorbent process and the adsorption mechanism, derived from the van't Hof equation: (Shikuku, V. O et al., 2018) .

$$\Delta G = -RT.\ Ln(k_c) \qquad \text{(I. 10)}$$

$$\Delta G = \Delta H - T\Delta S \qquad \text{(I. 11)}$$

$$K_C = \frac{Cads}{Ce} \qquad \text{(I. 12)}$$

$$\ln(K_C) = -(\frac{\Delta H^0}{RT}) + (\frac{\Delta S^0}{R}) \qquad \text{(I. 13)}$$

**$K_c$**: equilibrium constant, **$\Delta G^\circ$**: free enthalpy (J/mol), **$\Delta H^\circ$**: enthalpy change (J/mol), **$\Delta S^\circ$**: entropy change (J/mol. K), **T**: absolute temperature (K). **$C_{ads}$**: is the difference, where $K_d$ is the distribution coefficient) and $R$ is the universal gas constant (8,314 J. $mol^{-1}$. $K^{-1}$) (Tran, H. N.; You. S. J., Chao, H. P 2016).

### I. 2. 6. Classification of adsorption isotherms

The Figure I. 6 of the isotherm varies according to the adsorbent–adsorbent pair studied. The adsorption isotherms of solutes with limited solubility have been classified by (Gilles et al., 2000) Of the four main classes Figure I. 6.

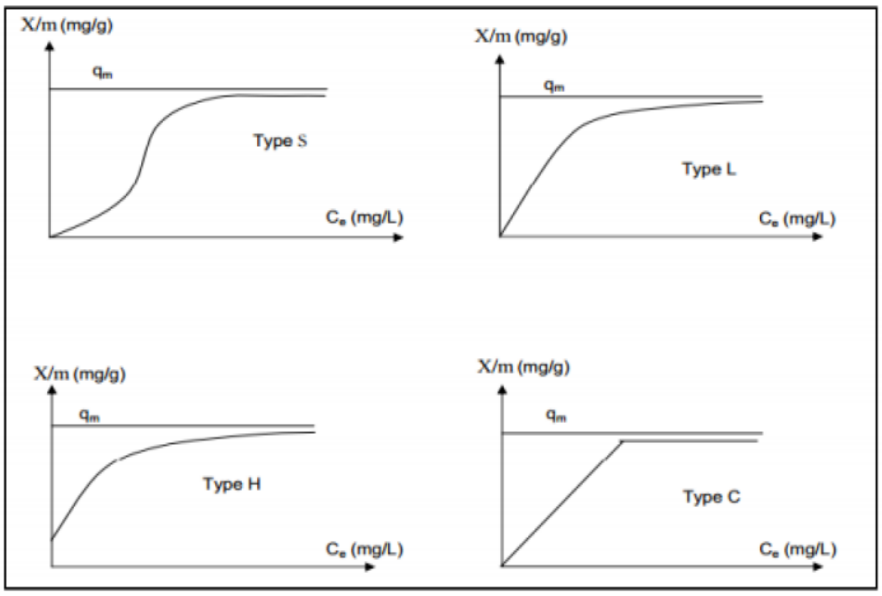


**Figure I. 6:** Classification of adsorption isotherms.

**S:** sigma; **I :** Langmuir; **H:** high affinity; **WITH:** Score unchanged.

The adsorption isotherm is a curve that binds, at a fixed temperature, the amount of product adsorbed per initial mass of adsorbent to the concentration remaining in the liquid phase after adsorption equilibrium. The isotherm allows hypothesis about the mode of adsorption.

Indeed, its appearance is representative of several related phenomena: monolayer or multilayer adsorption, whether there are lateral interactions between molecules or not. The isothermal adsorption curve is determined by plotting the concentration of the contaminant in the solid phase (in mg/g of adsorbent) at equilibrium as a function of the contaminant concentration in the solid phase equilibrium (in mg/l) in solution.

A fixed quantity at equilibrium is determined by the following relationship:

$$q_e = \frac{(c_0 - c_e)v}{m} \qquad \text{(I. 14)}$$

With:

**$q_e$:** amount of adsorbent present on the adsorbent (mg/g).

**$C_e$:** equilibrium concentration of adsorbent (mg/l).

**$C_0$:** initial concentration of adsorbent (mg/l).

**m:** Initial mass of adsorbent (g).

**V:** solution volume (L).

To quantify the relationship between $q_e$ and $C_e$, two widely used models are those of Freundlich and Langmuir. Correction for spectrophotometric estimation of residual concentrations in mixture systems was performed using the equivalent equations (I. 15 and I. 16) (Ghemit, R et al, 2019; Djebri, N et al., 2017)

$$C_a = \frac{(k_{b2} * A_1 - k_{b1} * A_2)}{(k_{a1} * k_{b2} - k_{a2} * k_{b1})} \qquad \text{(I. 15)}$$

$$C_b = \frac{(k_{a1} * A_2 - K_{a2} * A_1)}{(K_{a1} * k_{b2} - k_{a2} * k_{b1})} \qquad \text{(I.16)}$$

where $k_{a1}$, $k_{a2}$, $k_{b1}$ and $k_{b2}$ are the calibration constants for Polluant (A) and Polluant (B) at the two wavelelenghts lambda max 1 and lambda max 2. $A_1$ et $A_2$ are the measured absorbances of each pharmaceutical compound.

**Table I. 4**: Comparative analysis of PARA/DIC removal by different sorbents in the single and binary systems.

| Pollutants | Adsorbent | Adsorption capacity(mg/g) | Contac t time | Reference |
|---|---|---|---|---|
| **Pharmaceuticals (PARA/DIC)** | | | | |
| **Paracetamol (acetaminophen)** | STL-AC | 59.2 | | **(Tran, H. N et al., 2020)** |
| **Paracetamol (single system)** | SAC | 356.22 | 4h | **(Spessato, L et al., 2019)** **(Barczak, M et al., 2018)** |
| **Authers pharmaceuticals** | | | | |
| **ciprofloxacin (CIP)** | biochar modified MBC | 44.44 | 6 h | **Hu, B et al., 2021** |
| **tetracycline (TC) (single system)** | | 119.05 | | |
| **ciprofloxacin (CIP)** **tetracycline (TC)** **(binary system)** | biochar modified MBC | 31.15 117.65 | 6 h | |
| **Auther pollutants (pharmaceutical- pollutant)** | | | | |
| **Pb (II)** **(Single system) Atenolol (ATE)** | Cc-Mt | 139.78 86.86 | 150 min | **(Fu, C et al., 2020)** |
| **Cu(II)** **Zn(II)** | polyhydr oquinone /graphen e | 58.82 µg. $g^{-1}$, 131.58 µg. $g^{-1}$, | | **Ali, I et al., 2019** |
| **Pb2+** **Cu2+** **$Pb^{2+}$ ($Pb^{2+}$ + $Cu^{2+}$)** **$Cu^{2+}$ ($Pb^{2+}$ + $Cu^{2+}$)** | grapesee d activated carbon | 55.56 11.628 12.987 7.874 | | **Baylan, N., & Meriçboyu, A. E., (2016).** |

### I. 2. 6. a) Langmuir model

The theory proposed by Langmuir is based on the kinetic view of the adsorption of molecules on a flat surface: There is no accumulation of molecules, the molecules are continuously directed towards the surface, and an equilibrium of adsorption and desorption of molecules is established at the top. The assumptions of this model are as follows: (Langmuir, I., 1918).

- ✓ The adsorption sites on the solid surface are energetically homogeneous: we talk about "homogeneous adsorption surface"
- ✓ There is no interaction between the adsorbent and the solute in the solution;
- ✓ Adsorption is limited to monolayer only.

According to Langmuir at equilibrium, describe the following equation:

$$q_e = \frac{K_L C_e}{1+K_L C_e} \qquad \text{(I. 17)}$$

With:

$q_e$: amount of solute adsorbed at equilibrium (mg/g or mmol/g);

$C_e$: equilibrium solute concentration (mg/L or mmol/L).

After linearization, we can use the following relationship:

$$\frac{\boldsymbol{c_e}}{\boldsymbol{q_e}} = \frac{\mathbf{1}}{\boldsymbol{k_f q_e}} + \frac{\boldsymbol{c_e}}{\boldsymbol{q_e}} \qquad \text{(I. 18)}$$

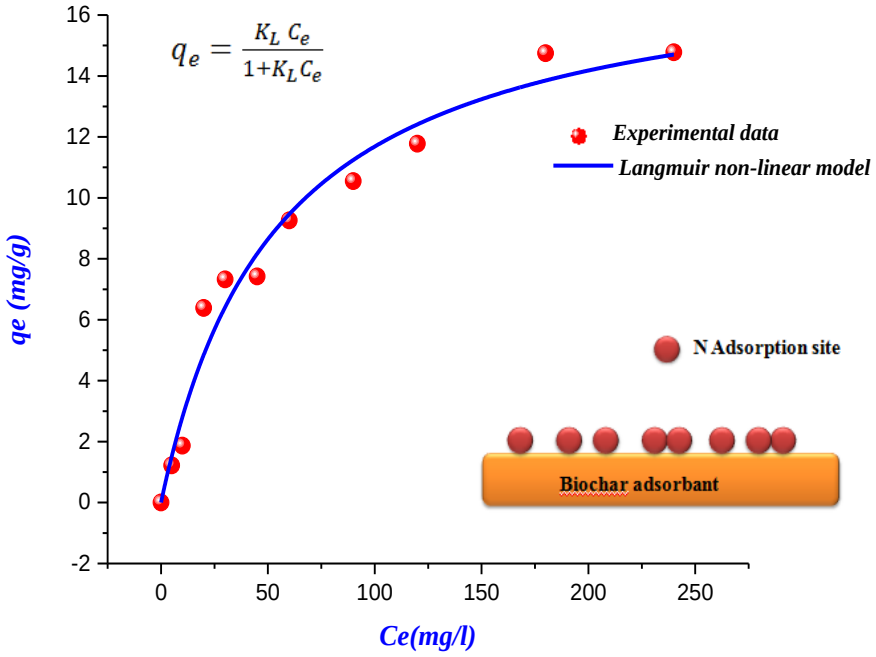


**Figure I. 7:** Langmuir isotherm and adsorption model

The shape of the isotherm can be used to predict whether the sorption system is favorable or not. The essential characteristic of the Langmuir isotherm can be expressed by a dimensionless factor ($R_L$), also known as a separation factor.

defined an RL parameter as follows: (Hall, K. R et al., 1966)

$$R_L = \frac{1}{(1+K_L C_0)} \qquad \text{(I. 19)}$$

$C_0$: initial concentration of solute in solution in mg. $l^{-1}$.

$K_L$ (l/ mg): is the Langmuir equilibrium constant.

$R_L$: indicates the conformational property of the isotherm.

* $R_L$>1 Adsorption is not favorable.

* 0 <$R_L$ <1 Favorable adsorption.

* $R_L$ = 0 Irreversible adsorption.

* $R_L$=1 Linear adsorption.

### I. 2. 6. b) Freundlich 's model

The Freundlich adsorption isotherm was first demonstrated in 1926, it is an experimental isotherm based on adsorption on heterogeneous surfaces. It is assumed that the more binding sites are occupied, the lower the binding decreases as site occupancy increases. In general, the Freundlich isotherm is given by the following equation: (Freundlich, H., 1906).

$$q_e = K_F * (C_e)^{\frac{1}{n}} \quad \text{(I. 20)}$$

Linearize this equation for:

$$lnq_e = lnK_f + \frac{1}{n_f} lnC_e \quad \text{(I. 21)}$$

$q_e$: adsorption capacity.

$C_e$: equilibrium concentration of adsorbent in solution.

$K_f$: characterizes the adsorption capacity of the carrier.

1/n: is the affinity of the solute for the adsorbent and represents the slope to the right. Depending on the values of 1/n,

We distinguish:

* 1/n=1: linear isotherm of type C.

* 1/n > 1: concave isotherm of type S.

* 1/n < 1: L- shaped convex isotherm.

* 0< 1/n < 1: H-shaped isotherm.

It is a straight line with slope 1/n and coordinates at the origin log K.

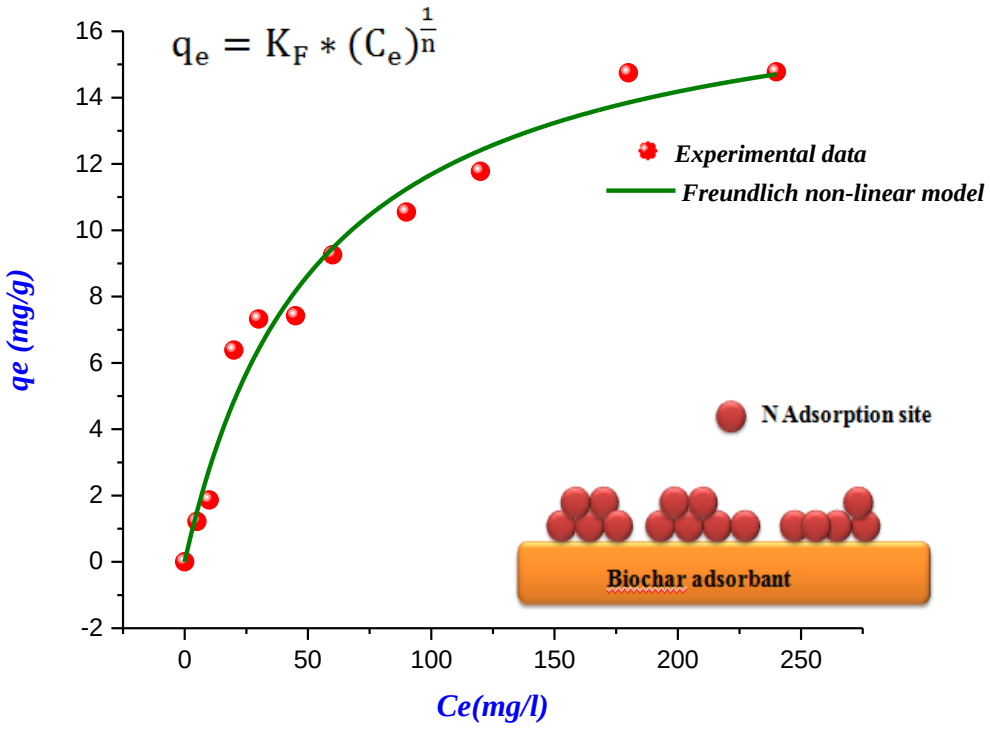


**Figure I. 8:** Multilayer adsorption model according to Freundlich.

### I. 2. 6. c) Temkin model

Temkin studied the effects of several indirect adsorbents/ Adsorbed on the adsorption isotherm, these interactions lead to The heat of adsorption of every molecule in the layer decreases linearly cover (Emmett, P. H, Kummer, J. T., 1943). The Temkin isotherm was used in the form:

$$q_e = \frac{RT}{b_t} \times Ln(K_T \times C_e) \qquad \text{(I. 22)}$$

$q_e$: amount of metal ions adsorbed (mg/g).

$C_e$: equilibrium solute concentration (mg/l).

R: universal ideal gas constant (J/mol. K).

T: absolute temperature (K).

bT: adsorption energy variation (J. mol/g. mg) This model allows to describe the phenomena occurring in the first minutes of the adsorption process.

### I. 2. 6. d) B.E.T isotherms (Brunauer, Emmett, Teller)

Brunauer, Emmett, and Teller explained that multi-layer physisorption at high pressure and low temperature reduces the thermal energy of the gas. Therefore, more gas molecules may be available per unit. Nitrogen gas is commonly used as an adsorption standard for surface analysis, except for the quantitative characterization of microporous materials (< 0.7 nm), where the use of $N_2$ gas is declining. Proved to be inappropriate. Argon and carbon dioxide are therefore used as alternative adsorbent molecules for microporous materials (Djemai, I., 2021)

The BET isotherm makes some assumptions. The most important of these assumptions is that the successive heats of adsorption of all but the first layer are equal to the heats of condensation of the adsorbates. Furthermore, this model assumes that the surface of the adsorbent is energetically uniform and that there are no interactions between the adsorbed molecules.

$$\frac{P}{N_a(P_0-P)} = \frac{1}{N_{am}.c} + \frac{c-1}{N_{am}.c}.\frac{P}{P_0} \qquad \text{(I. 23)}$$

Where:

P: is the equilibrium pressure,

$P_0$: is the saturation pressure,

$N_a$: is the amount of gas adsorbed,

$N_{am}$: is the amount of gas corresponding to a monolayer covering the entire solid, and c is the BET constant (approximately) given by:

$$c = \exp\left(\frac{E_1 - E_L}{R.T}\right) \qquad \text{(I. 24)}$$

And: $E_1$ is the heat of adsorption of the first layer and EL is the heat of liquefaction. The constant c is a measure of the affinity of adsorbent molecules for solids. Equation (I. 23) is usually valid in the range $05 \leq \frac{p}{p_0} \leq 0.3$, Here we get a straight line.

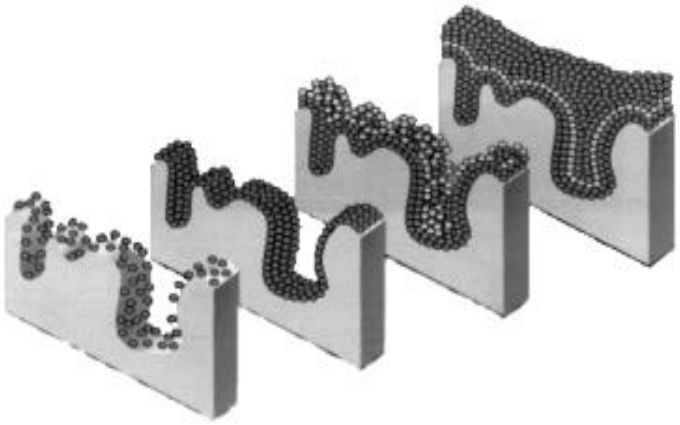

**Figure I. 9:** Representation of the adsorption of the adsorbent on the surface of the adsorbent (Arias, M et al., 2002)

### I. 2. 7. Adsorbent

All materials can be adsorbents, but only materials with high adsorption capacity are interested in industrial applications. This adsorption capacity is partly related to the internal structure of the material as: specific area, pore size….

### I. 2. 7. a) Adsorbent Pore sizes

The adsorbent consists of pores of different sizes, the distribution of which varies depending on the nature of the material. The classification of pores applied by IUPAC is based on their size, the pores sizes classified into three types:

- Microspores with the size less than 2 nm.
- Mesoporous the size from 2 to 50 nm.
- Macrospores with the size greater than50 nm.

Granular structure Figure I. 10 distinguishes two main types of adsorbents according to their structure:

- ✓ Homogeneous adsorbents with a porous structure spanning the entire particle scale (such as activated carbon);
- ✓ Particle heterogeneous adsorbents consist of homogeneous micro particles of the adsorbent agglomerated by a binder (such as a zeolite).

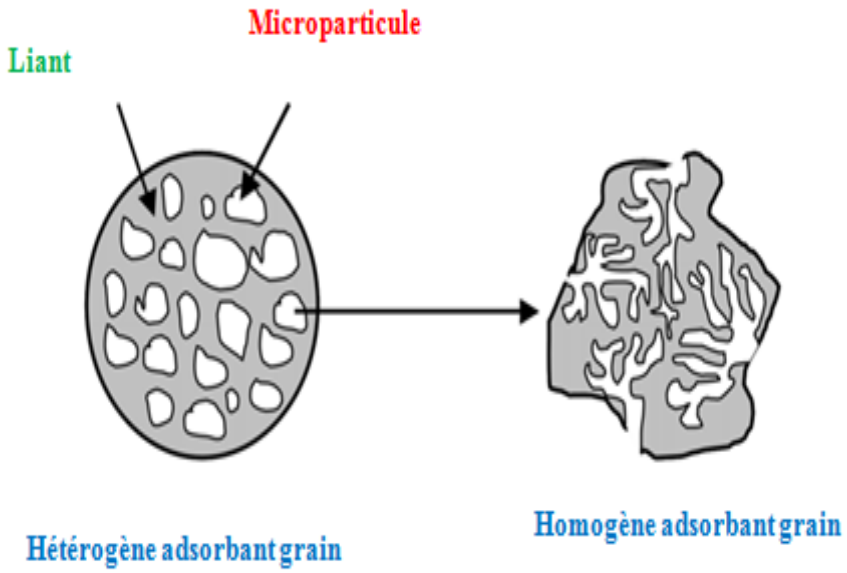


**Figure I. 10:** Schematic illustration of the grain shape of heterogeneous and homogeneous adsorbents

**2. 7. b) Factors that affect adsorption**

The adsorption balance between adsorbent and adsorbent depends on many factors, the main ones being as present in the Table I .5

**Table I. 5:** Factors that affect adsorption

| Adsorption factors | Adsorption factors: | Factors related to operating conditions: |
|---|---|---|
| **Specific surface The pore** | Polarization | Ambient temperature |
| **Diameter distribution** | Molecular mass | Stirring rate of the reaction medium |
| **Mass of adsorbent** | Particle size | Competition between species present in the environment |

| | | |
|---|---|---|
| **The nature of functional groups** | Solubility of the adsorbent | Contact time between adsorbent and adsorbent<br>Ionic strength |

## 2. 8. Application of adsorption

Adsorption is used industrially in the separation and purification of gases and liquids, in many fields such as petrochemicals, chemicals, pharmaceuticals and the environment. Industrial applications only use the physical adsorption property of the material because this phenomenon does not change the molecular structure of the adsorbent. Furthermore, it is reversible, allowing for the recovery of the adsorbed molecule and thus regeneration of the adsorbent. The main uses of adsorption are:

1) Purification of petroleum products and animal and vegetable fats.
2) Recovery of solvent and alcohol during fermentation.
3) Discoloration of the liquid.
4) Gas phase chromatography (fractionation method based on the difference in adsorption rates of different substances, on a given adsorbent).
5) Drying industrial organic products.
6) Water treatment for various industries (agricultural products, textiles, etc.) (Amimer, G et Kedadouche, S., 2015)

The performance and properties of biochar are influenced by the kind of feedstock precursors, the preparation temperature, and modification methods, among other factors (Ambaye et al., 2021)

# Experimental part: Materials and Methods

# Chapter II: adsorption of Ibuprofen by PS700 Adsorbent

## INTRODUCTION

Preparation of biochar as an efficace adsorbant and use to remove IBP. This chapter consists of fabrication a natural adsorption (biochar) from pepper stem (PS) wastes, as a potential adsorption capacity for IBP elimination from water media. Then passed to characterization techniques as: FTIR, BET analyzer, XRD, SEM-Eds, $pH_{PZC}$ method) to ascertain the adsorbent's physical characteristics. Additionally, this chapter examined and addressed the kinetics, equilibrium, and adsorption behavior (capacity and processes) of IBP on PS700 adsorbent.

### I.1.1. Preparation of PS700

The pepper stem considered as agricultural waste with a low financial value, collecte from pepper farming in the Biskra region, Algeria Figure II.1 (Pepper Stem). It is reducing into portions of approximately 0.5 cm, wash again and again with deionized water, after which drie at 110° C. for twenty-four hours to take away residual water. The dried pepper stem crush into debris of 0.1- 0.25 mm. The powder passe to the carbonization, which heat in a traditional tubular furnace at a temperature 700 °C (PS700) with the dew time growing scale of 10° C/min below $O_2$ restrained condition.

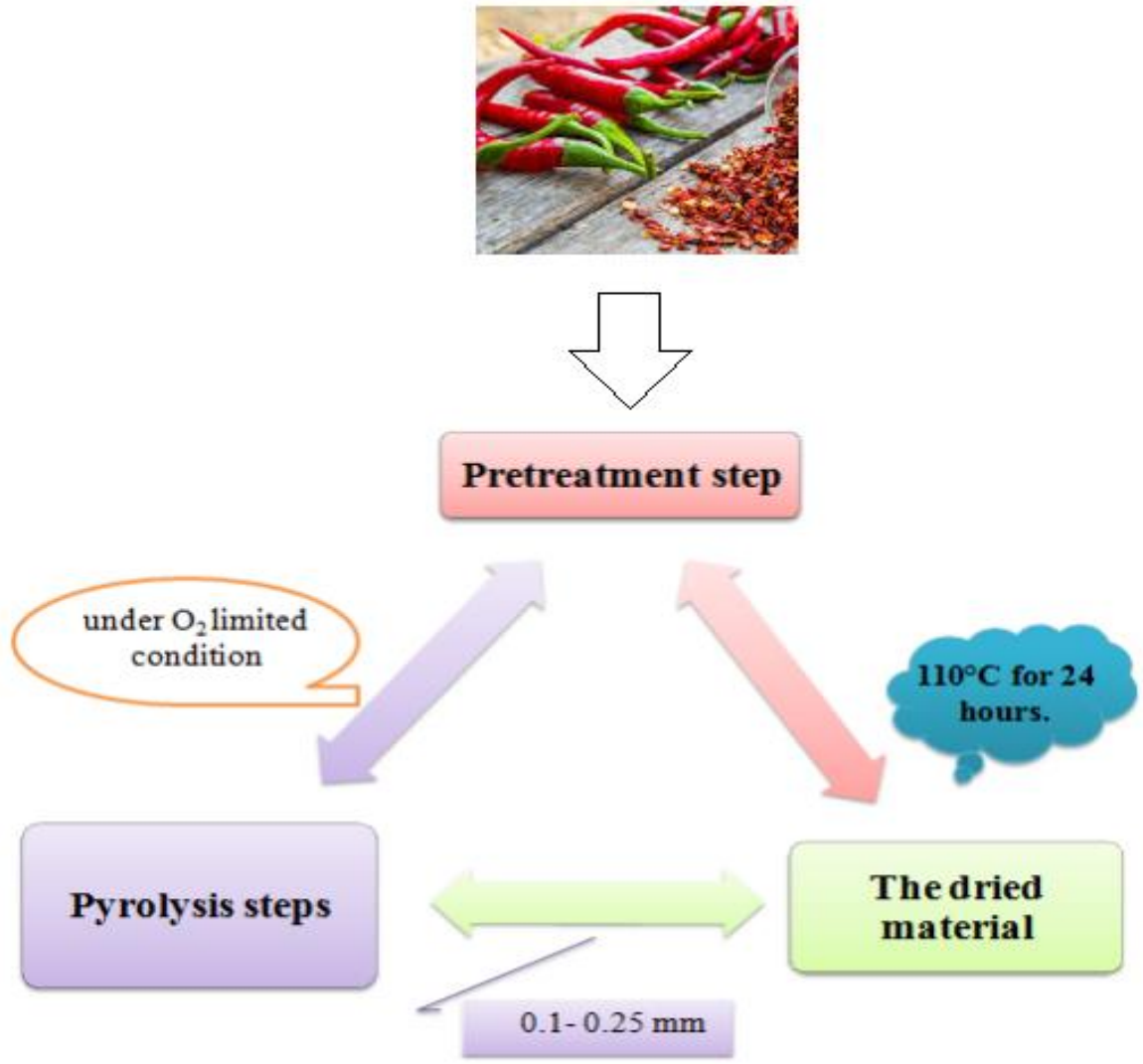


**Figure II. 2:** PS700 adsorbent preparation steps

### II. 1. 2- PS700 adsorbent characterization

After fabrication of PS700 adsorbent the samples pass to the characterization by using the analysis techniques as: BET; SEM- EDS; FTIR; DRX; $pH_{PZC.}$

### II.1. 2.1- Textural properties of PS700

Textural characteristics of PS700 samples obtained from nitrogen isotherms (Micromeritics ASAP 2020 equipment) at 77 K. Porosity ($V_{Total}$) and surface ($S_{BET}$) parameters estimated using the Brunauer method -Emmett-Teller (BET). Barrett-

Joyner Hallender (BJH) method used to determine micropore properties from the desorption isotherm.

The PS700 adsorbent sample's $N_2$ isotherm is shown in Figure II. 2. This isotherm, which belongs to category I in the IUPAC classification system, is typical of materials with modest exterior SBETs that are microporous. The presence of a mesoporous structure in this area is associated with the appearance of hysteresis loops (H4-type) at relative pressures larger than 0.4 (Nguyen et al., 2017).

According to the t-plot-De Boer method, the exterior $S_{BET}$ ($S_{Ext}$, $m^2/g$) and micropores volume ($V_{Micro}$, $cm^3/g$) were calculated. The PS700-biochar is a moderately mesoporous substance, according to the results, with a high volume of pores ($V_{Total}$ = 0.36 $cm^3/g$) and great surface area ($S_{BET}$ = 727.5 $m^2/g$). Additionally, the mean pore diameter and exterior surface area were 217.3 $m^2. g^{-1}$ and 1.97 nm, respectively.

Using the Dubinin-Radushkevich method, the characteristic energy of adsorption $E_0$ was 16.47 KJ/mol (higher than 16 KJ/mol), indicating that the generated biochar is microporous (Sevilla et al., 2011).

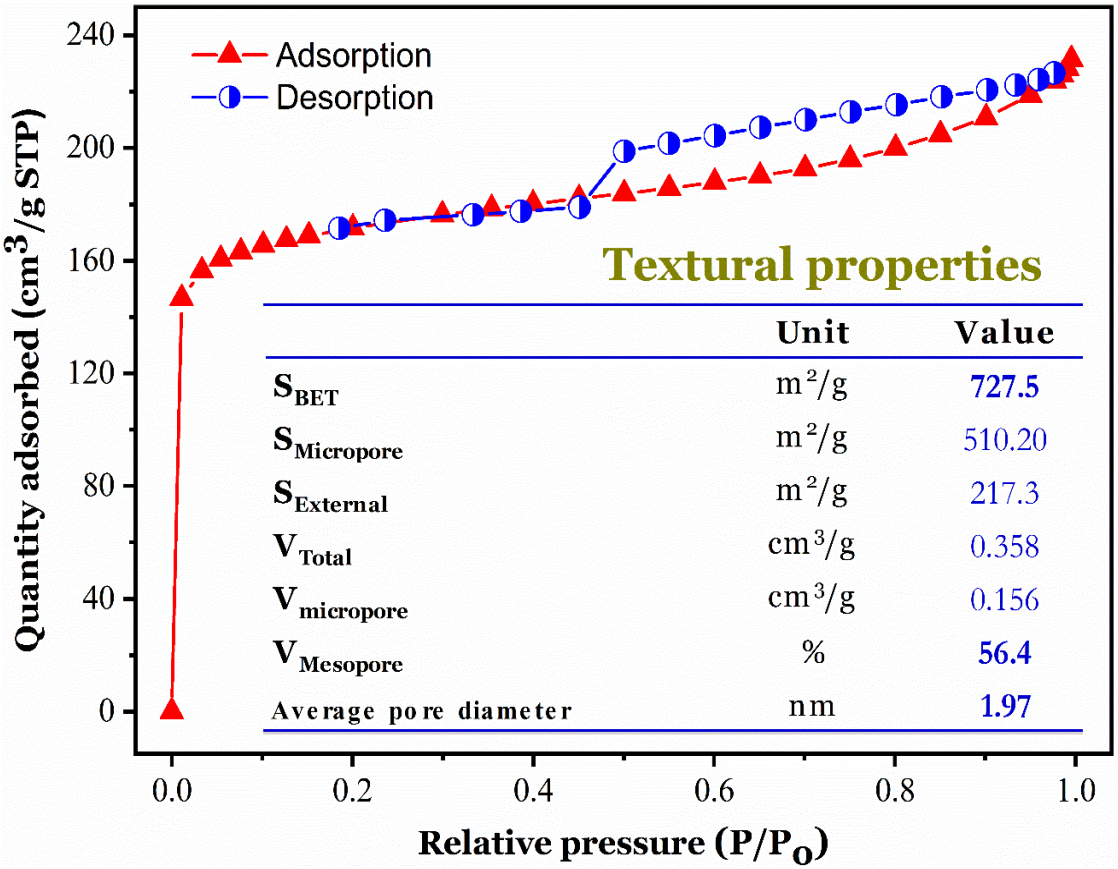

**Figure II. 2:** $N_2$ adsorption/desorption isotherm of PS700 adsorbent at 77 K and its textural characteristics.

**Table II. 1:** Textural parameters of sample PS700 adsorbent

| | $S_{BET}$ ($m^2/g$) | $S_{Lang}$ ($m^2/g$) | $S_{Micr}$ ($m^2/g$) | $S_{Ext}$ ($m^2/g$) | $V_{total}$ ($cm^3/g$) | $V_{Micro}$ ($cm^3/g$) | $V_{Non-micro}$ ($cm^3/g$) | $L_0$ (nm) | Average particle size (nm) | $E_0$ (kJ/mol) |
|---|---|---|---|---|---|---|---|---|---|---|
| **PS700** | 521.22 | 742.37 | 216.19 | 305.03 | 0.278 | 0.181 | 0.097 | 2.13 | 11.51 | 16.47 |

### II. 1. 2. 2- Scanning electron microscopy (SEM) and (EDS) analysis of PS700

Scanning electron microscopy (SEM) combined with energy dispersive X-ray spectroscopy (EDS) technique "Tescan Vega 3" was used for surface morphology and elemental analysis of the prepared material. The morphological properties show clearly that the PS700 sample possesses heterogeneous pores with tunnel form. The creation of a highly porous structure was explained by the conversion of cellulose and lignin to $CO_2$ (Changmai et al., 2018).

The EDS result of the elemental composition of the prepared PS-biochar indicates that C and O are the main elements in the PS700 composition. The high content of carbon (77.15 %) shows that the PS700 is a carbon-rich adsorbent, thus it is categorized as a mesoporous carbonaceous biochar.

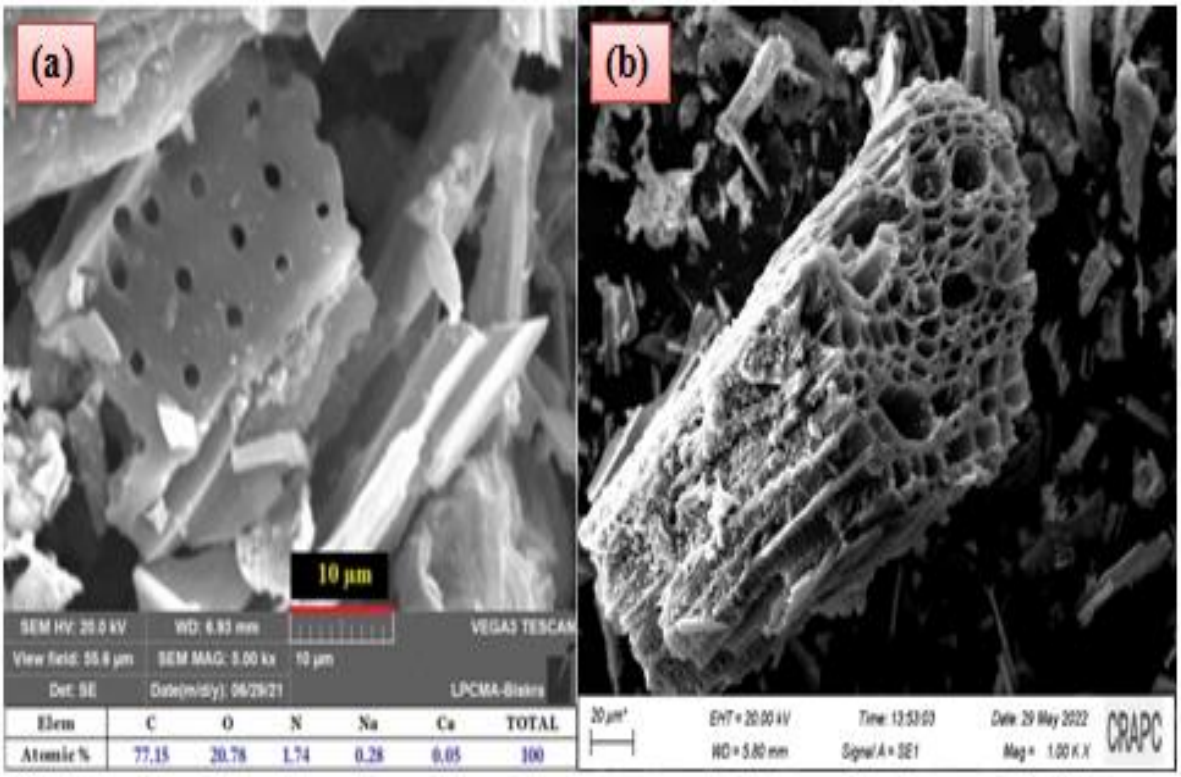


**Figure II.3:** (a) and (b) SEM images coupled by EDX spectrum before and after adsorption, for sample PS700 adsorbent.

### II.1.2. 3. X-ray diffraction analysis

The structure of PS700 was studied by X-ray diffraction (XRD) by a "PANalytical" diffractometer with CuKα radiation (λ= 1.5406 Å) at 30 mA and 40 kV. The 2θ values were between 2 and 70° with a scan rate of 2° $min^{-1}$. The prepared carbon's X-ray powder diffraction pattern showed no strong reflections in any area, indicating that the structure is not crystalline. The (002) and (100) plane amorphous carbon are responsible for the large peaks that arose at approximately 2θ = 22.8° and 43.2°, respectively (Zbair et al., 2018). The spacing value of the (002) plane is 0.39 nm, which is extremely similar to the results from earlier studies.

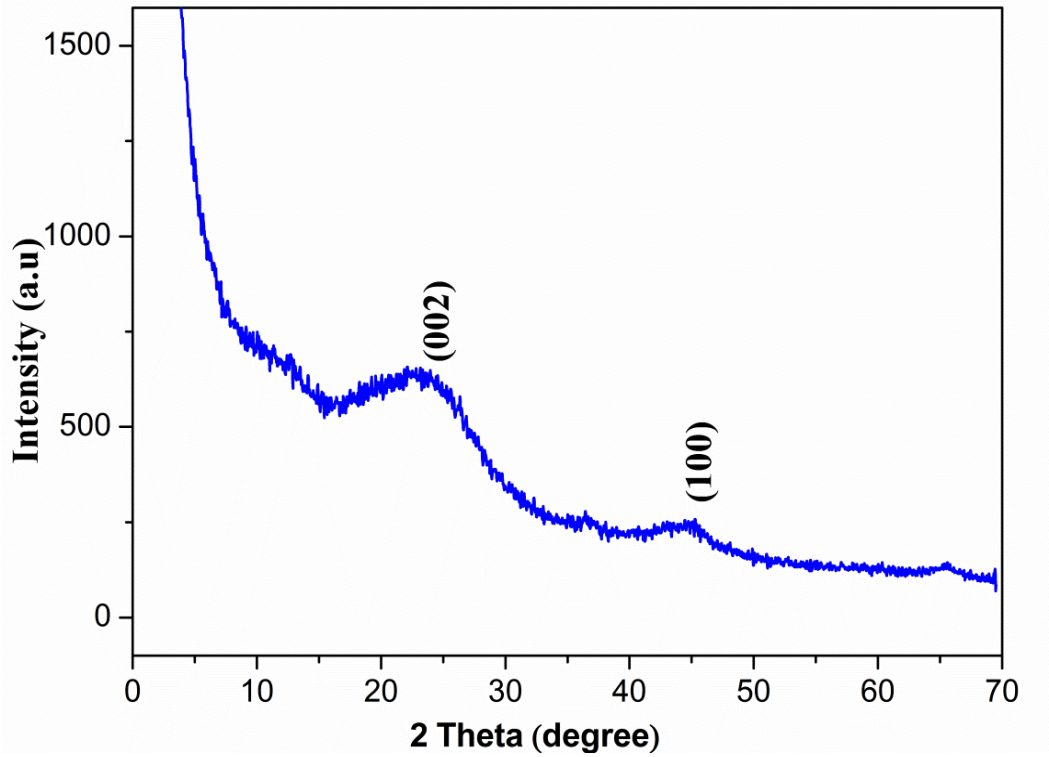


**Figure II.4:** X-ray diffraction pattern, for PS700 adsorbent.

### II.1.2.4. Infrared (IR) spectrometry

The surface properties of the synthesized PS700 were studied using FTIR spectroscopy. The spectra of the samples were acquired using the KBr disc technique (between 400 and 4000 $cm^{-1}$). FTIR spectrum of PS700 indicates the spectroscopic assignments of all functional groups of the adsorbent surface. The –OH stretching vibrations (of water, phenols, or carboxylic acids) are responsible for the broadband at nearly 3418 $cm^{-1}$. The triple bond (C≡C) in disubstituted alkynes was observed at the peak of 2377 $cm^{-1}$. Other function groups such as (C = O) and (C-O) were identified at around 1620 $cm^{-1}$ and 1120 $cm^{-1}$, respectively (Changmai et al., 2018). The sharp peak around 1384 $cm^{-1}$confirms the presence of carboxylate radical (–COO-) groups. Finally, the vibration of aromatic C–H bonds is responsible for the band at roughly 520 $cm^{-1}$.

After adsorption, the PS700 adsorbent's spectrum shows that the bands belonging to the hydroxyl (-OH) and carbonyl (C = O) groups have vanished. Peaks between 1200 and 600 $cm^{-1}$ are indicative of the IBP molecules' distinctive vibrations. A peak of 3418 $cm^{-1}$ disappeared as well.

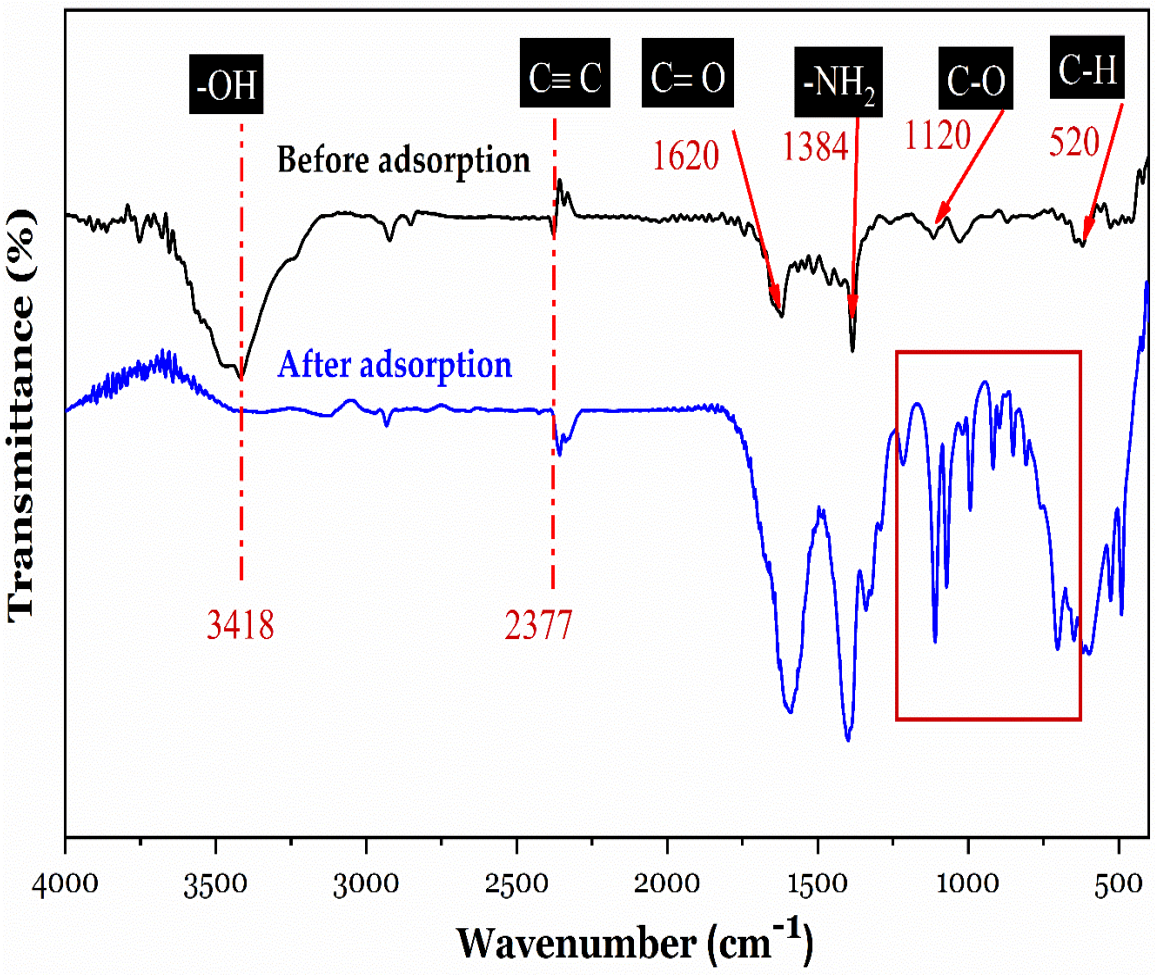


**Figure II. 5:** Fourier transforms infrared spectroscopy (FTIR) spectra of the PS700 adsorbent.

### II. 1. 2. 5. Point of zero charges ($pH_{PZC}$) and pH effect

The definition of the point of zero charges ($pH_{PZC}$) was taken from earlier research (Chahinez et al., 2020). In summary, drops of 0.1 M HCl solution or NaOH 0, 1 M solution were used to modify the initial pH ($pH_0$) of 0.01 M NaCl solutions (50 ml) to pH values from 2 to 12. Following that, each solution was agitated for 24 hours at room temperature while receiving 50 mg of PS-biochar. The $pH_{PZC}$ was then calculated by plotting ($pH_F$-$pH_0$) as a function of pH0 following the measurement of the final pH of the solutions.

With the exception of the experiment investigating the impact of pH, all adsorption tests were carried out at a pH of 7.0. IBP solutions with a concentration of 20 mg/L were utilized in a series of flasks for the adsorption kinetic experiment. Using 20 mg/L IBP solutions and 30 mg of PS700 adsorbent for 240 min of stirring, the effects of the initial pH (ranging from 2 to 12) on the IBP elimination were

investigated. After adsorption, it is possible that the hydrogen bonding mechanism played a role in the IBP adsorption process. This discovery demonstrates that IBP is present in the PS700 adsorbent. To better understand the charge property of the PS700 surface, it is vital to know the pH of point zero charges ($pH_{PZC}$). Understanding the mechanics of adsorption and identifying the ideal pH for adsorption requires knowledge of $pH_{PZC}$. The PS700 adsorbent responds as a negative surface when the pH of the solution is greater than $pH_{PZC}$, and it responds as a positive surface when the pH of the solution is lower than $pH_{PZC}$ ($pH_{PZC}$ = 6.3), as shown in Figure II. 6 (a).

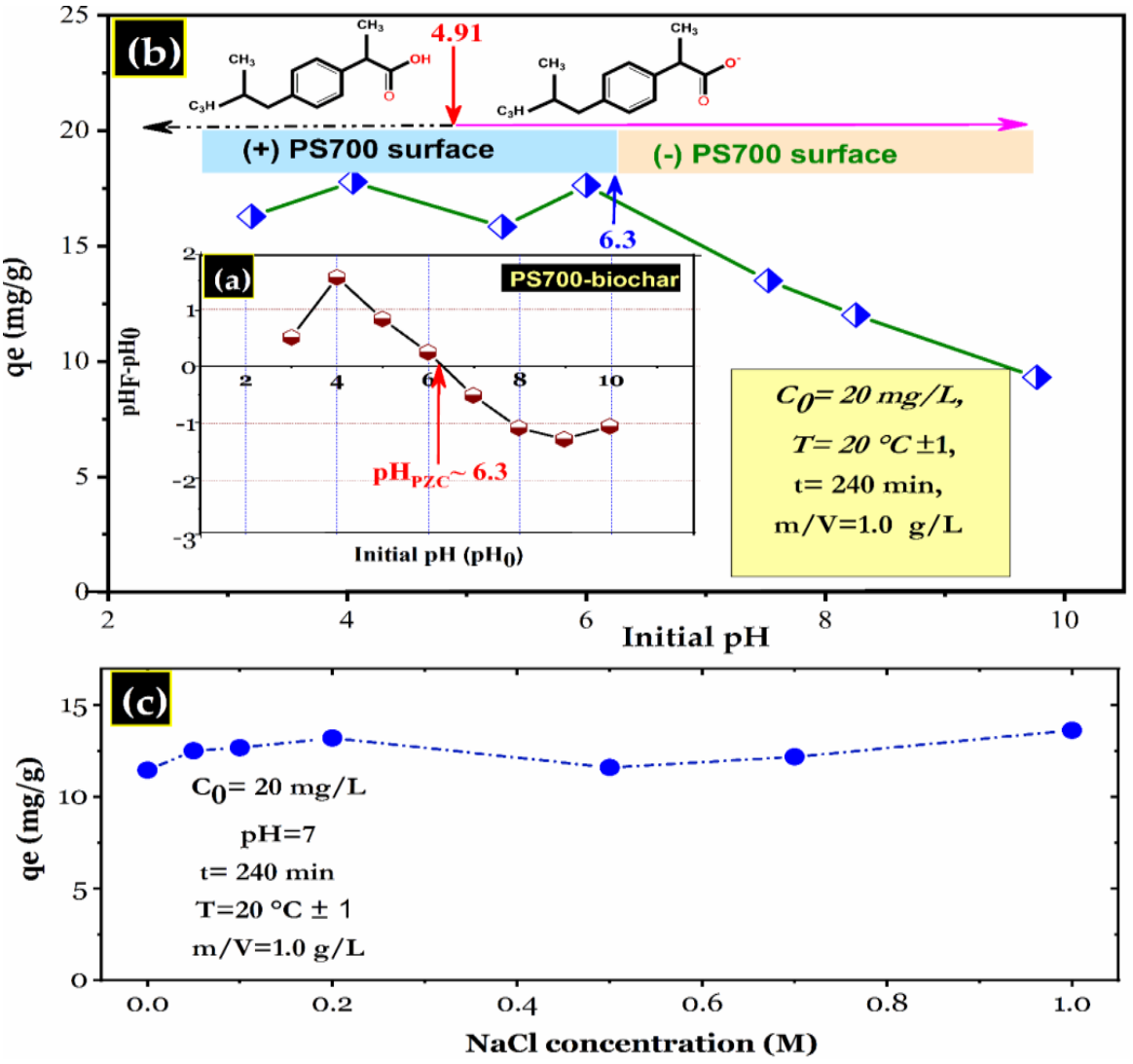


**Figure II. 6:** (a) $pH_{PZC}$ of PS700 sample; effect of (b) initial pH value and (c) ionic strength on adsorption capacity of PS700 adsorbent on antibiotic IBP.

## II. 2. The Adsorbate (Ibuprofen)

All chemicals (Aldrich, USA) were reagent grade (99%). Ibuprofen (IBP) was chosen as the adsorbate. All solutions were prepared with distilled water and the pH was adjusted using HCl (0.1 M) or NaOH (0.1 M). All compounds were used without further purification.

**Table II. 2:** Characteristics of Ibuprofen.

| **Nomenclature** | **acide (+/-) 2-(4-isobutyphényl) propionique** |
|---|---|
| **Chemical formula** | $C_{13}H_{18}0_2$ |
| $\mathbf{M_W}$ | 206.3 g/mol |
| $\lambda_{max}$ | 222 nm |
| **PKa** | 4.91 |
| **melting temperature** | $75\ ^0C$ |

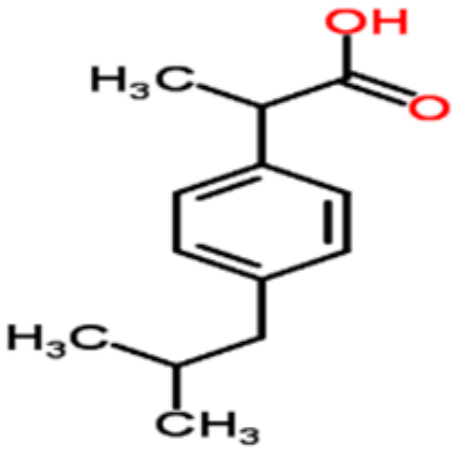


**Figure II. 9:** Molecular structure of Ibuprofen (IBP).

### II. 2. 1: calibration curve

Calibration was performed by measuring the absorbance of solutions with IBP concentrations from1to 30mg/l at wavelength $\lambda_{max}$ = 222 nm. The structure of the standard curve is shown in (Figure II. 10).

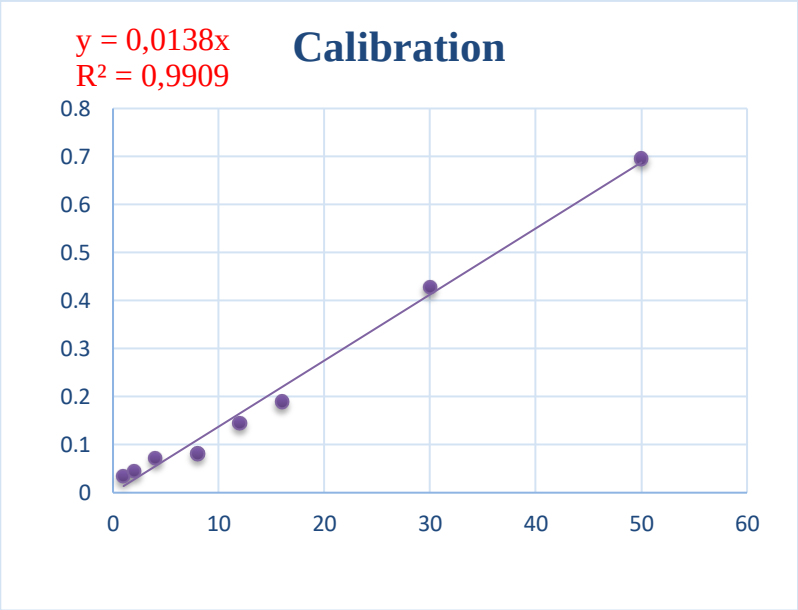


**Figure II. 10:** calibration curve of IBU

### II. 2. 3: Influence of contact time

Investigation of the effect of stirring time on IBP removal by PS700, conducted his PS700 on Biskra region for 4 hours' excitement (Figure II. 11) showing the effect of contact time on IBP adsorption by PS700. The influence of stirring time on the elimination of IBP at an initial content of 20 mg/L is presented in (Figure II. 11). It can be seen that as the shaking time increases, the adsorption rate of IBP increases and a rapid equilibrium is reached (approximately 120 min). About 80% (corresponding to 16.01 mg/g) of the total IBP was eliminated from the solution after only 30 minutes of contact.

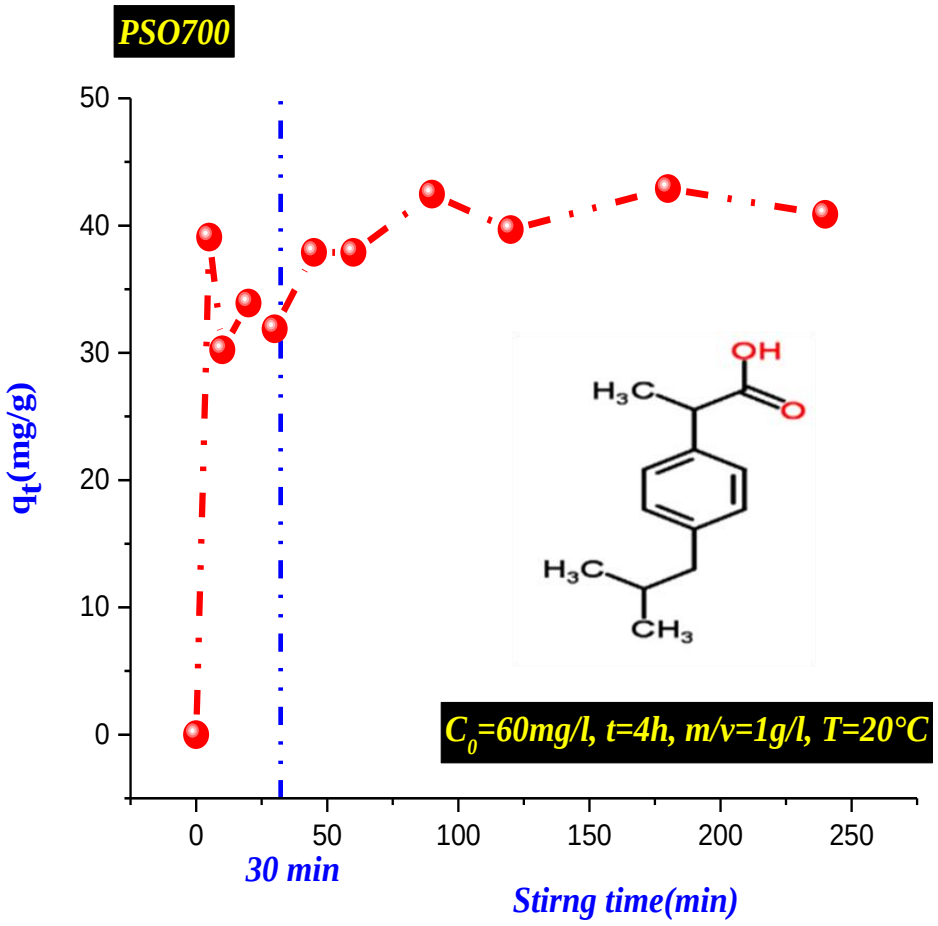


**Figure II. 11:** Effect of contact time on amount of IBP adsorbed ($C_0$= 20 mg/l, m/v= 1g/l, T= 20 °C)

### II. 3. Adsorption experiments

Adsorption tests were carried out discontinuously at 293 K (except for temperature effect experiments) and studied three repetitions of the same experiment. All IBP solutions tested were made from 500 mg. $L^{-1}$ stock solution. In 100 ml Erlenmeyer flasks containing 30 ml of IBP at a specified concentration, 30 mg of PS700 adsorbent was introduced. The mixtures were stirred at a speed of 300 rpm for the desired time. The solutions were then filtered through a 0.45 µm membrane filter and the residual IBP content was detected by a UV-vis spectrophotometer (Optizen 2120 UV model) at 222 nm. In the isotherm study, IBP solutions with concentrations ranging from 5 to 300 mg/L were used at a constant temperature (~293 K).

The equilibrium data of IBP adsorption were described using the Langmuir, Freundlich, Redlich-Peterson, and Liu isotherm models (Figure II. 13). These models' adsorption parameters were calculated using a non-linear optimization technique. The data demonstrate that the qe=f (Ce) plot resembles the L-type (high affinity) isotherm (Giles et al., 1974), which is characterized by a high solid adsorption capacity at low concentrations. The isotherm data is better explained by the Langmuir ($R^2$ = 0.982), Redlich-Peterson ($R^2$ = 0.988), and Liu ($R^2$ = 0.986) models than by the Freundlich ($R^2$ = 0.946) model, according to the estimated values in Table 3.

The Liu model postulates that adsorption sites on the biochar surface cannot have the same energy while the Langmuir model contends that IBP molecules were adsorbed in monolayers and multilayers (Grabi et al., 2021). Additionally, using the Langmuir equation, it was discovered that the PS-biochar's maximum adsorption capacity ($Q^0$max) was 569.6 mg/g, highlighting the excellent effectiveness of the made-up adsorbent in removing IBP from water.

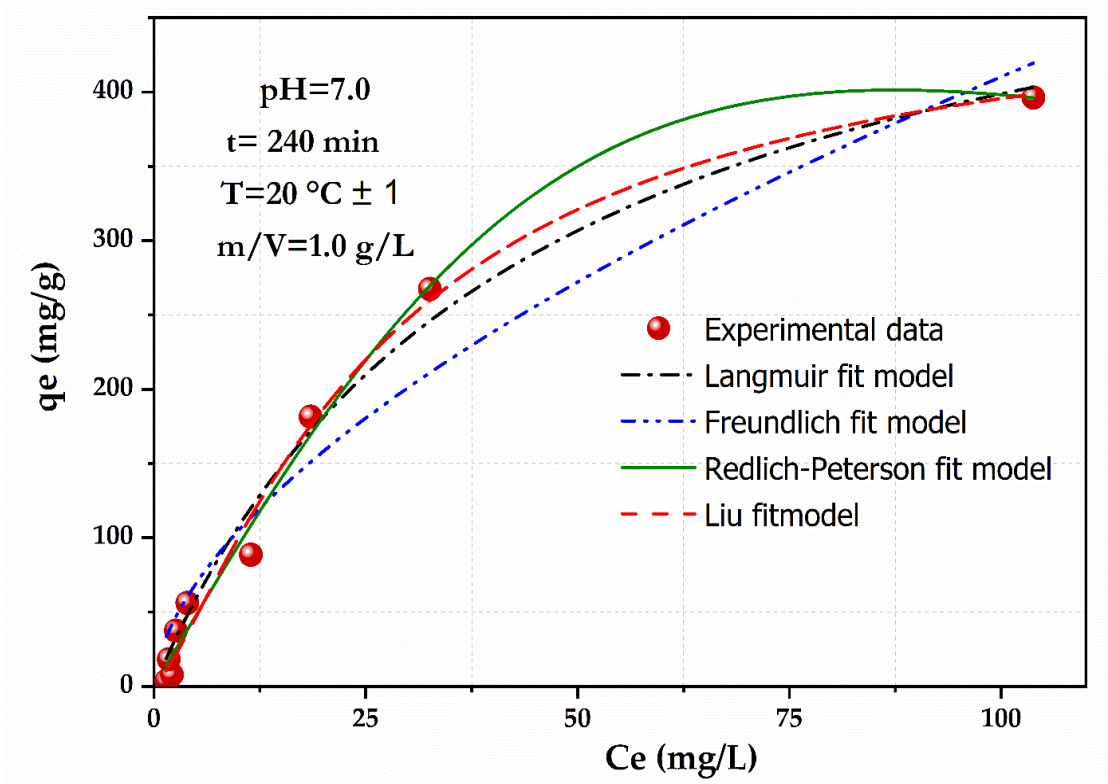


**Figure II. 13:** IBP adsorption isotherm on PS700 and fitting curves of isothermal models

The value of the Langmuir adsorption capacity was compared to the results of various adsorbents that have been described in the literature in order to support the ability of the PS700 as an efficient adsorbent for IBF from aqueous solutions. According to data in Table I. 2, the generated biochar used in this work has a higher $Q^{o}_{max}$ value (569.6 mg. $g^{-1}$) than other types of biochar, processed biochars (12.2-311 mg. g-$^{1}$), and activated carbons (139- 495 mg. $g^{-1}$) in the literature.

**Table II. 3:** Isothermal constant parameters for IBP adsorption on PS700 adsorbent.

| Model | Unit | Value | Standard Error |
|---|---|---|---|
| **Langmuir** | | | |
| $\mathbf{Q^{o}_{max}}$ | mg/g | 569.64 | 50.23 |
| $\mathbf{K_L}$ | L/mg | 0.023 | 0.004 |
| $\mathbf{R^2}$ | — | 0.982 | — |
| $\chi^2$ | — | 329.58 | — |
| **Freundlich** | | | |
| $\mathbf{K_F}$ | $(mg/g)/(mg/L)^{-1/n}$ | 26.81 | 7.68 |
| $\mathbf{n_F}$ | — | 0.59 | 0.198 |
| $\mathbf{R^2}$ | — | 0.946 | — |
| $\chi^2$ | — | 1119.69 | — |
| **Redlich–Peterson** | | | |
| $\mathbf{K_{RP}}$ | L/g | 9.681 | 1.198 |
| $a_{RP}$ | $(mg/L)^{-g}$ | $2.25*10^{-4}$ | $8.33*10^{-4}$ |
| **G** | — | 1.91 | 0.756 |
| $\mathbf{R^2}$ | — | 0.988 | — |
| $\chi^2$ | — | 216.87 | — |
| **Liu** | | | |
| $\mathbf{Q_{max}}$ | mg/g | 472.66 | 46.92 |
| **Kg** | L/mg | 0.0358 | 0.008 |
| $\mathbf{n_L}$ | | 1.281 | 0.185 |
| $\mathbf{R^2}$ | — | 0.986 | — |
| $\mathbf{R^2}$ | — | 0.986 | — |
| $\chi^2$ | — | 265.79 | — |

## II. 4. Kinetic study

To obtain the right equation to explain the IBP adsorption process on PS700, the kinetic data were fitted to the aforementioned mathematical models. All of the kinetic models' important estimated parameters have been compiled in (Table II. 4).

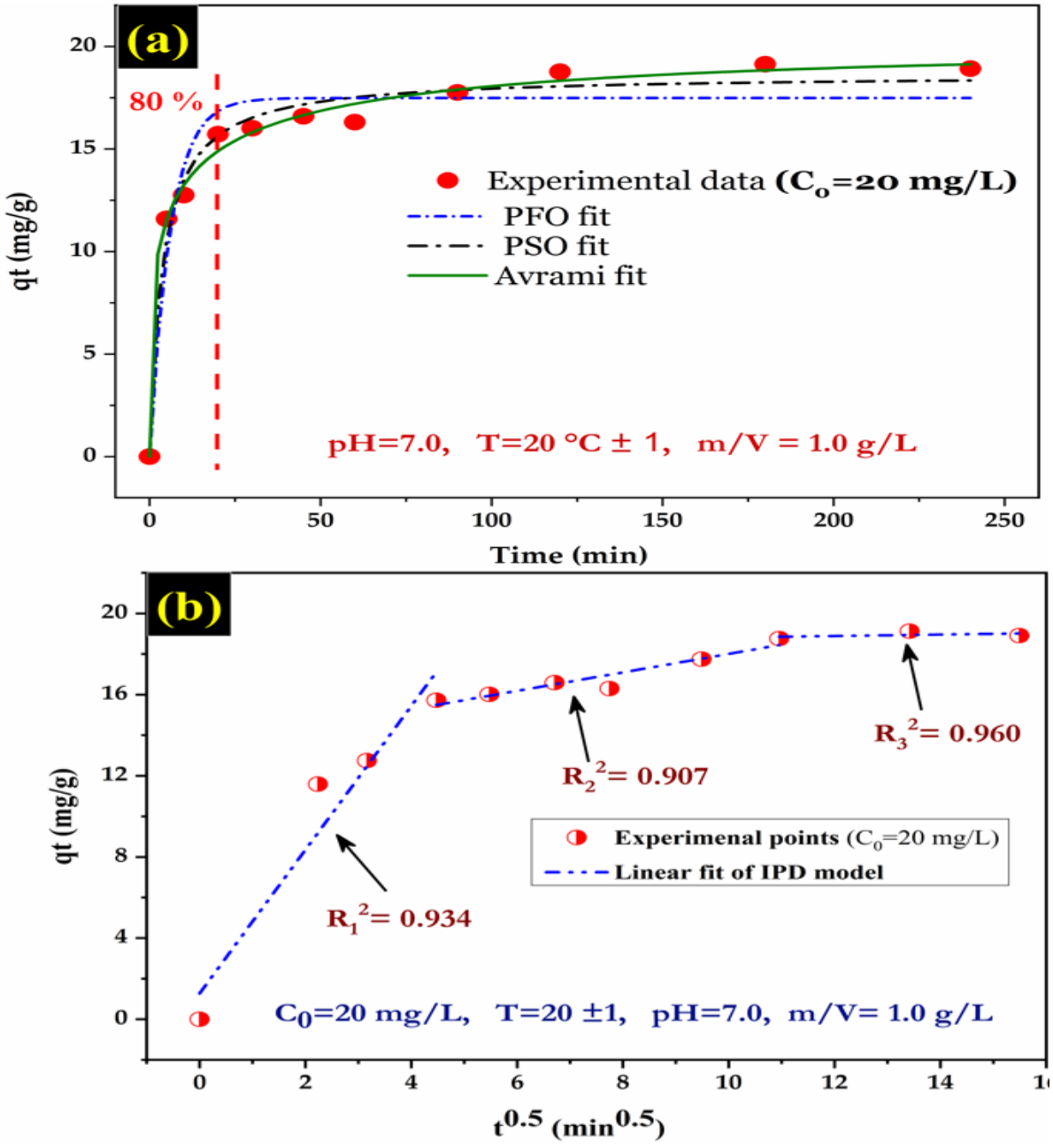


**Figure II. 14:** (a) the effect of contact time and nonlinear adjustment of the PFO, PSO, and Avrami kinetic models, (b) the linear relationship of the intraparticle diffusion model

Based on the correlation coefficient ($R^2$) and chi-square (2) values, the PSO ($R^2$ = 0.980, $\chi^2$ = 0.589) and Avrami ($R^2$= 0.987, $\chi^2$ = 2.629) models describe the kinetic data more accurately than the PFO and internal diffusion of particles model (Table 4). The measured value (18.23 mg/g) and the predicted value of the adsorption capacity ($q_{ecal}$ = 18.63 mg/g) agreed well. The half-life of the whole reaction was 5.1 min, and Avrami's rate constant was discovered to be 1.25 (L/min), demonstrating the efficiency of the adsorption process. In a practical engineering design, the speed of the equilibrium reaction is an important consideration when choosing an adsorbent.

The Weber and Morris model was applied to the analysis of the kinetic data of IBP adsorption on PS700 material in order to specify the deciding steps of the entire process and confirm the existence of the diffusion mechanism during adsorption. Figure 17(b) depicts the curve of qt vs $t^{0.5}$ for the intraparticle diffusion model. The findings are displayed in Table II. 4 and demonstrate that the IPD model satisfactorily suited the kinetic data ($R^2$ = 0.907-0.960). The straight-line plot displays a three-linear type with a different slope and intercept, as was seen. This result demonstrated that intraparticle diffusion is a phase in the adsorption process, but it was not the only one that limited the rate of the entire reaction (Somkiewicz et al., 2019).

The three steps that control the adsorption of IBP molecules on PS-biochar powder are, according to (Foroutan et al. 2019), (1) film diffusion mechanism, whereby adsorbed substances immediately penetrate the solid surface, (2) intra-particle diffusion, and (3) equilibrium condition. The order of the diffusion rate constant ($K_{IP}$) values, $K_{IP1} > K_{IP2} > K_{IP3}$, shows that the adsorption rate is initially higher and then gradually declines with time.

**Table II. 4:** Kinetic parameters of IBP adsorption on PS700 adsorbent at $C_0$ = 20 mg/L.

| Model | | Paramètre | Unit | Value | Standard Errer |
|---|---|---|---|---|---|
| **Experiment** | | **$q_{exp}$** | **mg/g** | **18.23** | — |
| **PFO** | | $k_1$ | L/min | 0.166 | 0.006 |
| | | $q_e$ | mg/g | 17.48 | 0.416 |
| | | $R^2$ | — | 0.938 | — |
| | | $\chi^2$ | — | 1.850 | — |
| **PSO** | | $k_2$ | g/mg×min | 0.014 | $2.2 \times 10^{-4}$ |
| | | $q_e$ | mg/g | 18.63 | 0.228 |
| | | $R^2$ | — | 0.980 | — |
| | | $\chi^2$ | — | 0.589 | — |
| **Avrami** | | $K_{AV}$ | $min^{-1}$ | 0.147 | 0.004 |
| | | $n_{AV}$ | — | 1.248 | 0.045 |
| | | q | mg/g | 20.04 | 0.306 |
| | | $t_{1/2}$ | min | 5.1 | — |
| | | $R^2$ | — | **0.987** | — |
| | | $\chi^2$ | — | 2.629 | — |
| **Intraparticle-diffusion** | First step | $K_{IP}$ | $mg/g/min^{1/2}$ | 3.54 | 0.169 |
| | | C | mg/g | 1.28 | 2.07 |
| | | $R^2$ | — | 0.934 | — |
| | | $\chi^2$ (RSS) | — | 9.39 | — |
| | Second step | $K_{IP}$ | $mg/g/min^{1/2}$ | 0.45 | 0.008 |
| | | C | mg/g | 13.45 | 0.628 |
| | | $R^2$ | — | 0.907 | — |
| | | $\chi^2$(RSS) | — | 0.63 | — |
| | Third step | $K_{IP}$ | $mg/g/min^{1/2}$ | 0.04 | 0.004 |
| | | C | mg/g | 18.46 | 0.905 |
| | | $R^2$ | — | 0.960 | — |
| | | $\chi^2$ (RSS) | — | 0.0535 | — |

## II. 5. Thermodynamic behaviors

The ΔH and ΔS values of IBP on PS700 were determined graphically by plotting Ln Kc as a function of 1/T. The results in Table II. 5 indicate that the Gibbs free energy is negative (ΔG<0), suggesting that the IBP adsorption process is spontaneous and favorable in the temperature range examined. ΔG values are between -20 and 0 kJ/mol. K, indicating that the process is dominated by physisorption (i.e. π-π interaction, pore filling, hydrogen bonding).

On the other hand, the standard change in enthalpy was found to be negative (ΔH<0), reflecting the exothermic nature of the IBP adsorption onto PS700. Moreover, the negative value of ΔS suggests that there is less disorder at the solid/liquid interface throughout the adsorption process (Grabi and Lemlikchi, 2021). This finding confirms that the adsorption of IBP occurred mainly by spontaneous and exothermic interactions with weak attraction forces. A similar observation was reported by several researchers for the exothermic nature of IBP antibiotic adsorption onto carbonaceous materials (Iovino et al., 2015).

**Table II. 5:** Thermodynamic parameters of IBP adsorption by PS700 at different temperatures.

| T (K) | $K_C$ | Van 't Hoffequation | ΔG (kJ/mol) | ΔH (kJ/mol) | ΔS (J/mol) K) |
|---|---|---|---|---|---|
| **293.15** | 7.189 | y = 4939.48 x –14.80 | -5.351 | -41.047 | -123.037 |
| **303.15** | 5.12 | $R^2$ = 0.947 | -3.529 | | |
| **313.15** | 2.439 | | -1.707 | | |

### I. 6. Regenerative potential of PS700 adsorbent

The possibility of reusing the absorbent fabric in diverse absorbent exams may be very essential economically and environmentally. To look at the regeneration of PS700, numerous re-desorption assays (four cycles) have been observed through adsorption and regeneration experiments as defined in a preceding study. 200 mg biochar changed into introduced to a 40 mg/L IBP answer and mixed (three hundred rpm) for four hours. The biochar charge changed into dried and reused for the following cycle after every adsorption experiment. After numerous cycles, and while the IBP elimination reduced through much less than

50%, the accumulated biochar changed into immersed in 100 mL of NaOH (0.1 M) solution for four h, after which washed with ultrapure water. Finally, the washed material changed into dried and used for regeneration experiments. The clearance percentage (%) of IBP at regular state changed into calculated as follows:

$$\textbf{Pourcentage}\ (\%) = \frac{(C_0 - C_e)}{C_0} * 100$$

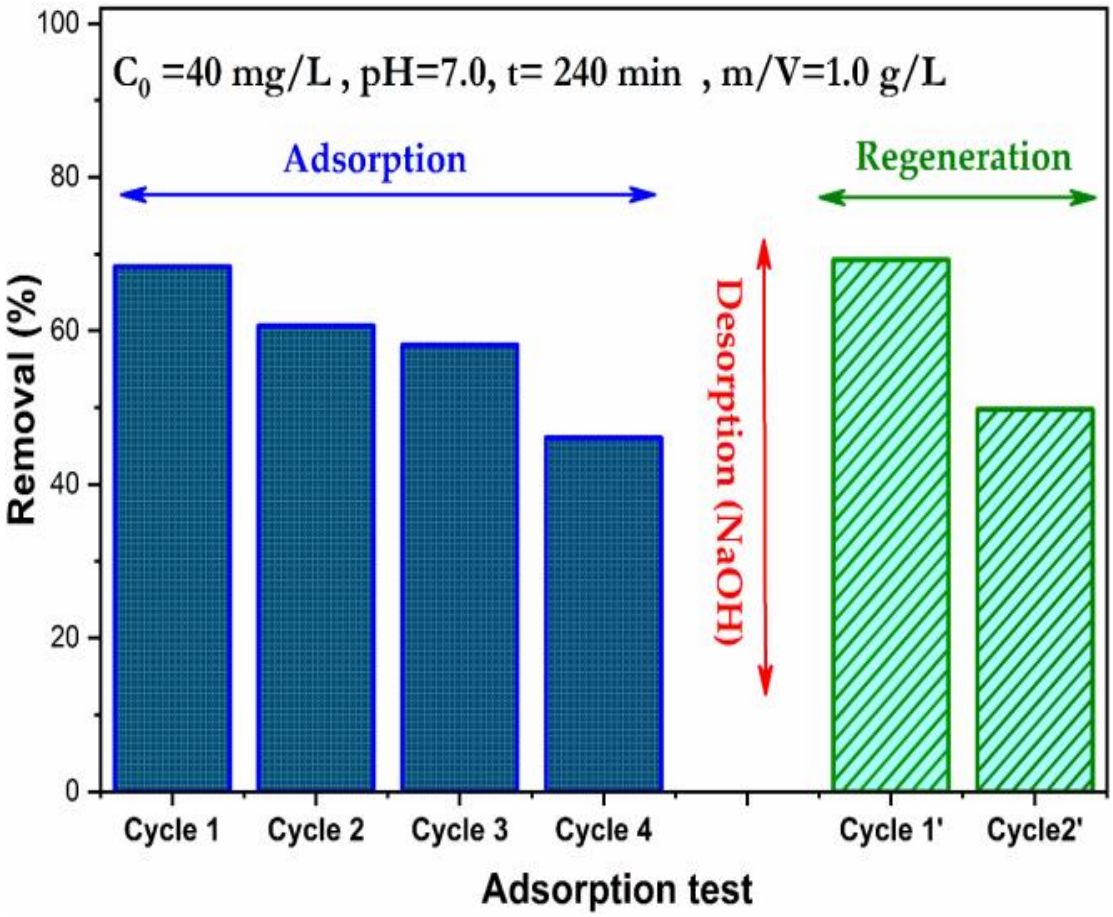


**Figure II. 15:** Reuse and regeneration tests of prepared PS700 adsorbent.

Figure II. 16 suggests an evaluation of the adsorption capacities of PS700 with the ones received the usage of biochar oxidized via way of means of $HNO_3$ (PS700 $HNO_3$). The quantity adsorbed of IBP acquired via way of means of the 2 biochar samples in an extensive variety of concentrations (from 20 to 300 mg/L) from the adsorbate. The effects offered on this figure suggest a marked lower in the quantity adsorbed from IBP on PS700 after $HNO_3$ oxidation. This end result confirms the crucial contribution of the π-interaction to the complete method of IBP adsorption on PS700.

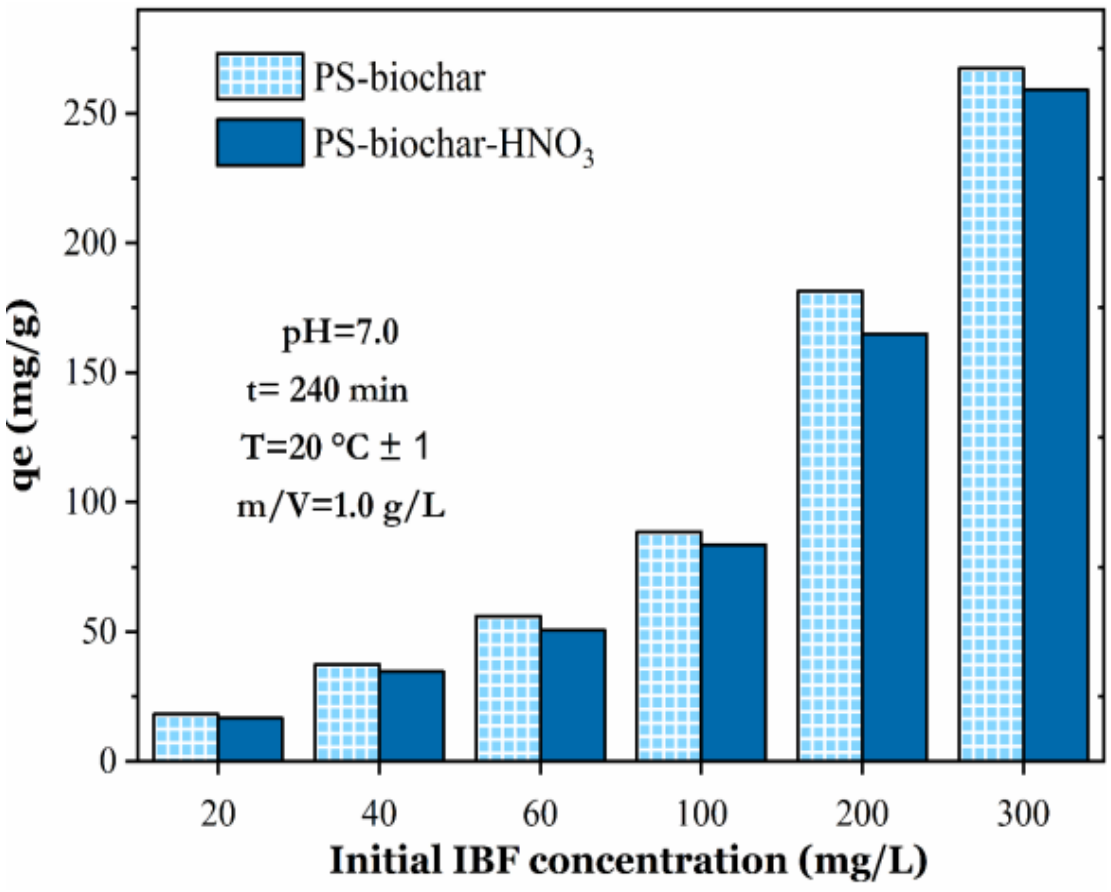


**Figure II. 16:** Comparison of IBP adsorption capacities on oxidized and non-oxidized PS700 adsorbent at different initial IBP concentrations

The results of trying out and evaluation of the capacity of the organized biochar to absorb 4 pollutants (diclofenac, hydrated acid, chromium, and methylene blue) are shown Figure II. 17. The organized adsorbents gave excellent elimination efficiencies for all of the studied pollutants on the studied concentrations of IBP (10, 20, 30 mg/L). The excessive quantity of adsorption in the case of wet acid elimination and methylene blue is (28.8 and 29.7 mg/g), respectively. Accordingly, synthesized biochar need to be a capacity adsorbent for the treatment of water weighted down with diverse organic pollutants

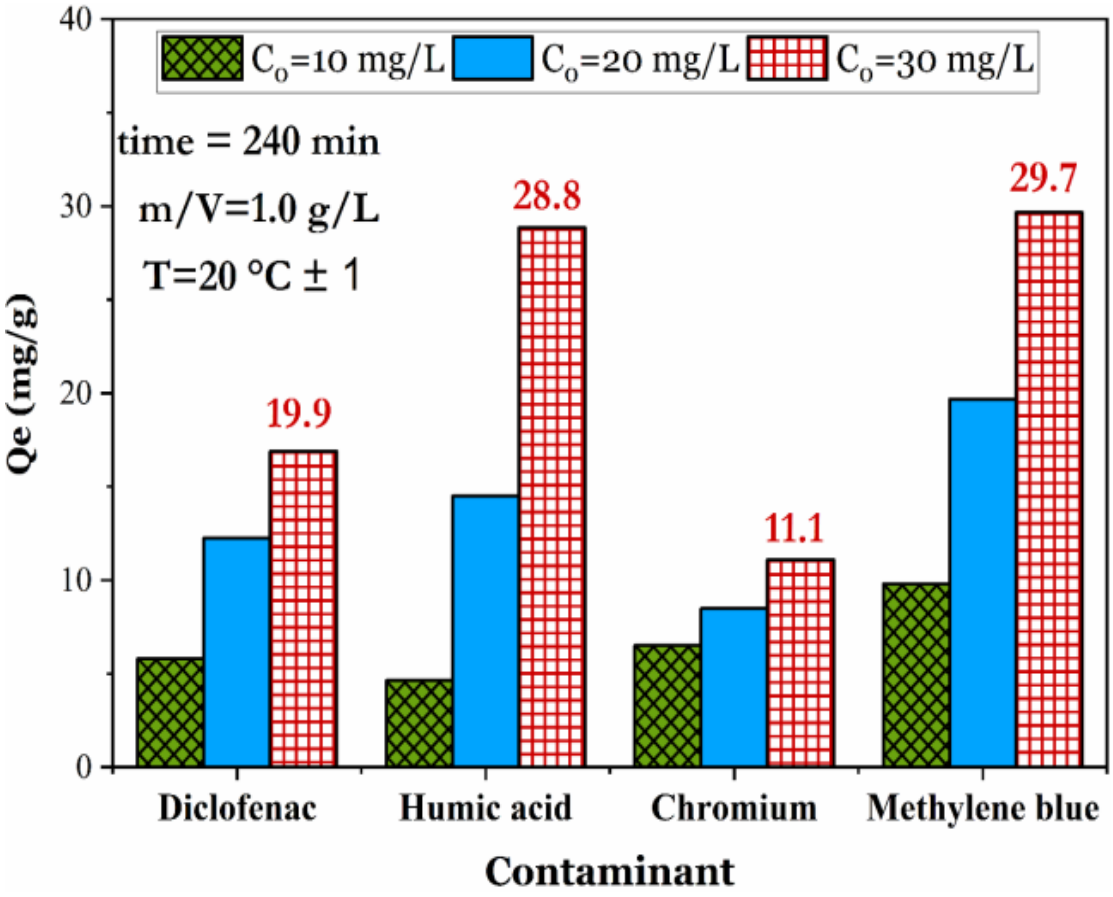


**Figure II. 17:** comparison of the capacities of PS700 adsorbent against different types of contaminants (pH=7.0 for the adsorption of organic contaminants and 5.5 for Chromium)

## Conclusion

Biochar prepare from pepper stem (PS700) give great results and proved effective for IBP absorption. Through the results obtained, PS700 is a medium porous carbon adsorbent material with advanced structural properties ($S_{BET}$ = 727.5 m 2 / g and $V_{Total}$ = 0.36 cm 3 / g). The π-π interaction, pore filling, and hydrogen bonding contributed to the adsorption process. The monolayer adsorbent quantity for the Langmuir model became 569.6 mg/g. PS700 confirmed excellent reusability for IBP elimination with extremely good applicability to other forms of water contaminants....

# **Chapter III:** Adsorption of Diclofenac and Paracetamol in the single system

## III. INTRODUCTION

This chapter consist of samples characterizations after removal of DIC and PARA by PS700 adsorbent in a single system adsorption, and Study isotherm, kinetics, and thermodynamic systems.

### III. 1. Samples characterization

#### III. 1. 1- Morphology and crystalline characteristics of PS700 in the Single system

Following the adsorption of PARA and DIC, the EDS analysis of the fundamental composition of the produced PS700 shows that C and O are the primary elements in the PS700 adsorbent composition. Its classification as mesoporous carbonaceous biochar is based on Figure III. 1, which demonstrates that the PS700 is a carbon-rich adsorbent.

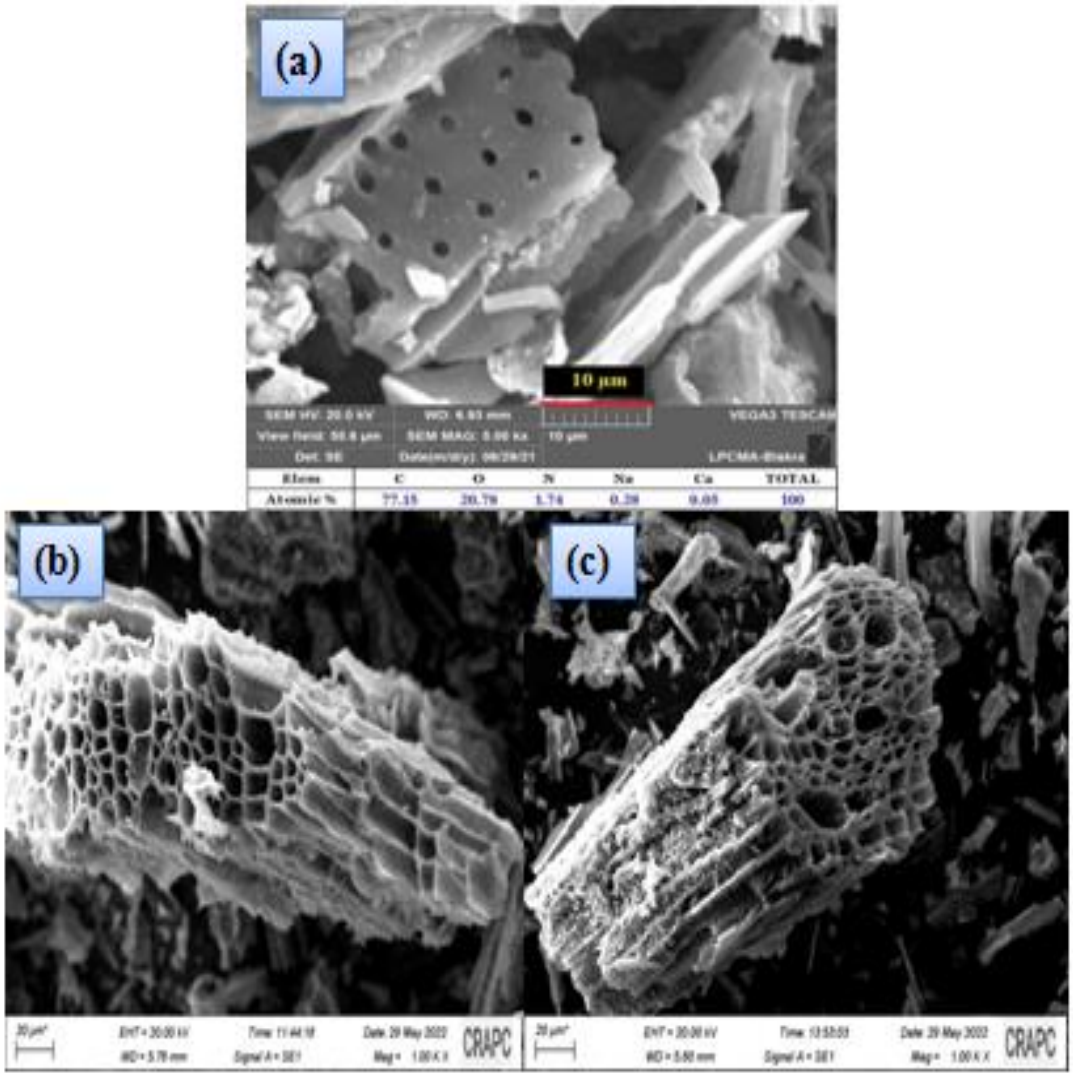


**Figure III. 1:** Present SEM images PS700 before adsorption (a), and (b), (c) SEM images coupled with EDX spectrum PS700 after adsorption of PARA and DIC respectively in the single system.

## III. 2. Adsorption phenomena

### III. 2. 1 - The Adsorbat (Diclofenac)

Diclofenac (NSAID, Figure III. 2(a)), a non-steroidal anti-inflammatory Drug, is widely used in human medicine. It enters the aquatic environment via human waste. DIC removal efficiency in sewage treatment plants is very low (Verlicchi et al., 2012).

All chemicals Aldrich, (USA Figure III. 2(b)) were reagent grade (99%), a no-steroidal anti-inflammatory drug. Paracetamol $C_8H_9NO_2$. It is a weakly acidic drug of the analgesic class, (Ocampo-Perez, R et al, 2017; García-Mateos, F. J et al., 2015).

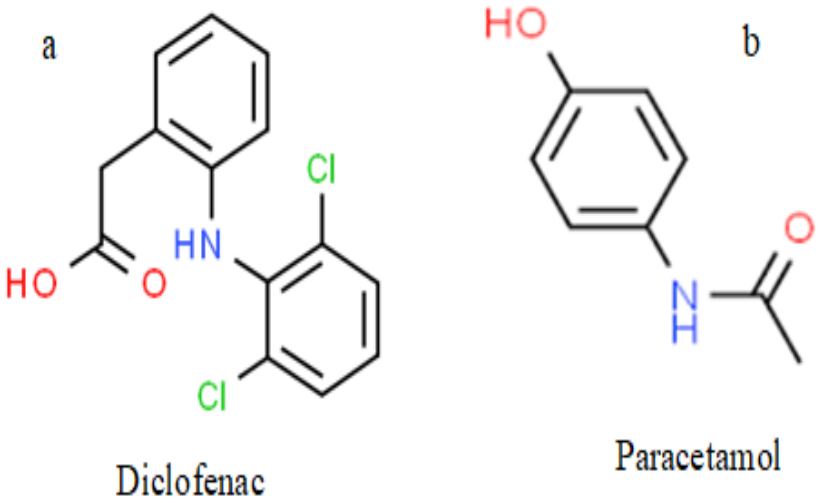


**Figure III. 2: a-** Diclofenac Molecular structure, **b-** Paracetamol Molecular structure

**Table III. 1:** Characteristics of Diclofenac and Paracetamol

| Nomenclature | Diclofenac | Paracetamol |
|---|---|---|
| **Chemical formula** | $C_{14}H_{10}CL_2NNaO_2$ | $C_8H_9NO_2$ |
| $\mathbf{M_w}$ | 318.13 g. $mol^{-1}$ | 151.16 g. $mol^{-1}$ |
| $\boldsymbol{\lambda_{max}}$ | 276 nm | 242 nm |
| **pKa** | 4.15 | 9.46 |
| **Solubility** | | 20 °C |

### III. 2. 2) Calibration curve

Calibrations were performed by measuring the absorbance of solutions with DIC and PARA concentrations from (1 to 30 mg/l) at wavelength $\lambda_{max}$ = 276 nm and 242 nm, respectively. The structure of the standard curves is shown in (Figure III.a,b 3).

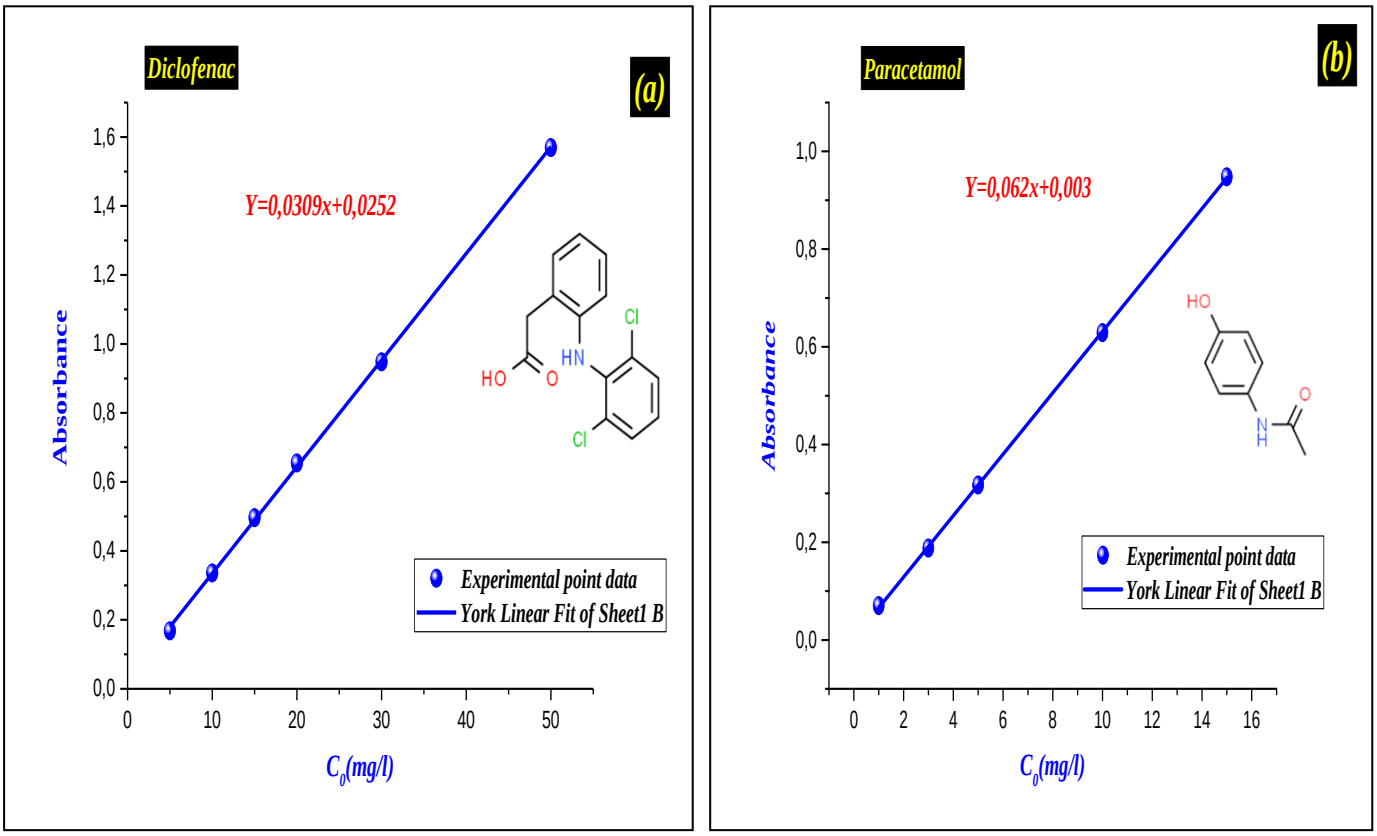


**Figure III. 3.a, b: C**alibration curve of DIC and PARA

In the DIC and PARA concentrations ranges up to 30 mg/l you mean Fig III. a, the curves obtained are linear and have a high correlation coefficient ($R^2$) (thus confirming the Beer-Lambert law). The results of this calibration are used to derive the residual concentration of DIC and PARA in given solutions by substituting its absorbance into the equation **($A = \varepsilon \times l \times c$).**

### III. 2. 3- Parameters Effect

#### III. 2. 3. 1. Influence of pH on the adsorption of DIC

The DIC and PARA adsorption efficiency were investigated by changing the pH from (3 to11) using hydrochloric acid solution HCl (0.1N) or NaOH (0.1N), depending on the desired pH. Below these pH conditions, a mass of 0.06 g of adsorbent was stirred in 60 ml of PARA with 20 mg/l and DIC solution in the single system. The results obtained during these tests are shown in Figure III. 4. The adsorption capacity of DIC and PARA adsorbent is given by the following formula:

$$q_e = \frac{(c_0 - c_e)v}{m} \qquad \text{(III. 1)}$$

Figure III. 4 (a) demonstrates how solution pH affects DIC adsorption on PS700. It is obvious that the pH value (which ranges from 3 to 10) affects the adsorption efficiency. A lower pH value increases the quantity of DIC adsorbed at equilibrium. The PS700 adsorbent's surface need to be positively charged (pHpzc = 6.3). Thus, the electrostatic attraction contributes in the uptake of $C_{14}H_{10}CL_2NNaO_2^-$, because the biochar's surface charge is mostly positive and the DIC molecule is neutral at pH 3 (pka= 4.15).

Figure III. 4 (b) demonstrates how the pH of the medium affects the adsorption of PARA onto PS700. Clearly, the pH range (pH 3 to 10) affects the adsorption efficiency. With a falling pH value, the amount of PARA adsorbed at equilibrium increases. Adsorbent should have a positively charged surface. Due to the biochar's mostly positive surface charge and the PARA molecule's neutral pH 3 (pka=9.46), electrostatic attraction plays a role in the uptake of $C_8H_9NO_2+$.

From Figure 4 (a) and (b), it can be clearly seen that the adsorption capacity increased gradually with increasing solution pH, reaching maximum values of 12.03 and 14.95 mg/g for DIC and PARA at pH 7, respectively. The pH dependent adsorption behavior can be explained by variations in the surface charge of the adsorbent due to protonation or deprotonation mechanisms (Jung, K.-W, et al. 2018)

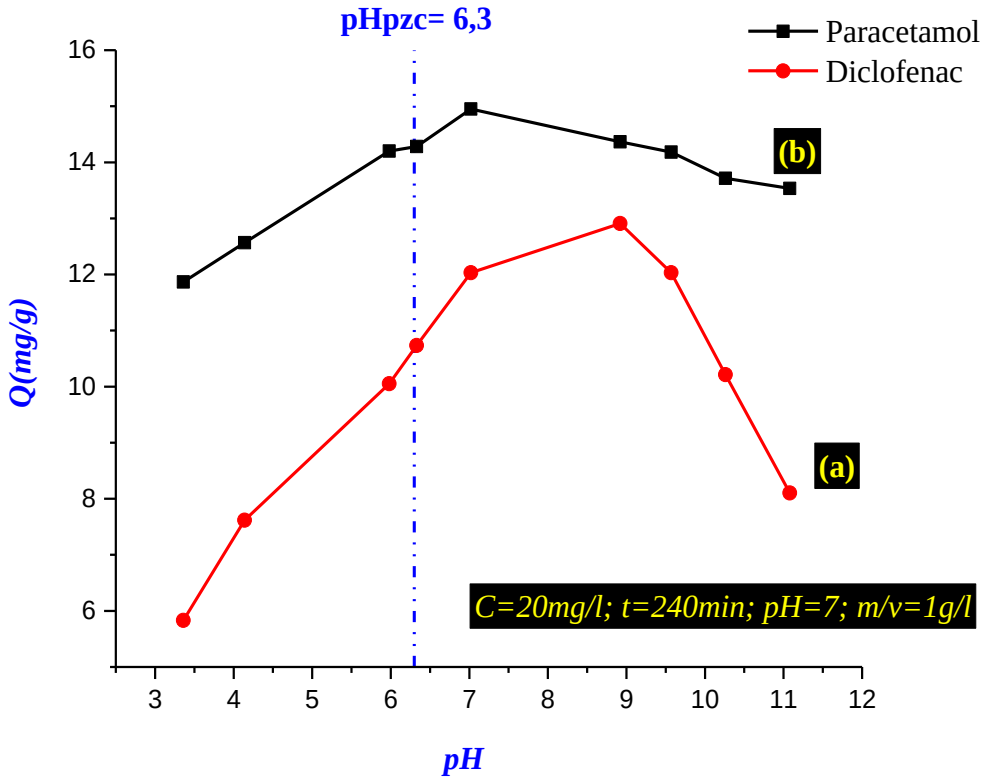


**Figure III. 4:** Effect of initial pH (a, b) on the amount of DIC and PARA adsorbed by PS700 in the single system (*m/v =1g/l, $C_0$=20mg/l, T=293k ± 2, t= 240min*).

### III. 2. 3. 2. Influence of ionic strength

The effect of ionic strength during DIC and PARA adsorption by PS700 between (0-1M) NaCl was investigated and the experimental results are shows in the Figure III 5. All materials appeared to be inhibited at low ionic strength (0- 0.2 M). When the ionic strength reaches a certain level at a certain concentration (> 0.2 M), the DIC and PARA removal ability by PS700 gradually increases with increasing NaCl concentration, this justifies that ions can penetrate the diffusion layer on the surface of PS700.

The influence of ionic strength on the adsorbed amount (*qe*, mg/g) was investigated further to understand the role of electrostatic attraction in the DIC and PARA uptake process. The capacity of DIC and PARA adsorption onto the synthesized biochar considerably varies when the ionic strength value is altered in the range of (0-1.0 M), according to the results of Figure III. 5 (a) and (b).

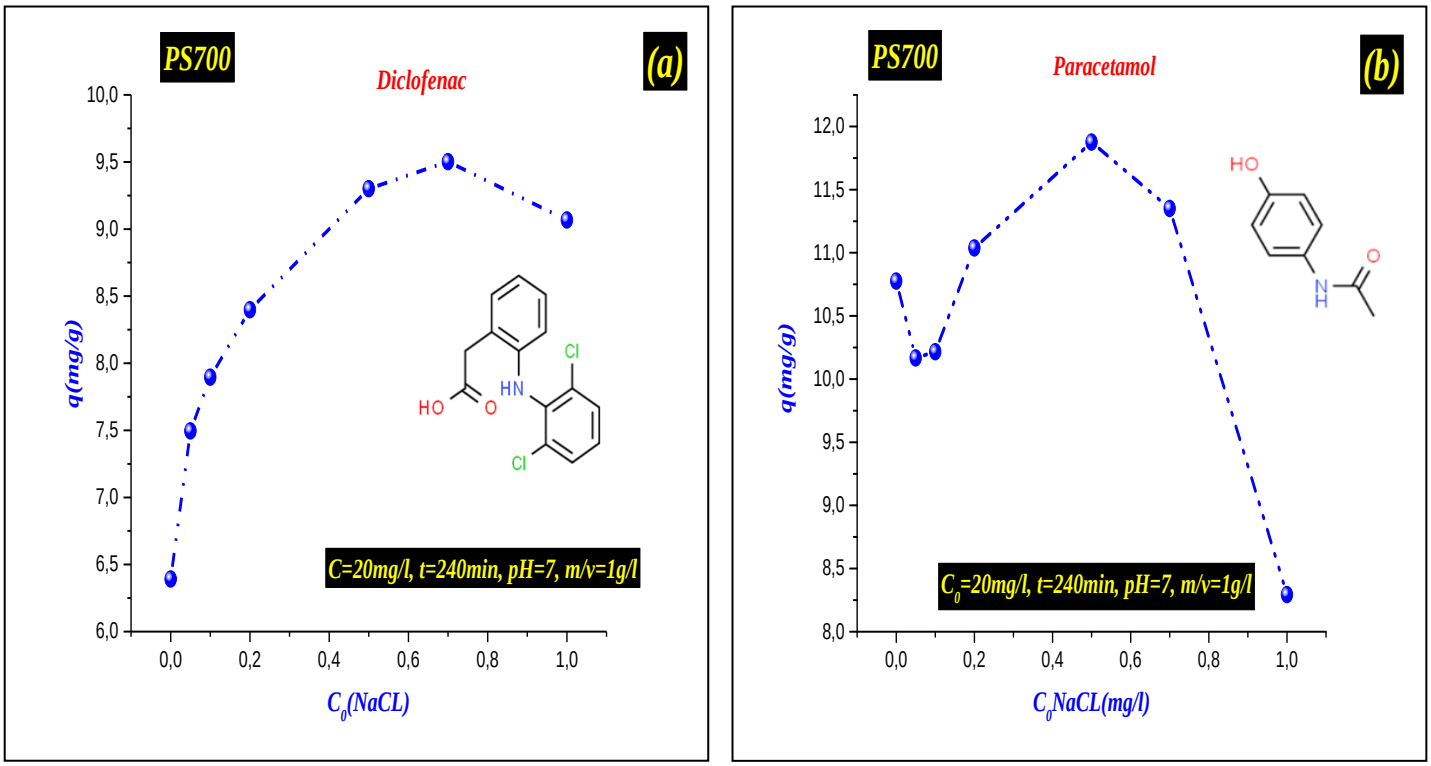


**Figure III. 5**: Influence of ionic strength DIC and PARA adsorbed (m/v = 1g/l, $C_0$ = 20mg/l, T=20°C**)**

### III. 2. 3. 3. Effects of contact time

DIC and PARA solutions tested were prepared from 500 mg/L stock solutions. 60 mg of PS700 adsorbent was placed in 100 mL Erlenmeyer flask containing 60 mL of DIC and PARA at specified concentrations in a single system. The mixture was stirred at a speed of 300 rpm for the desired time. The solution was then filtered through a 0.45 µm membrane filter and residual DIC and PARA content was detected with a UV-Vis spectrophotometer (Optizen 2120 UV model) at 276 nm and 242 nm.

Figure III. 6 show the effect of contact time on the adsorption of DIC and PARA by PS700 adsorbent. Equilibration time is one of the most important parameters in designing an economical wastewater treatment system. The results obtained show that the adsorption capacity increases with stirring time and plateaus. For maximum efficiency the adsorption rate very high during the first 10 minutes Figure III. 6 (a) and 50 minutes Figure III. 6 (b), finally reached equilibrium after approximately 120 minutes of stirring. Rapid adsorption on first contact results in

surface of the adsorbent. Subsequently, the adsorption efficiency decrease and the sites became more occupied.

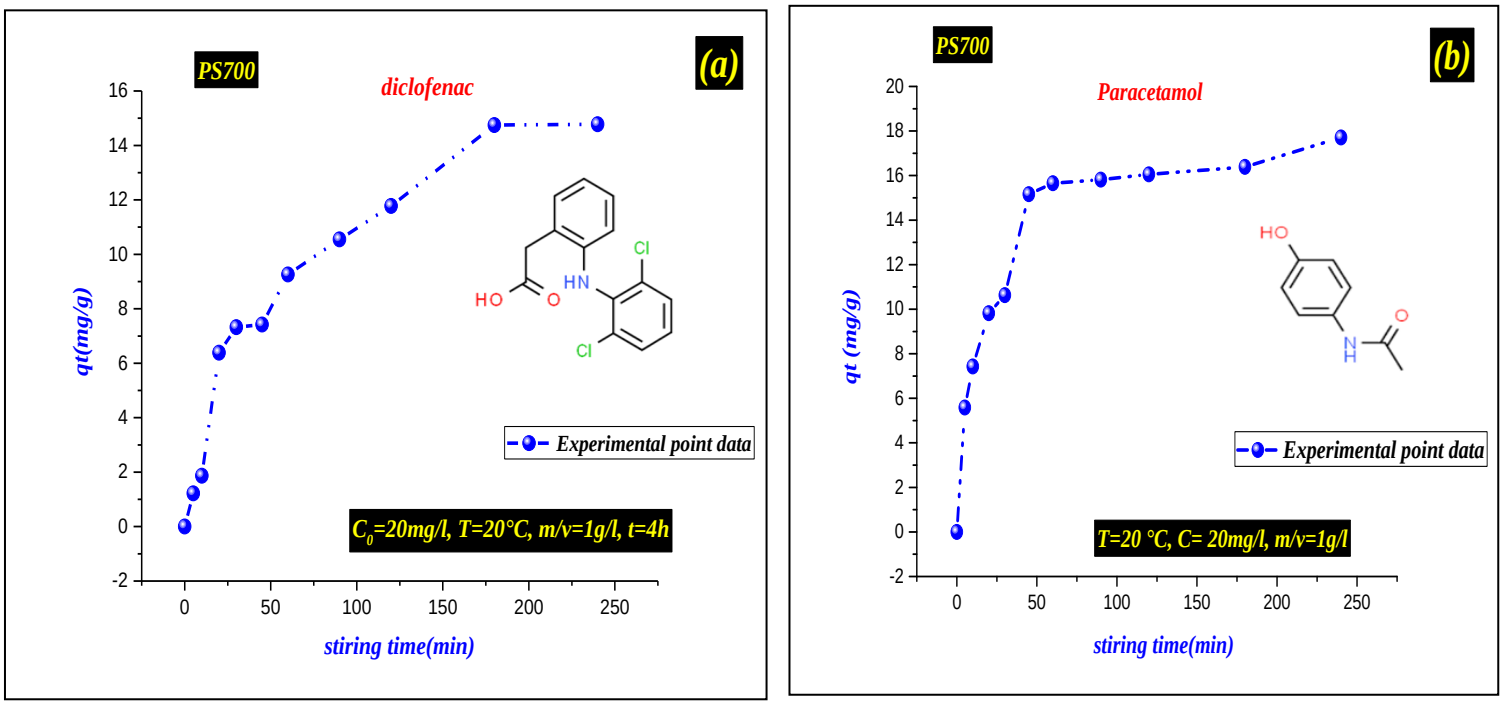


**Figure III. 6:** (a) and (b) Effect of contact time on the amount of DIC and PARA, respectively adsorbed (m/V=1g/l, $C_0$= 20 mg/l, T= 20 °C, t = 240 min).

### III. 3. Batch adsorption experiments

#### III. 3. 1. Adsorption isotherm

Experiments on adsorption are carried out in batch a state of equilibrium mode. Until the equilibrium period was reached, 60 mg of prepared samples were added to 60 ml of DIC solution or PARA solution (60 mg/L) and stirred. The starting and final concentrations of DIC or PARA in liquid phases were measured with an ultraviolet spectrophotometer (Optizen 2120 UV model) at 276 and 242 nm for DIC and PARA, respectively, and were used to calculate the amount of drugs adsorbed. On the adsorption capacity, the effects of the starting concentration, contact time, pH and adsorbent dose were investigated.

The following equations are used to compute the R% elimination:

$$R(\%) = \frac{(C_0 - C_e)}{C_0} * 100 \qquad \text{(III. 2)}$$

Where:

$C_0$: is the initial equilibrium concentration (mg/L);

$C_e$: is the equilibrium concentration (mg/L);

V: is the volume of solution (L).

m: is the mass of adsorbent(g).

Where $C_0$ and $C_e$ are the initial and equilibrium concentration (mg/l) of the adsorption solution. Also; V(L) is the volume of the solution and m(g) is the mass of the adsorbent Langmuir and Freundlich isotherm models were used to analyze the adsorption behavior of the adsorbents (Bing et al., 2017; Dai et al., 2020; Yan et al., 2020; Yang et al., 2020).

Adsorption equilibrium isotherm studies are fundamental for determining the capacity and mode of adsorption. Our goal is to identify an isotherm that best describes the adsorption of DIC and PARA by PS700 at room temperature. Experiments were performed at temperatures of 293, 303 and 313K and pH 7.

### III. 3. 1. a- Diclofenac

The equilibrium data of DIC adsorption were described using the Langmuir, Freundlich, Redlich-Peterson, and Temkin isotherm models (Figure III. 7). These models' adsorption parameters were calculated using a non-linear optimization technique. The data demonstrate that the $q_e = f(C_e)$ plot resembles the L-type (high affinity) isotherm (Giles et al., 1974), which is characterized by a high solid adsorption capacity at low concentrations. In Table 2 approximate parameters indicate that the isotherm data is more adequately described by Langmuir ($R^2$ = 0,928, $R^2$ = 0,925, $R^2$ = 0,909) and Redlich-Peterson ($R^2$ = 0,917, $R^2$ = 0,915, $R^2$ = 0,896) and Temkin ($R^2$ = 0,895; $R^2$ = 0,903; $R^2$ = 0,897) than the Freundlich ($R^2$ = 0,898, $R^2$ = 0,893, $R^2$ = 0,883) model at different temperature (293, 303 and 313k), respectively. The maximum adsorption capacity was found (400,16 mg/g; 397,40 mg/g and 382,46 mg/g) at different temperatures (293, 303, and 313k), respectively.

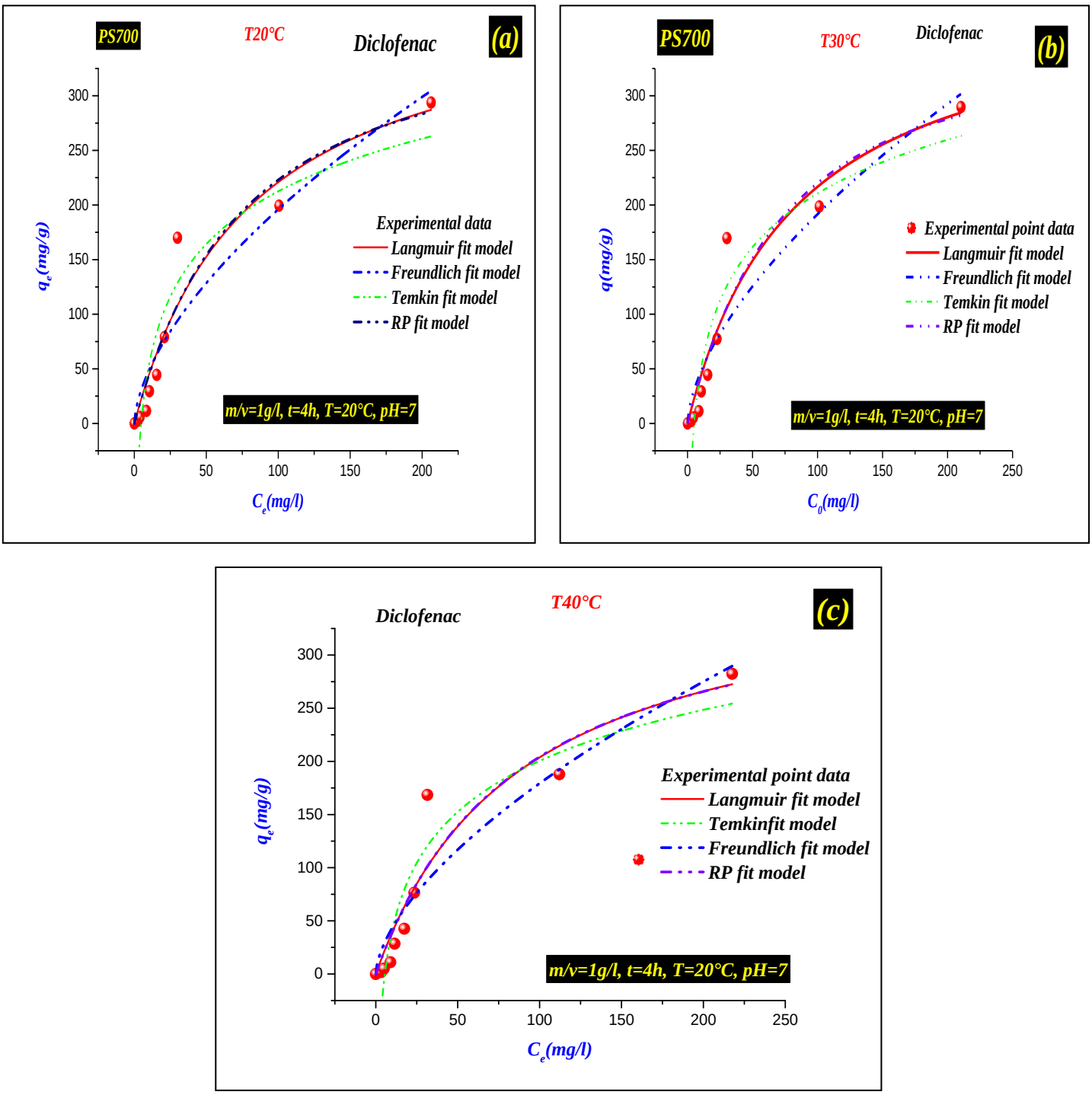


**Figure III. 7:** (a), (b), and (c) DIC adsorption isotherm on PS700 adsorbent and fitting curves of isothermal models

**Table III. 2:** Isothermal constant parameters for DIC adsorption on PS700 adsorbent.

| Model | Unit | Value | | | Standard Error | | |
|---|---|---|---|---|---|---|---|
| **Langmuir** | | **293** | **303** | **313** | **293** | **303** | **313** |
| $Q^0_{max}$ | mg/g | 400,16582 | 397,4080 | 382,46603 | 68,60547 | 69,72494 | 74,7234 |
| $K_L$ | L/mg | 0,01232 | 0,01199 | 0,0114 | 0,00463 | 0,00458 | 0,00487 |
| $R^2$ | — | **0,92805** | **0,92525** | **0,90957** | — | — | — |
| $\chi^2$ | — | — | — | — | — | — | — |
| **Freundlich** | | | | | | | |
| $K_F$ | (mg/g)/(mg/ | 11,85276 | 11,5065 | 10,47264 | 5,37939 | 5,36574 | 5,27029 |
| $n_F$ | — | 1,64149 | 1,63738 | 1,62127 | 0,25513 | 0,25999 | 0,27247 |
| $R^2$ | — | 0,89838 | 0,89317 | 0,8834 | — | — | — |
| $\chi^2$ | — | | | | | | |
| **Redlich–** | | | | | | | |
| $K_{RP}$ | L/g | 4,77816 | 4,5442 | 4,33223 | 2,16687 | 1,99365 | 2,40779 |
| $a_{RP}$ | $(mg/L)^{-g}$ | 0,00891 | 0,0072 | 0,01062 | 0,03344 | 0,02772 | 0,04713 |
| **G** | — | 1,05408 | 1,08514 | 1,01185 | 0,61047 | 0,62997 | 0,70865 |
| $R^2$ | — | 0,91795 | 0,915 | 0,89666 | | | |
| $\chi^2$ | — | | | | | | |
| **Temkin** | | | | | | | |
| **A** | | 0,21163 | 0,19557 | 0,18084 | 0,04755 | 0,04096 | 0,03894 |
| **B** | | 69,62897 | 70,83224 | 69,24814 | 8,26885 | 8,03478 | 8,14243 |
| $R^2$ | | 0,89533 | 0,90364 | 0,89717 | | | |
| $\chi^2$ | | | | | | | |

### III. 3. 1. b- Paracetamol

This study described the equilibrium data of PARA adsorption using the Langmuir, Freundlich, Redlich-Peterson, and Temkin isotherm models (Figure III 8). These models' adsorption values were calculated using a nonlinear optimization approach. The high solid adsorption capacity at low concentrations is an isotherm attribute. The estimated values in Table 3 show that Langmuir's description of the isotherm data is more accurate. ($R^2$ = 0,928, $R^2$ = 0,925, $R^2$ = 0,909) and Temkin ($R^2$ = 0,959; $R^2$ = 0,971; $R^2$ = 0,942) than the Freundlich ($R^2$ = 0,898, $R^2$ = 0,893, $R^2$ = 0,883) and Redlich-Peterson ($R^2$ = 0,917, $R^2$ = 0,915, $R^2$ = 0,896) model at different temperature (293, 303 and 313k), respectively.

Furthermore, using the Langmuir equation, the calculated maximum adsorption capacities ($Q_{0\ max}$) for the PS700 asdsorbent were found to be 411,99 mg/g, 383,33 mg/g and 365,055 mg/g, respectively. The outstanding performance of this preparation demonstrates the adsorbent in removing DIC. From water the results of the effect of temperature on PARA adsorption are shown in Figure III 13. Since then the adsorption capacity of PARA increased from 411.99 as the solution temperature increased from 293K to 313K 383.33 and 365.05 mg. $g^{-1}$ for PS-biochar.

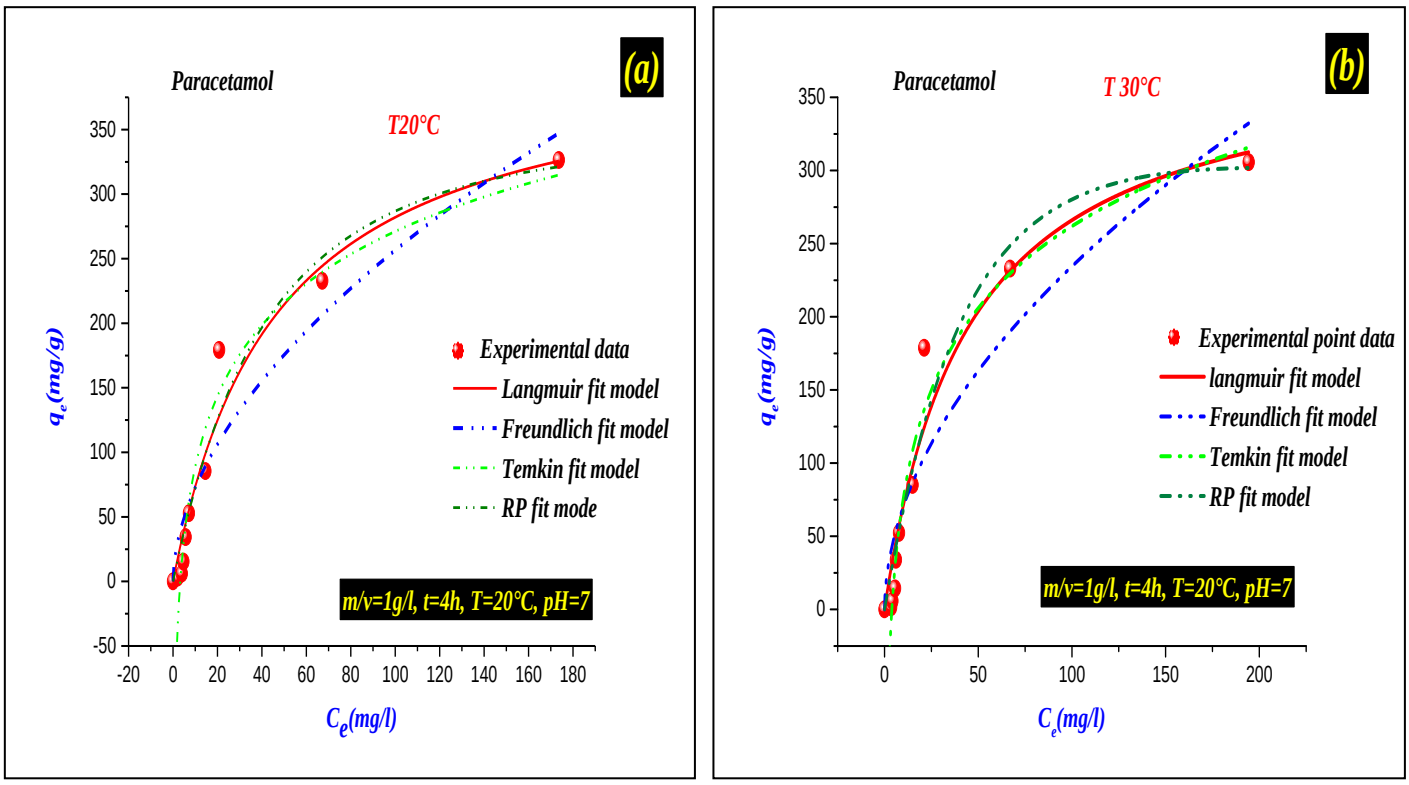

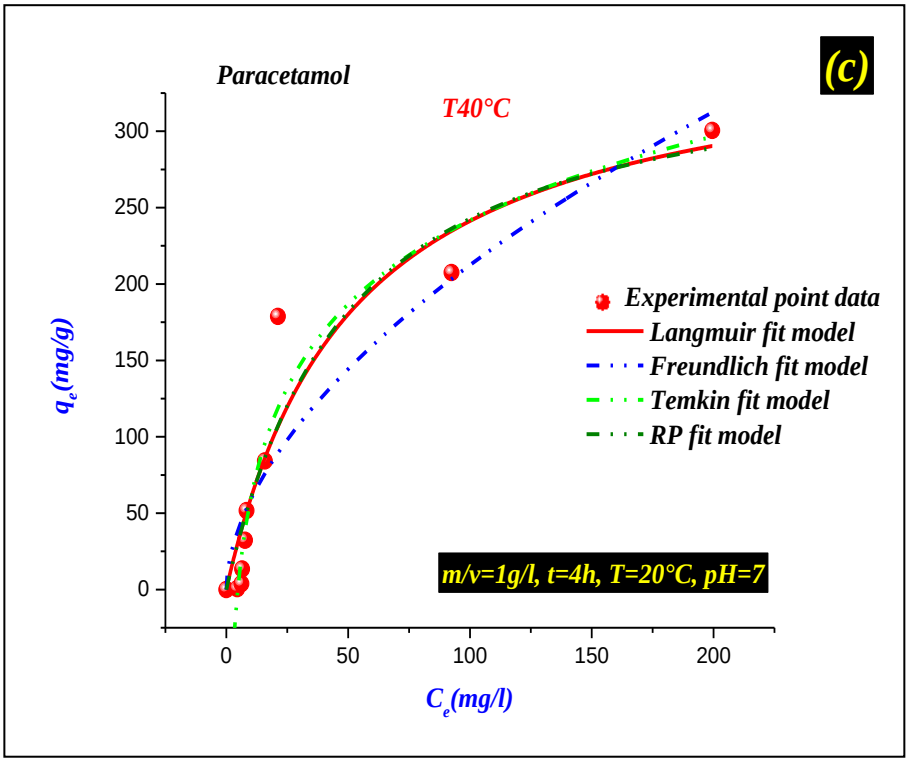


**Figure III. 8:** PARA adsorption isotherm on PS700 and fitting curves of isothermal models

**Table III. 3:** Isothermal constant parameters for PARA adsorption on PS700.

| Model | Unit | Value | | | Standard Error | | |
|---|---|---|---|---|---|---|---|
| **Langmuir** | | **293** | **303** | **313** | **293** | **303** | **313** |
| $Q^o_{max}$ | mg/g | 411,99 | 383,33 | 365,055 | 45,02472 | 45,43095 | 59,64192 |
| $K_L$ | L/mg | 0,0217 | 0,02267 | 0,01948 | 0,00574 | 0,00656 | 0,00786 |
| $R^2$ | — | 0,95638 | 0,94091 | 0,89721 | — | — | — |
| $\chi^2$ | — | | | | — | — | — |
| **Freundlich** | | | | | | | |
| $K_F$ | $(mg/g)/(mg/L)^{-1/n}$ | 20,55619 | 20,95762 | 16,22886 | 7,40312 | 8,58351 | 7,6678 |
| $n_F$ | — | 1,8243 | 1,90702 | 1,79068 | 0,26228 | 0,32172 | 0,32055 |
| $R^2$ | — | 0,90503 | 0,8639 | 0,85714 | — | — | — |
| $\chi^2$ | — | | | | — | — | — |
| **R-** | | | | | | | |
| $K_{RP}$ | L/g | 8,25606 | 7,37623 | 6,98401 | 2,47857 | 1,95895 | 3,4697 |
| $a_{RP}$ | $(mg/L)^{-g}$ | 0,01136 | 0,0051 | 0,01644 | 0,02305 | 0,0107 | 0,05222 |
| G | — | 1,10916 | 1,25255 | 1,02882 | 0,33668 | 0,35361 | 0,51343 |
| $R^2$ | — | 0,95139 | 0,94061 | 0,88262 | — | — | — |

| | | | | | | | |
|---|---|---|---|---|---|---|---|
| $\chi^2$ | — | | | | — | — | — |
| **Temkin** | | | | | | | |
| **A** | | 0,30644 | 0,25619 | 0,21167 | 0,0413 | 0,02763 | 0,03175 |
| **B** | — | 79,23347 | 80,76645 | 79,17906 | 5,65895 | 4,85354 | 6,80006 |
| $\mathbf{R^2}$ | — | 0,95956 | 0,9711 | 0,94261 | — | — | — |
| $\chi^2$ | — | | | | | | |

## III. 3. 2- Kinetic behaviors

The adsorption capacity $q_t$ at any time point (t) can be calculated using the following formula (Ma et al., 2019; Zhang et al., 2019).

$$q_t = \frac{(c_0 - c_t)}{m} \qquad \text{(III. 4)}$$

Where $C_0$ and $C_t$ (mg/L) represent the DIC concentration at the beginning and each time point (t), respectively and v (L) represents the volume of the solution, m (g) represents mass adsorbent.

### III. 3. 2.1 Kinetic behaviors Diclofenac

The fitting results are shown in Table 4. The correlation coefficients PSO model was high, but the correlation coefficient of the pseudo nonlinear models less Which is more suitable for describing the adsorption kinetics of DIC on PS700. Furthermore, the Qe value is theoretical values calculated by a PSO model. The PSO ($R^2$ = 0,972, $R^2$ = 0,956, $R^2$ = 0,959) and Elovich ($R^2$ = 0,862, $R^2$ = 0,985, $R^2$= 0,959) models in the concentration 20, 40, 80 mg/l had better describe the kinetic data than the PFO model, based on the correlation coefficient $R^2$ Table 4. The calculated value of the adsorption capacity ($q_{ecal}$ = 18, 03 mg/g, $q_{ecal}$ = 26, 36mg/g, $q_{ecal}$ =56, 13mg/g).

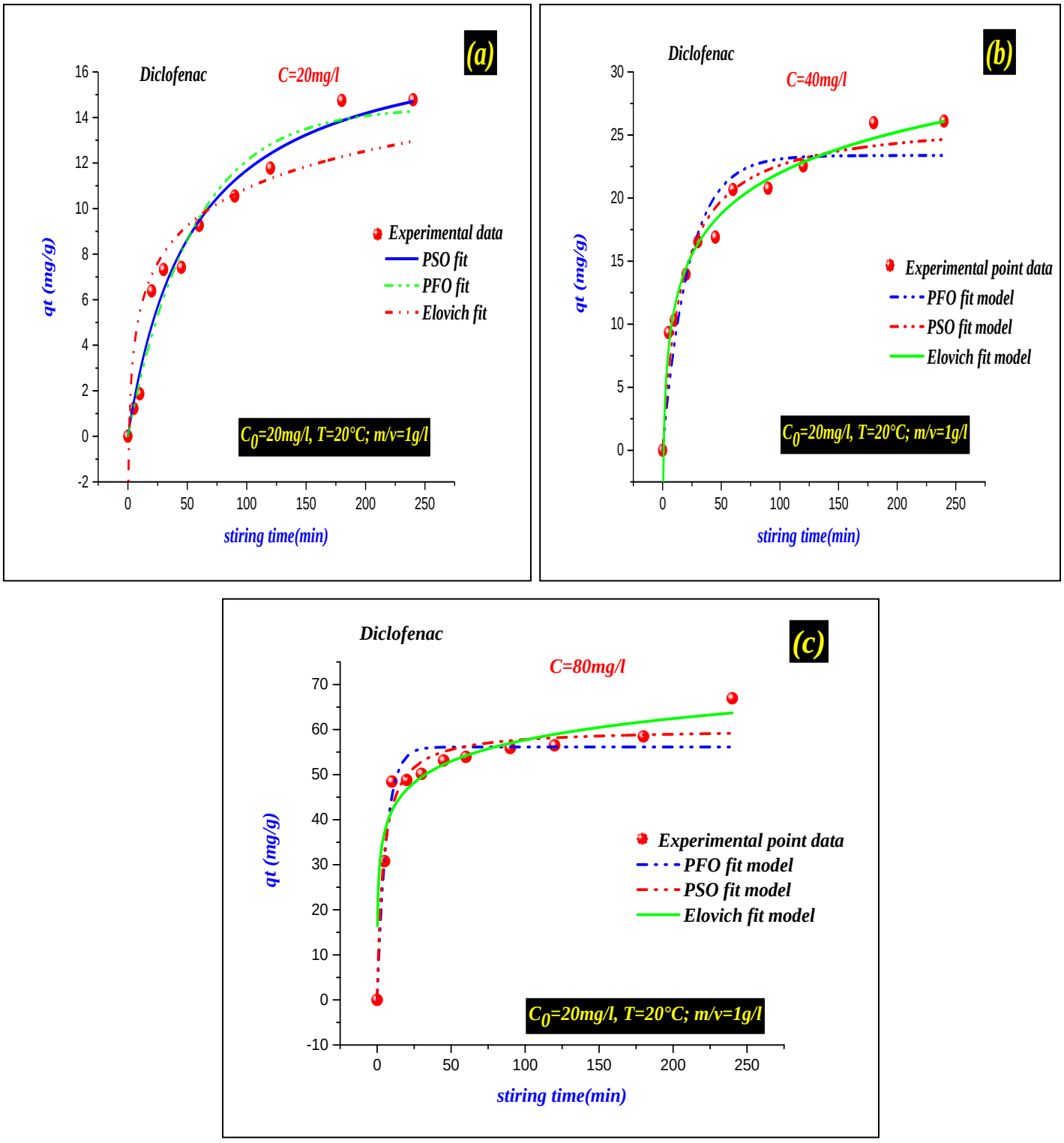


**Figure III. 9:** the effect of contact time and nonlinear adjustment of the PFO, PSO and Elovich kinetic models

Table 4 shows the model parameters for the adsorption of DIC on PS700. The results show a higher ($R^2$ = 0.972) at the concentration of 20mg/l.

**Table III. 4:** Kinetic parameters of DIC adsorption on PS700 at $C_0$ = 20 mg/, 40mg/L and 80mg/l.

| Model | Paramètre | Unit | Value | | | Standard Errer | | |
|---|---|---|---|---|---|---|---|---|
| **Experiment** | $q_{exp}$ | **mg/g** | **20** | **40** | **80** | **E1** | **E2** | **E3** |
| **PFO** | $k_1$ | L/min | 0,01814 | 0,04418 | 0,16327 | 0,00269 | 0,00883 | 0,0307 |
| | $q_e$ | mg/g | 14,45217 | 23,37538 | 56,13086 | 0,81495 | 1,26184 | 1,76242 |
| | $R^2$ | — | 0,95981 | 0,89692 | 0,93033 | — | — | — |
| | $\chi^2$ | — | — | — | — | — | — | — |
| **PSO** | $k_2$ | g/mg×min | 0,00102 | 0,00227 | 0,16327 | 2,4607E-4 | 5,2356E-4 | 0,0307 |
| | $q_e$ | mg/g | 18,03162 | 26,36887 | 56,13086 | 1,19926 | 1,21749 | 1,76242 |
| | $R^2$ | — | 0,97291 | 0,956 | 0,95995 | — | — | — |
| | $\chi^2$ | — | | | | | | |
| **Elovich** | a | | 1E-14 | 0,47455 | 26,19176 | 0 | 1,0077 | 3,84392 |
| | b | | 2,36385 | 4,67258 | 6,84234 | 0,15093 | 0,25204 | 0,9614 |
| | $R^2$ | — | 0,86213 | 0,98554 | 0,95995 | — | — | — |
| | $\chi^2$ | — | | | | | | |

### III. 3. 2. 2 Kinetic behaviors Paracetamol

According to the results shown in Table 5, the model is the PSO rissuitable for determining the order of adsorption kinetics by PARA by PS700. This is because the correlation coefficient is very high. Similarly, according to the value $q_e$ quoted in Table 5 (calculated according to a PSO model), Note that they are very close to those determined experimentally. Result A similar finding can be found in (Llado, Jet al., 2015). The PSO ($R^2$ = 0,973, $R^2$ = 0,941, $R^2$ = 0,983) and Elovich ($R^2$ = 0,959, $R^2$ = 0,983, $R^2$ = 0,994) models in the concentration 20, 40 and 80 mg/l had better describe the kinetic data than the PFO model, based on the correlation coefficient ($R^2$) values Table 5. The value of the adsorption capacity ($q_{ecal}$ =18, 42 mg/g, $q_{ecal}$ = 29,30 mg/g, $q_{ecal}$ = 61, 15 mg/g).

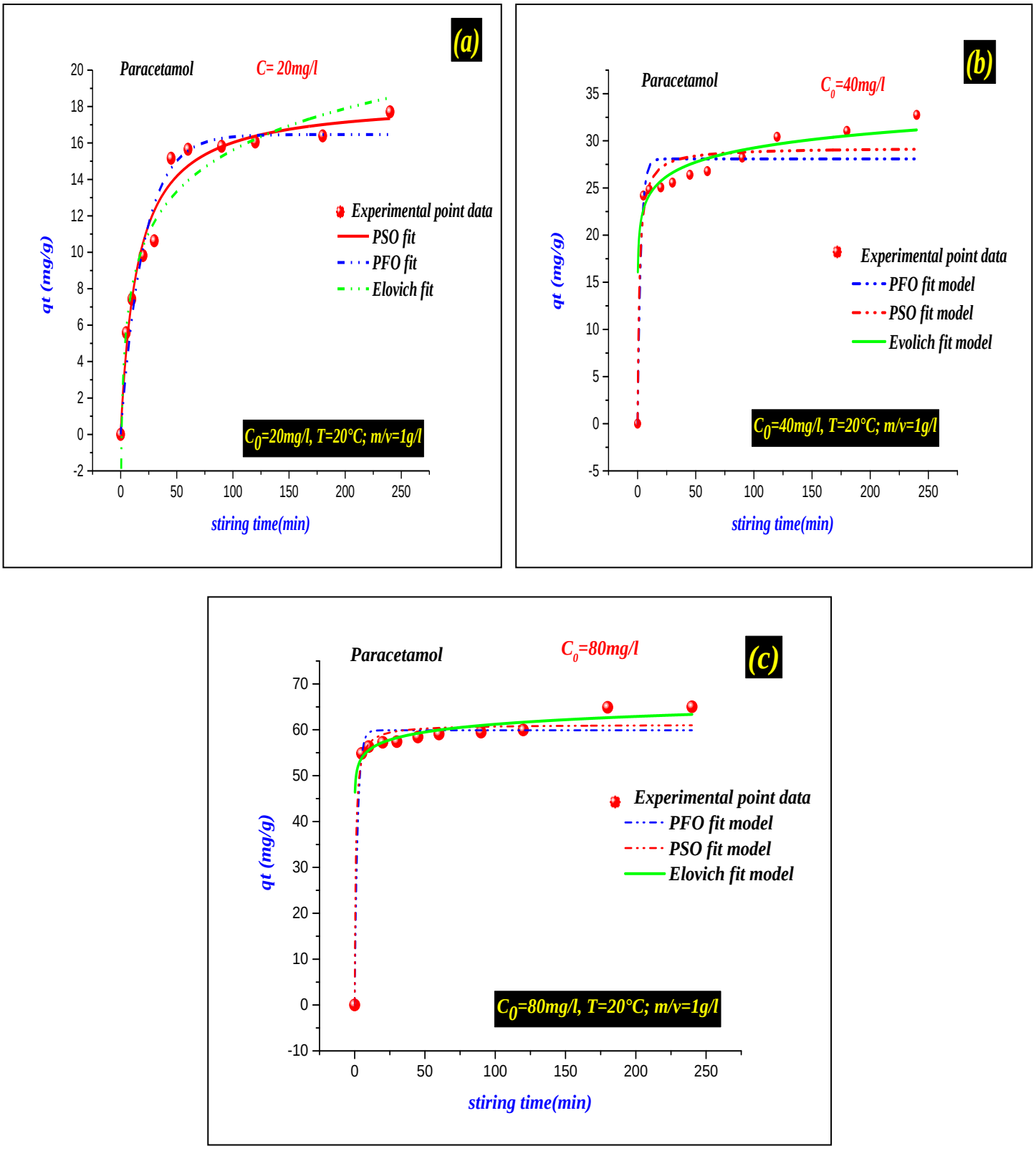


**Figure III. 10:** (a), (b) and (c) the effect of contact time and nonlinear adjustment of the PFO, and PSO kinetic models,

Table 5 shows the model parameters for the adsorption of PARA on PS700. The results show a higher ($R^2$ = 0,983) at the concentration of 80 mg/l

**Table III. 5:** Kinetic parameters of PARA adsorption on PS700 adsorbent.

| Model | Paramètre | Unit | Value | | | Standard Errer | | |
|---|---|---|---|---|---|---|---|---|
| **Experiment** | $q_{exp}$ | **mg/g** | **20** | **40** | **80** | **E1** | **E2** | **E3** |
| **PFO** | $k_1$ | L/min | 0,04859 | 0,35474 | 0,47276 | 0,00624 | 0,11292 | 0,10918 |
| | $q_e$ | mg/g | 16,46504 | 28,0811 | 59,88532 | 0,55054 | 0,91123 | 0,99325 |
| | $R^2$ | — | 0,95917 | 0,9093 | 0,97412 | — | — | — |
| | $\chi^2$ | — | | | | | | |
| **PSO** | $k_2$ | g/mg× min | 0,00362 | 0,02149 | 0,02196 | 6,49171E-4 | 0,0089 | 0,00806 |
| | $q_e$ | mg/g | 18,42463 | 29,30051 | 61,15968 | 0,64227 | 0,91733 | 0,98008 |
| | $R^2$ | — | 0,97393 | 0,94192 | 0,98315 | — | — | — |
| | $\chi^2$ | — | | | | | | |
| **Elovich** | a | | 0,48964 | 19,20294 | 49,9048 | 1,21107 | 1,18795 | 1,43776 |
| | b | | 3,28393 | 2,18127 | 2,45383 | 0,3029 | 0,29712 | 0,3596 |
| | $R^2$ | — | 0,95923 | 0,98371 | 0,99444 | — | — | — |
| | $\chi^2$ | — | | | | | | |

## III. 4- Thermodynamic behaviors

Effects of temperature and interactions thermodynamic processes between biochar and DIC were investigated at varying temperatures from (293 to 313K). A detailed description is provided in the supplementary material (Mariene, R. Cunha, et al, 2020). The ΔH and ΔS values of DIC and PARA on PS-biochar were determined graphically by plotting Ln $K_c$ as a function of 1/T. The results in Table 6 indicate that the Gibbs free energy is negative (ΔG < 0), suggesting that the DIC and PARA adsorption process are spontaneous and favorable in the temperature range examined. ΔG values are between (-20 and 0 kJ/mol. K) Indicating that the process is dominated by physic-sorption (i.e. π-π interaction, Pore filling, hydrogen bonding) (Shikuku, V. O et al., 2018, Cazetta, A. L et al, 2016; Sharma, P et al., 2013).

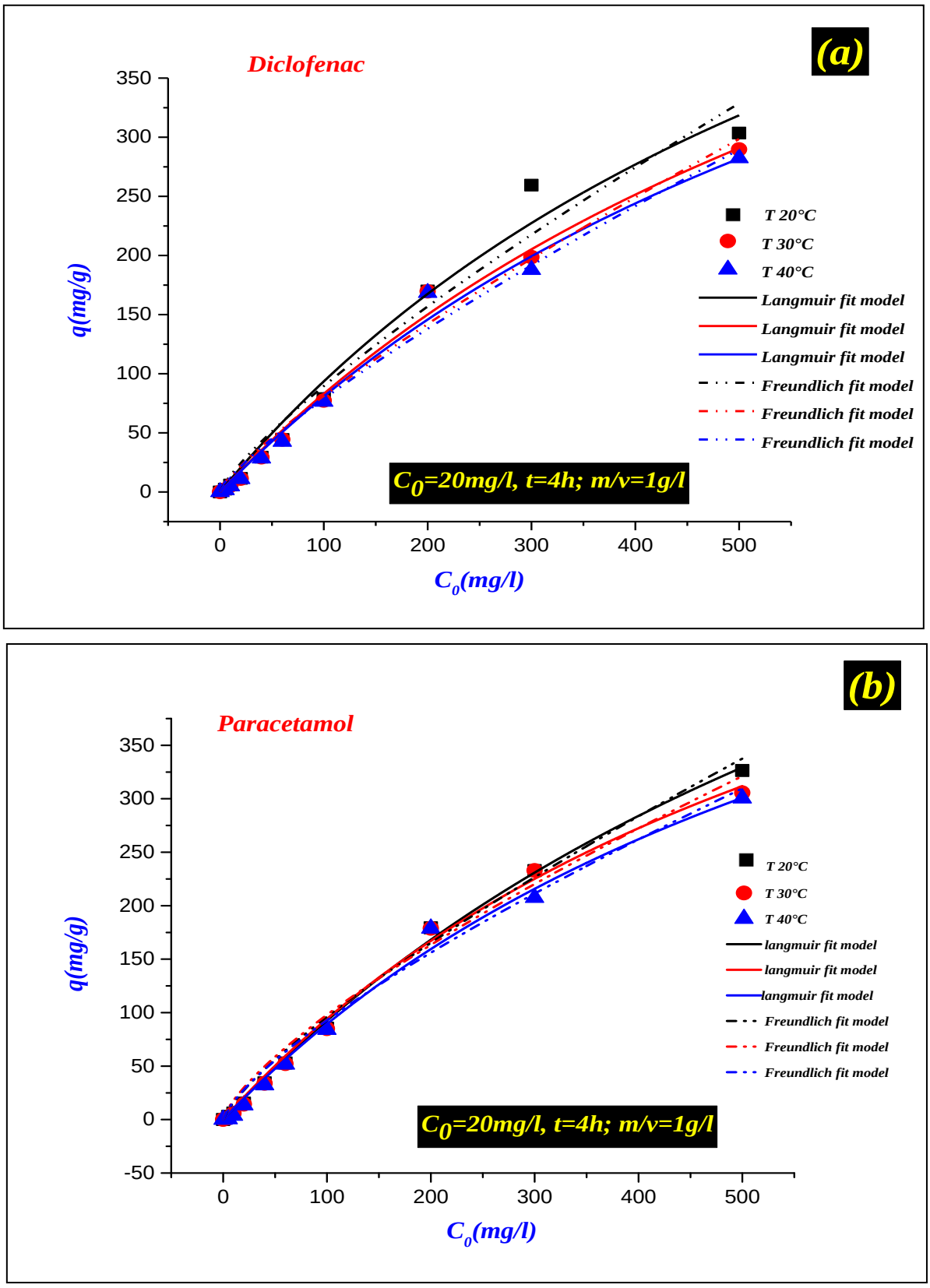


**Figure III. 11:** (a) and (b) are isothermal fittings for PARA and DIC adsorption in the single system at different temperatures on PS700 ($m/V$ = 1 g/L, pH = 7.0, $t$ = 4 h)

The values of changes in Enthalpy (ΔH) and Entropy (ΔS) of adsorption were calculated using the nonlinear Van't Hoff equation since, according to (Lima et al. 2020) linear Van't Hoff equation commonly used in most work on thermodynamics, the values of ΔH and ΔS are low compared to same value as the non-linear approach see in Figure III 12.

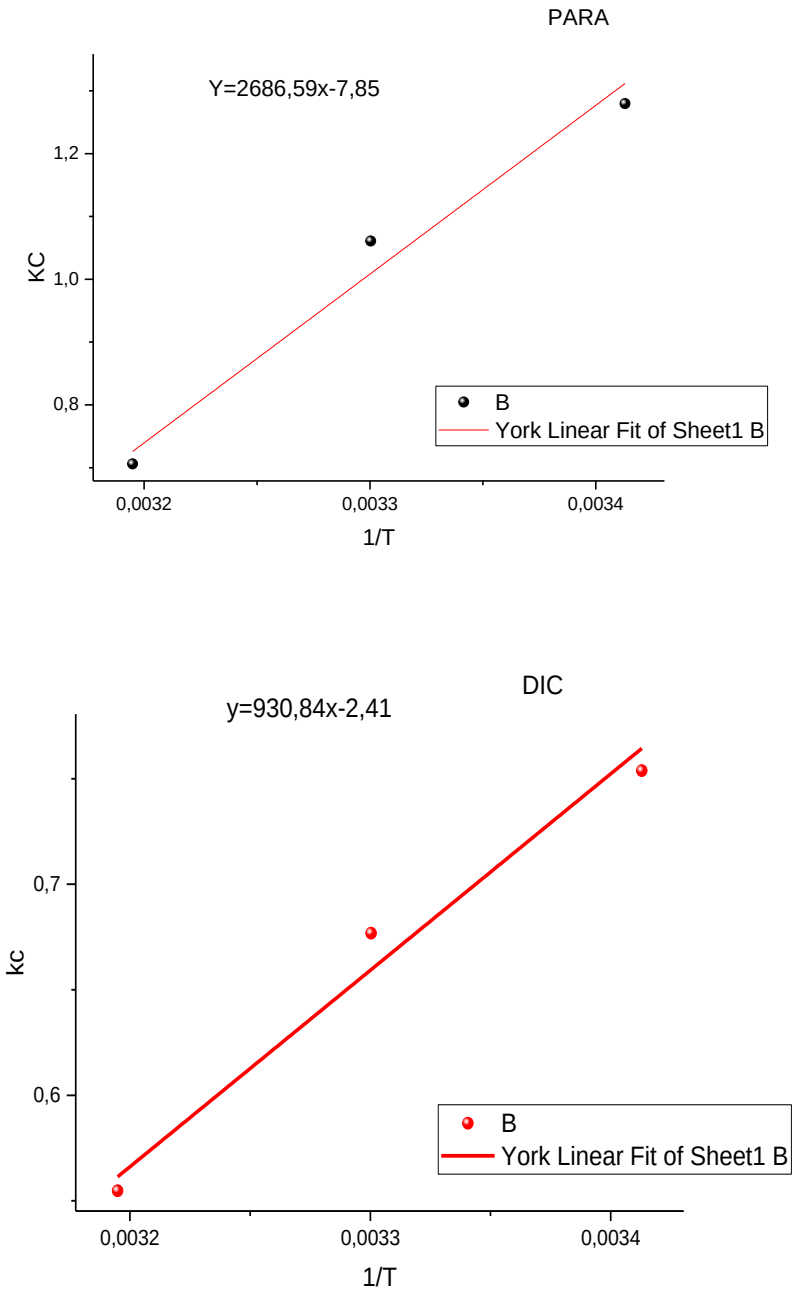


**Figure III. 12**: (a) and (b) Van't Hof plots for adsorption of DIC and PARA onto PS-biochar (Lima, E. C et al., 2019).

Thermodynamic equilibrium constants were obtained from the Liu isotherm model, for temperatures in the range (293– 313K). The change in Gibbs free energy was ($\Delta G < 0$) in the selected temperature range Table 6 (Mariene, R. Cunha, et al, 2020).However, there are some studies that report the PARA adsorption process on activated carbons being exothermic (Terzyk A. P and Rychlicki, G., 2000) and (L.. Cotoruelo, M et al., 2011).

**Table III. 6:** Thermodynamic parameters of DIC and PARA adsorption by PS700 at different temperatures.

| Single system | T | Qmax(mg/g) | van 't Hoff equation | ΔS (J/mol) | ΔH (kJ/mol) | ΔG (kJ/mol) |
|---|---|---|---|---|---|---|
| **DIC** | 293 | 400,16 | Y=930,84x-7,43 | 61,773 | -7.739 | -25.838 |
| | 303 | 397,40 | | | | -26.456 |
| | 313 | 382,46 | | | | -27.073 |
| **PARA** | 293 | 411,99 | y=2686,59x-7,85 | 65,264 | -22.336 | -41.458 |
| | 303 | 383,33 | | | | -42.111 |
| | 313 | 365,05 | | | | -42.764 |

## III. 6. Regenerative potential of PS700

The regeneration performance of biochar materials is very important in evaluating the adsorption performance. Therefore, we investigated the regeneration adsorption capacity of PS700. Ultrasonic vibration was used to desorb the adsorbed material in the NaOH solution. The results for 4 cycles are shown in Figure III 16. The results show that the adsorption capacity decreased slightly after regeneration, and the $q_e$ of PS700 after 4cycles, indicating its excellent stability and potential as an adsorbent.

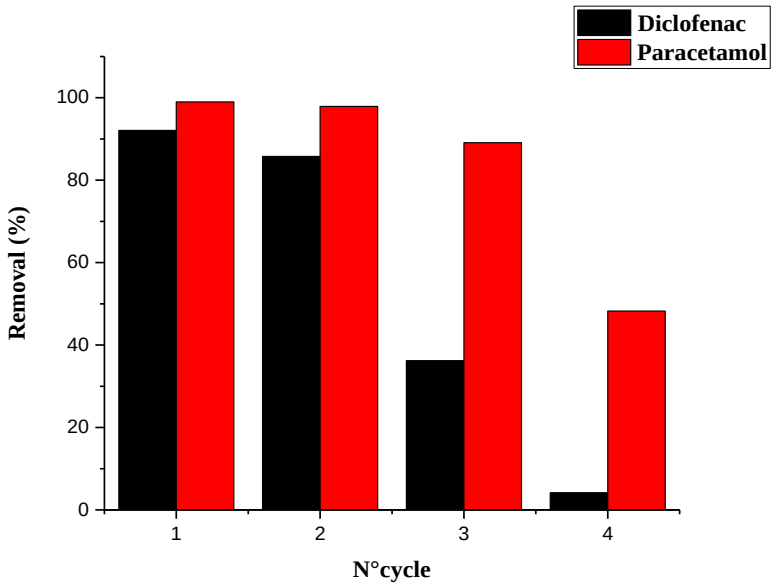


**Figure III. 13:** Reuse and regeneration tests of prepared PS700 adsorbent.

## Conclusion

The results obtained in this study demonstrate that PS700 is a highly efficient adsorbent for Diclofenac and Paracetamol adsorbents and has high adsorption capacity for these contaminants

- ✓ The surface of PS700 adsorbent should be positively charged. Thus, the electrostatic attraction contributes in the uptake of $C_{14}H_{10}CL_2NNaO_2^-$, because the biochar's surface charge is mostly positive and the DIC molecule (pka= 4.15). Thus, the electrostatic attraction contributes in the uptake of $C_8H_9NO_2^+$, because the biochars' surface charge is mostly positive and the PARA molecule (pka= 9.46). The pH dependent adsorption behavior can be explained by variations in the surface charge of the PS-biochar adsorbent due to protonation or deprotonation mechanisms.

- ✓ The isotherm data is more adequately described by and Redlich-Peterson and Temkin than the Freundlich model at different temperature (293, 303 and 313k), respectively. The maximum adsorption capacity was found (400,16 mg/g; 397,40 mg/g and 382,46 mg/g) at different temperatures (293, 303, and 313k), respectively.

- ✓ The isotherm data is more adequately described by Langmuir and Temkin than the Freundlich and Redlich-Peterson model at different temperature (293, 303 and 313k), respectively. The calculated maximum adsorption capacities ($Q_{0\ max}$) for the PS700 adsorbent were found to be 411,99 mg/g, 383,33 mg/g and 365,055 mg/g, respectively.

- ✓ The model is the PSO rissuitable for determining the order of adsorption kinetics PARA and DIC by PS700. The PSO and Elovich (models in the concentration 20, 40 and 80 mg/l.

- ✓ The Gibbs free energy is negative ($\Delta G < 0$), suggesting that the DIC and PARA adsorption process are spontaneous and favorable in the temperature range examined and the process is dominated by physic-sorption (i.e. $\pi$-$\pi$ interaction, Pore filling, hydrogen bonding).

- ✓ We investigated the regeneration adsorption capacity of PS700 Ultrasonic vibration was used to desorb the adsorbed material in the NaOH solution. The results for 4 cycles. the results show that the adsorption capacity decreased slightly after regeneration

# **Chapter IV:** Adsorption of Diclofenac and Paracetamol in the binary system

# IV. INTRODUCTION

This chapter consist, PS700 adsorbent to remove DIC and PARA from aqueous media in binary system adsorptions. Parameters effect, Kinetic studies, adsorption isotherm, thermodynamics studies and desorption regeneration analysis.

## IV. 1. PS700 characterization

## IV. 1. SEM and EDS Analysis

The morphological properties show clearly that the PS700 sample possesses heterogeneous pores with tunnel form. The EDS result of the elemental composition of the prepared PS700 indicates that C and O are the main elements in the PS700 composition after adsorption of (PARA+ 20 mg/l DIC). The high content of carbon **(79.33 %)** shows that the PS700 is a carbon-rich adsorbent Figure IV. 1, thus it categorized as a mesoporous carbonaceous biochar.

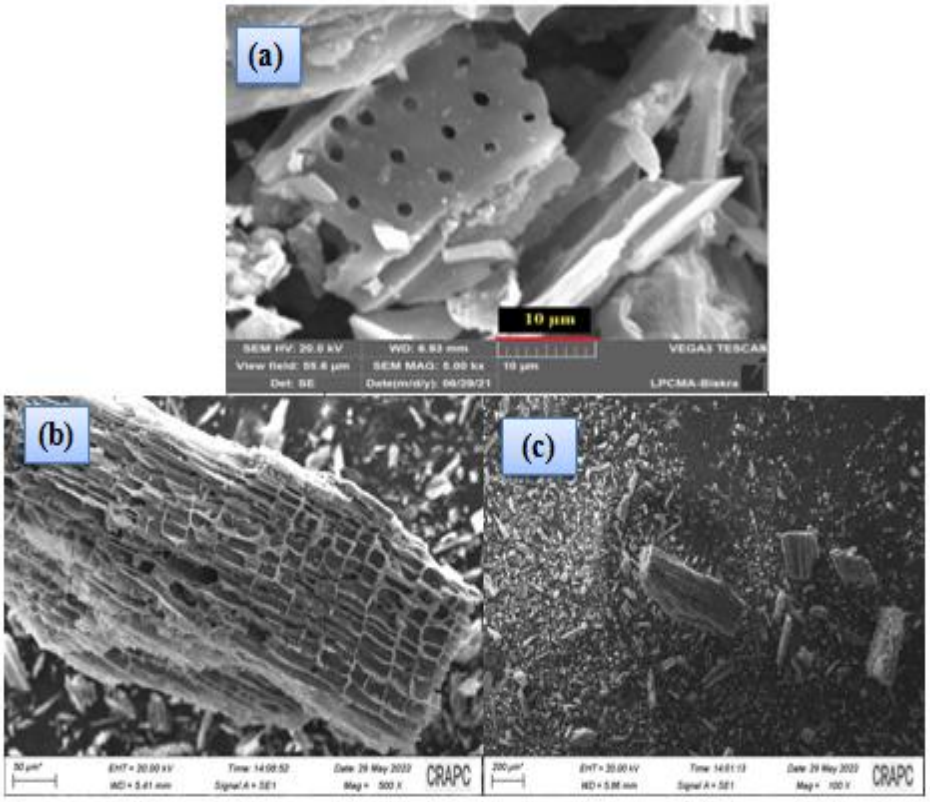


**Figure IV. 1:** (a) present the SEM of PS700 before adsorption, (b) and (c) S after adsorption of DIC and PARA, respectively, in binary system.

## I. 1. 2. 4. Fourier transforms infrared red (FTIR)

Figure IV. 2 shows the FTIR spectra of PS700 before and after of PARA and DIC adsorption in single and binary systems. Characteristic bands corresponding to functional groups commonly found in PS700 can be observed. A band at 3410 $cm^{-1}$ indicates the presence of O-H bonds in the hydroxyl groups of carboxyl's, alcohols, or phenols. The band at 1620 $cm^{-1}$ is assigned to the carboxyl asymmetric C=O vibrations. The band at 1365 $cm^{-1}$ is assigned to the C=C vibrations of aromatic rings. Finally, the band at 1120 $cm^{-1}$ could be related to the C–O bond of the hydroxyls of carboxyl's, alcohols or phenols. Changes are observed in all bands after the adsorption process. These changes indicate a possible adsorption between the DIC and PARA molecules and PS700 functional groups.

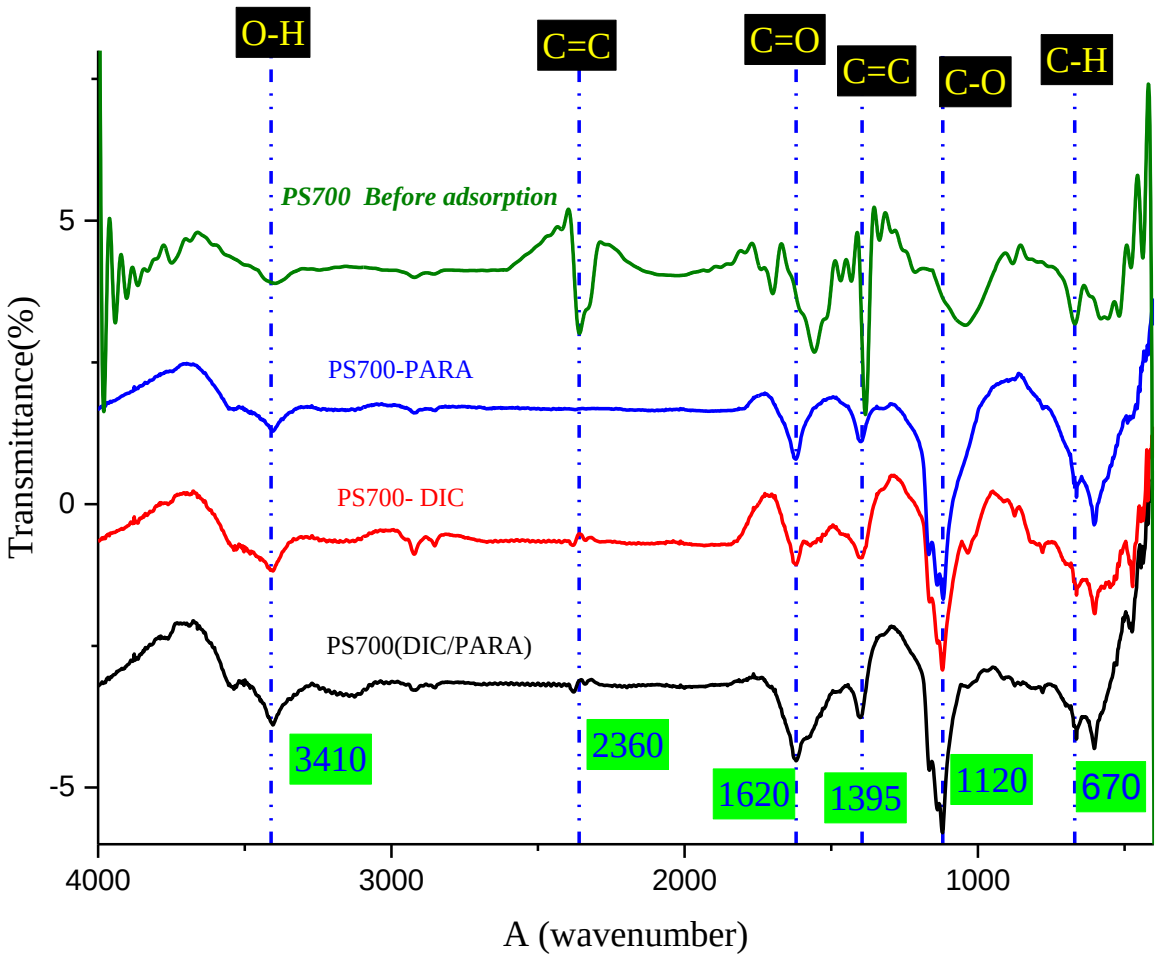


**Figure IV. 2:** Fourier transforms infrared spectroscopy (FTIR) spectra of PS700 before and after adsorption.

## IV. 2. 1- Binary adsorption

### IV. 2. 1. A) Paracetamol (PARA + 20 mg/l DIC)

Calibration performed by measuring the absorbance of solutions with (PARA + 20 mg/l DIC) concentrations from 1to 30 mg/l at wavelength ($\lambda_{1max}$ = 242 nm and $\lambda_{2\ max}$= 276 nm). The structure of the standard curve is shown in Figure IV 3.

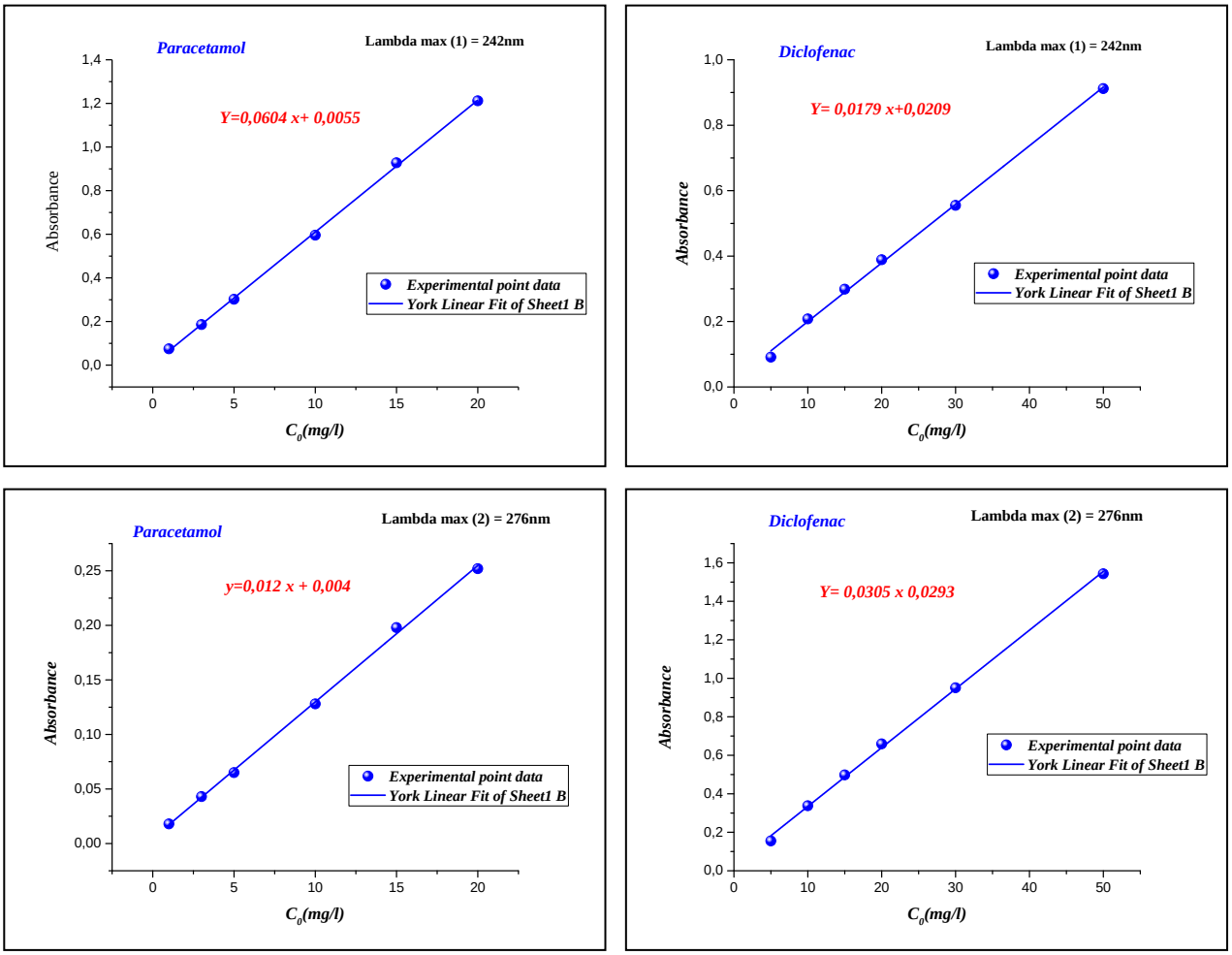


**Figure IV. 3:** Calibration Curve (PARA+ 20 mg/l DIC)

### IV. 2. 1. b. Diclofenac (DIC+20 mg/l PARA).

Calibration performed by measuring the absorbance of solutions with (DIC + 20 mg/l PARA) concentrations from1to 30 mg/l at wavelength ($\lambda_{1\ max}$= 242 nm and $\lambda_{2max}$= 276 nm). The structure of the standard curve is shown in Figure IV 4.

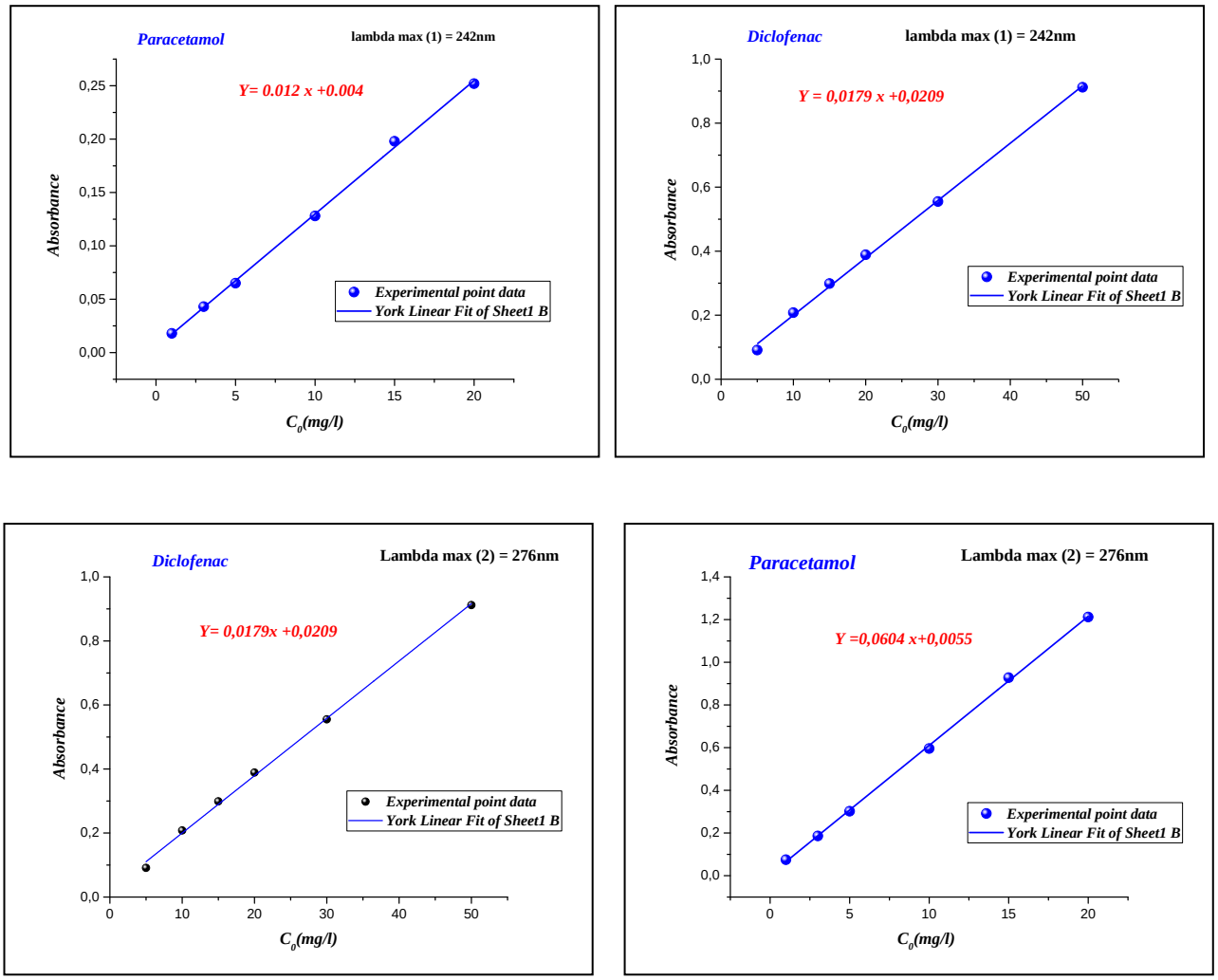


**Figure IV. 4:** Calibration curve (DIC+ 20 mg/l PARA)

The first step is to fix each time one of the concentrations, the concentration of DIC varied from (10 - 400 mg/l) with PARA (20 mg/l). the second step, the concentration of DIC was set at 20 mg. $L^{-1}$ and PARA concentration ranged from (10 to 400 mg. $L^{-1}$). both solutions (binary) were stirred for 24 min at 20 ± 1°C. Correction for spectrophotometric estimation of residual concentrations in mixing systems performed using the equivalent equations (1, 2) (Ghemit, R et al, 2019, Djebri, N et al., 2017);

$$c_a = \frac{(k_{b2} * A_1 - k_{b1} * A_2)}{(k_{a1} * k_{b2} - k_{a2} * k_{b1})} \qquad \text{(IV. 1)}$$

$$c_b = \frac{(k_{a1} * A_2 - K_{a2} * A_1)}{(K_{a1} * k_{b2} - k_{a2} * k_{b1})} \qquad \text{(IV. 2)}$$

where $k_{a1}$, $k_{a2}$, $k_{b1}$ and $k_{b2}$ are the calibration constants for PARA and DIC, at the two wavelengths lambda max 1 (242 nm) and lambda max 2 (276 nm). $A_1$ et $A_2$ are the measured absorbance of each pharmaceutical compound.

$$q_e = \frac{(c_0 - c_e) * v}{m} \qquad \text{(IV. 3)}$$

The adsorption carried out under conditions such as: initial concentrations of adsorbate with 500 mg. $L^{-1}$, isothermal with pH =7 and temperature (293 – 313K), The adsorption phenomena was done by mixing the two adsorbates with adsorbent (PS700) Figure IV.5; until close equilibrium time at 120 min, and the concentration of the two pharmaceutical products quantified by UV-Vis spectrophotometer.

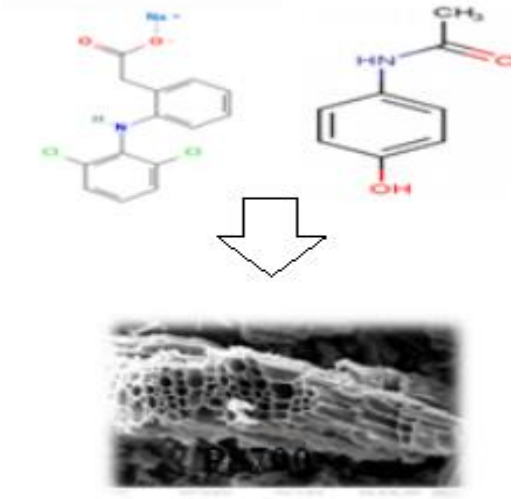

**Figure IV. 5:** Present binary system adsorption

### IV. 2. 3. Parameters Effect

#### IV. 2. 3. 1. Effect of pH

The effect of pH solution on the adsorption of DIC and PARA studied using PS700 as the adsorbent Figure IV. 6. Batch adsorption experiments conducted at the inherent solution pH ranging from (3–11), A mixture of 0.6 g PS700 dissolved in 60 ml to 20 mg. $L^{-1}$ stock solutions of PARA and DIC agitated on a mechanical shaker at 300 rpm and filtered for 240 min at selected times.

It can be clearly seen from Figure IV. 6 that the adsorption capacities gradually increased with increasing solution pH and reached maximum values of

(14.95 and 17.14 mg/g) for PARA in the single ad binary system, at pH 7,02 and 8,037 respectively. maximum values of (12,90 and 11,94 mg/g) for DIC in the single ad binary system, at pH 8.83 and 10.025, respectively (Fu, C et al., 2020). The pH-dependent adsorption behavior can be explained by the fluctuation of the surface charge of the adsorbent by protonation or deprotonation mechanisms (Jung, K. W et al, 2018).

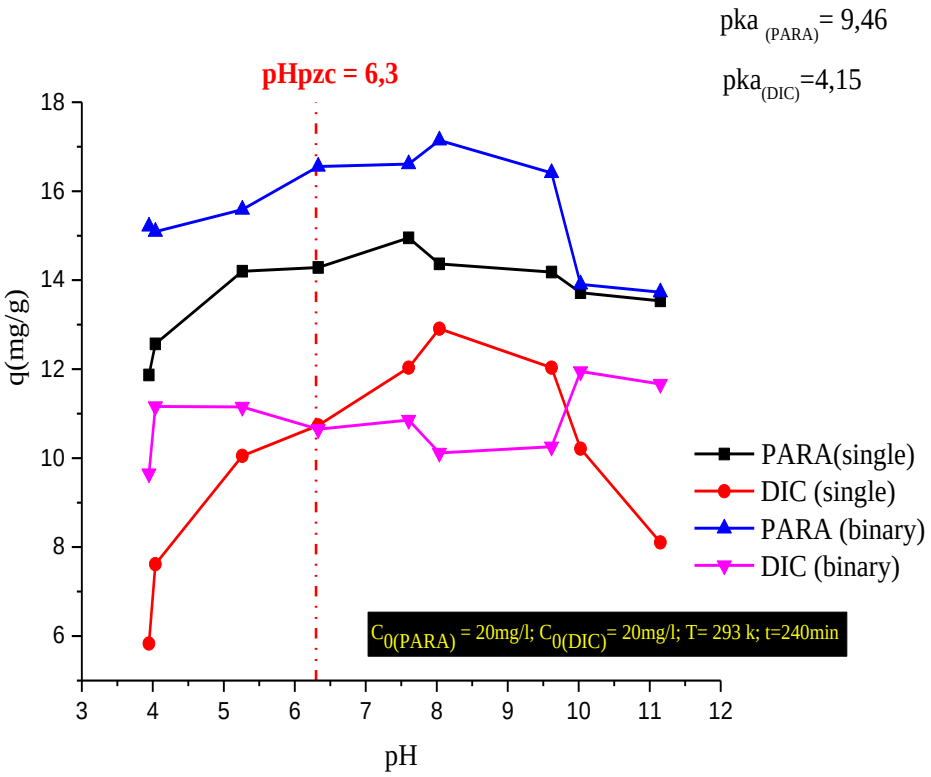


**Figure IV. 6:** Effect of pH on PARA and DIC adsorption in the binary system

### IV. 2. 3. 2. Ionic strength

Figure IV. 7 shows the effect of ionic strength on the adsorption behavior of PS700 for PARA and DIC. Increasing the ionic strength (NaCl concentration) from (0 to 1 g/L) gradually reduced the adsorption capacity of all contaminants. This trend could be due to either competitive adsorption of contaminants by electrolyte ions ($Na^+$) to the same binding sites on the adsorbent surface, or contaminant interfacial potentials affected by increasing ionic strength (Jung, K. W et al., 2018).

We found that PARA clearly inhibited adsorption of all substances at low ionic strength (0 - 0.2 M). Furthermore, when the ionic strength at a certain concentration (> 0.2 M) reaches a certain level, the removal capacity of PARA and

DIC by PS700 in single and binary systems gradually increases with increasing NaCl concentration increase. Possible explanations are: Ions can permeate the diffuse layer around the PS700 surface.

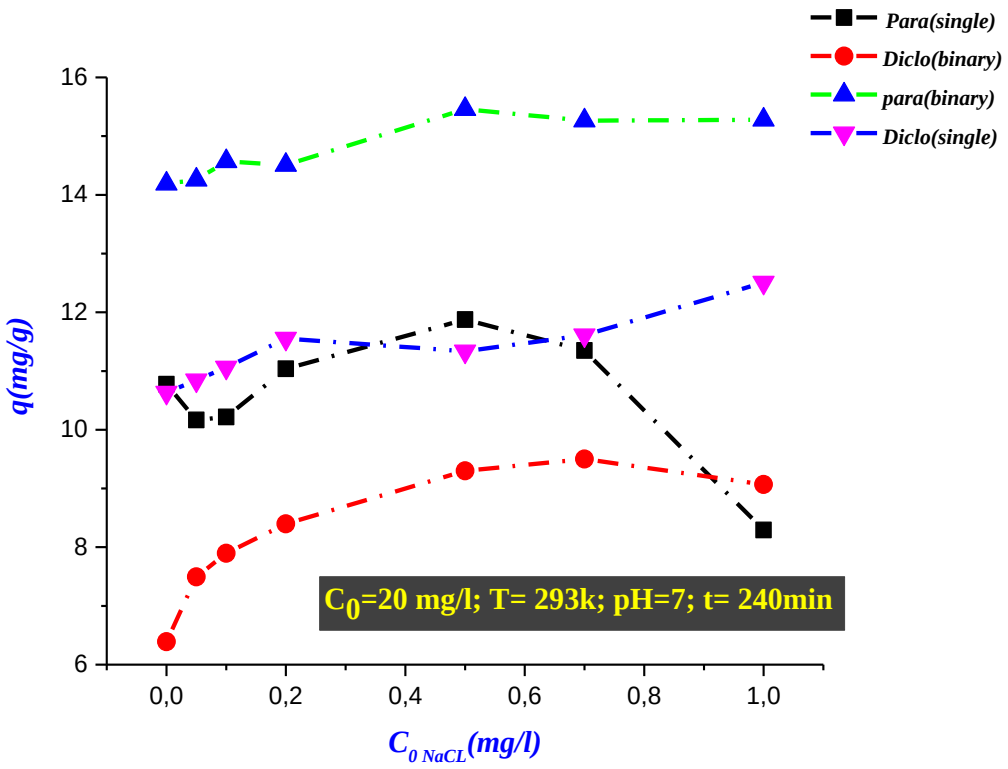


**Figure IV. 7:** Effect of ionic strength on adsorption of PARA and DIC in the single and binary system (m/v = 1 g/L, T = 20 °C, pH = 7.0, t = 4 h**)**

The adsorption process by the outer sphere adsorption mechanism may be more sensitive to ionic strength changes than the inner sphere adsorption mechanism, as the coexisting $Na^+$ may also form outer sphere surface complexes through electrostatic attraction (Uchimiya, M., 2014).

### IV. 3. 1. Adsorption isotherm

Figure IV. 8 illustrate the change in adsorption capacities for DIC and PARA as a function of equilibrium concentration for binary system. All general remarks Adsorption isotherms showed that the adsorption capacities decreased in the binary system at all temperatures tested, reflecting competitive adsorption between DIC and PARA. All DIC absorption capacities found to be higher than that of PARA in each

regimen. The same behavior was observed on the two systems, but the difference was less significant. Two statistical physics models were used to elucidate the absorption mechanisms of these antibiotics.

Adsorption equilibrium data of DIC and PARA onto PS700 present in Figure IV. 8 (a) and (b) in the binary system. The effects of different concentrations of the adsorption DIC (0- 400 mg. $L^{-1}$) on the presence PARA (20 mg. $L^{-1}$) Figure IV. 8 (a), When the concentration of PARA was 20 mg $L^{-1}$, the adsorption amount of PARA decreased from (400,16 mg. $g^{-1}$ to 158,96 mg $g^{-1}$) with DIC concentration increasing from (0 mg L−1 to 400 mg $L^{-1}$) at 293k. Reduced adsorption of DIC caused by the presence of PARA may be due to the PARA occupied part of the active sites (Baylan, N and Meriçboyu, A. E., 2016) and the retained high adsorption for PARA was the reason of electrostatic attraction and pore filling. Thus, PARA inhibits the adsorption of DIC on the adsorbent, which is competitive adsorption (Fu, C et al., 2020). The effects of different concentrations of PARA (0- 400 mg $L^{-1}$) on the adsorption of DIC (20 mg $L^{-1}$) Figure IV. 8 (b), When the concentration of PARA was 20 mg $L^{-1}$, the adsorption amount of PARA decreased from (411, 99 mg. $g^{-1}$ to 320, 72 mg $g^{-1}$) with DIC concentration increasing from (0 mg. $L^{-1}$ to 400 mg. $L^{-1}$) at 293k.

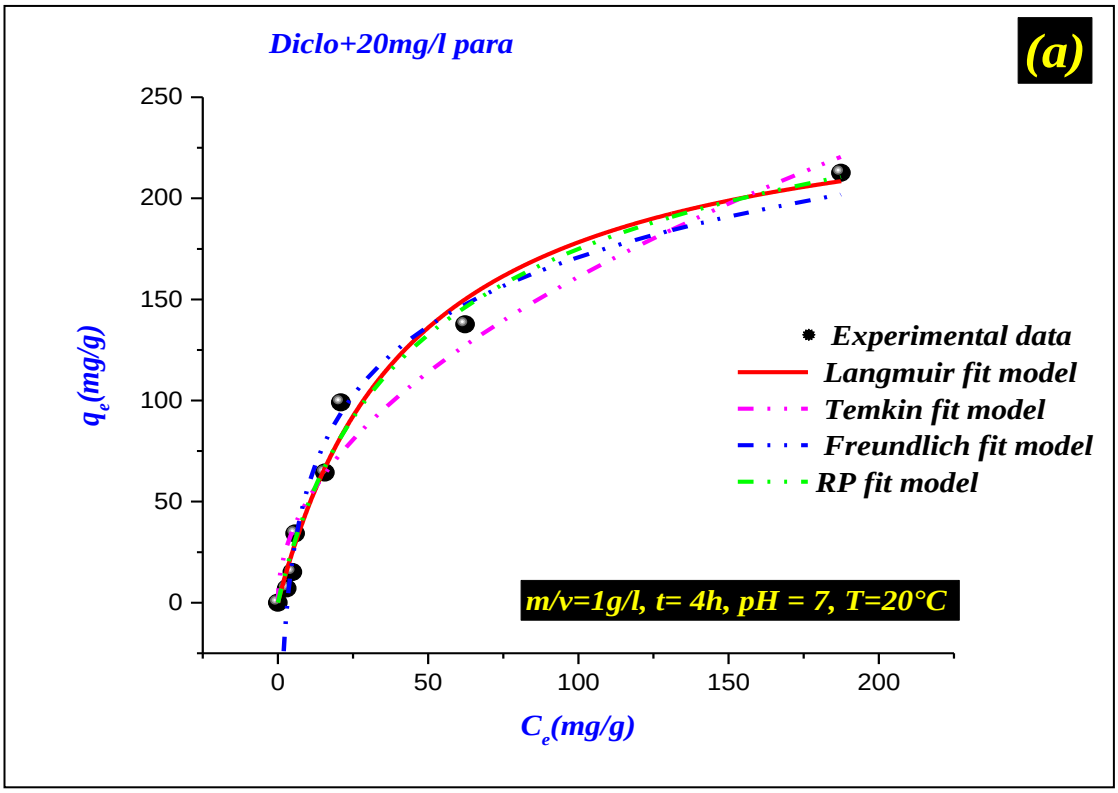


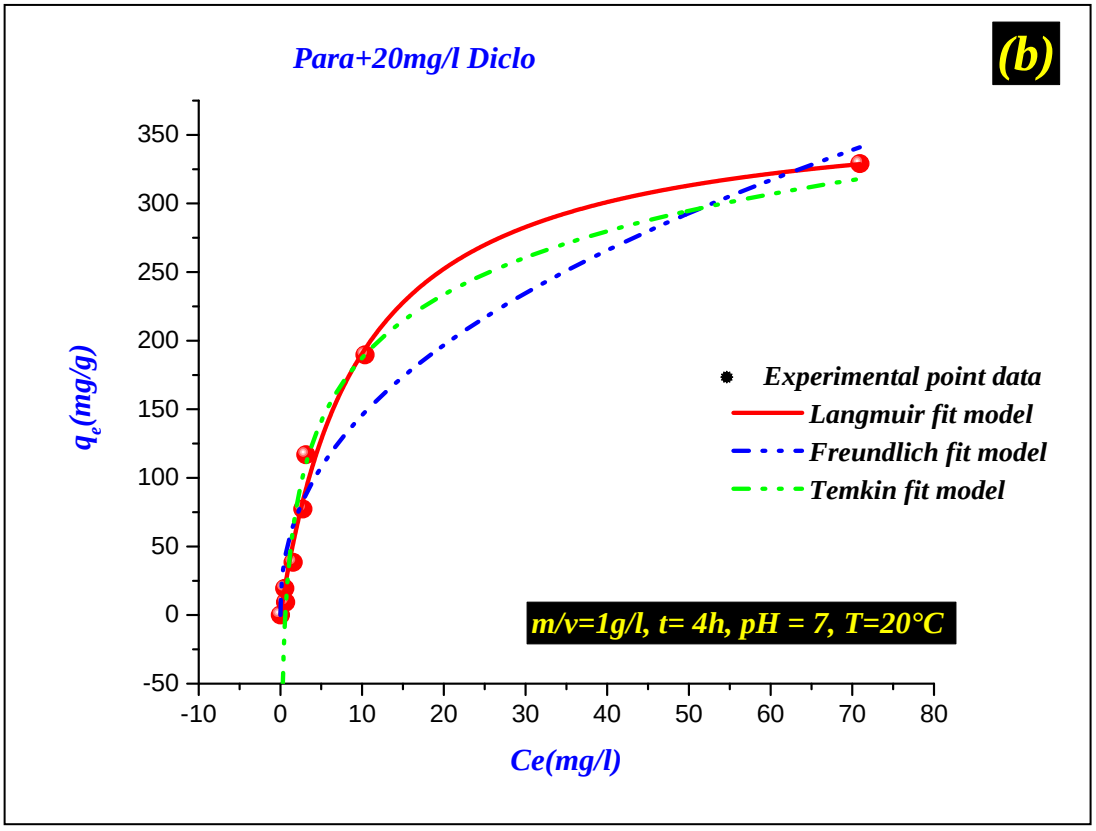


**Figure IV. 8:** (a) and (b) binary adsorption of DIC and PARA onto PS700 and fitting curves of isotherm models

**Table IV. 1:** Langmuir, Freundlich and Temkin isotherm adsorption parameters

| Antibiotics | system | T (k°) | Langmuir | | | Freundlich | | | Temkin | | |
|---|---|---|---|---|---|---|---|---|---|---|---|
| | | | $q_{max}$ ($mg.g^{-1}$) | K1 ($L.mg^{-1}$) | $R^2$ | nf | $K_F$ ($g.mg^{1}.min^{-1}$) | $R^2$ | A | B | $R^2$ |
| PARA | Binary | 293 | 320,72655 | 0,21453 | 0,8362 | 3,04752 | 67,62113 | 0,7346 | 2,4546 | 57,3201 | 0,8098 |
| | | 303 | 329,71696 | 0,0811 | 0,9353 | 2,45325 | 44,61807 | 0,8424 | 0,9347 | 64,4912 | 0,9338 |
| | | 313 | 302,32717 | 0,18919 | 0,8279 | 3,13006 | 62,66688 | 0,6999 | 1,9118 | 55,8806 | 0,8029 |
| DIC | Binary | 293 | 158,96838 | 0,04952 | 0,9439 | 2,72083 | 21,50076 | 0,8821 | 0,5184 | 32,3948 | 0,9597 |
| | | 303 | 142,55062 | 0,06272 | 0,9045 | 3,17332 | 25,01291 | 0,7720 | 0,6269 | 28,5028 | 0,8784 |
| | | 313 | 133,04951 | 0,0416 | 0,8938 | 2,9669 | 19,40266 | 0,7404 | 0,3856 | 27,9755 | 0,8669 |

## IV. 3. 2. Kinetic studies

The kenitics of adsorption analyzed using a PFO kenitic model equation (IV. 4) and and PSO Kenitic model equation (IV. 5) shows the non-linearized form (Shikuku, V. O. et al, 2018., Jemutai-K, S et al, 2019):

Pseudo-first-order model: $$q_t = q_e(1-e^{-K_1 t}) \quad \text{(IV. 4)}$$

Pseudo-second-order model: $$q_t = \frac{q_e^2 . k_2 . t}{1 + q_e . k_2 . t} \quad \text{(IV. 5)}$$

Batch kinetics conducted in duplicate for PARA and DIC using PS700, The samples removed at predetermined contact times of (0, 5, 10, 15, 20, 30, 45, 60, 120, 180 and 240min) and immediately filtered using 0.45 mm filters to separate the adsorbent from solution.

The effects of different times on the adsorption of DIC in the presence PARA (20mg. $L^{-1}$, 40 mg. $L^{-1}$, 80 mg. $L^{-1}$) by PS700 as a function of time (0-

240min) in a binary system DIC showed a rapid increase in compound adsorption kinetics to saturation within 45 min 70% Figure IV. 9 (a). Moreover, the effects of different times on the adsorption of PARA in the presence DIC (20 mg. $L^{-1,}$ 40 mg. $L^{-1}$, 80 mg. $L^{-1}$) by PS700 as a function of time (0- 240 min) in a binary system PARA showed a rapid increase in compound adsorption kinetics to saturation within10 min 90% Figure IV. 9 (b).

Table 2 shows the model parameters for the adsorption of DIC and PARA on PS700. PSO ($R^2$ = 0,973, $R^2$ = 0,976, $R^2$ = 0,905) and Elovich ($R^2$ = 0,959, $R^2$ = 0,898, $R^2$ = 0,975) models in the concentration 20, 40, and 80 mg/l better describe the kinetic data than the PFO model, based on the correlation coefficient $R^2$. The calculated value of the adsorption capacity ($q_{ecal}$ = 18,42 mg. $g^{-1}$, $q_{ecal}$ = 39,53mg. $g^{-1}$, $q_{ecal}$ = 60,29 mg. $g^{-1}$). PS700 showed higher PARA removal efficiency compared to DIC. From the results, it can be inferred that the pseudo-second- ordre –model can better represent the adsorption process of PS700 than the first-order pseudo-model and Elovich model due to the higher $R^2$ value Figure IV. 9 (a). Therefore, it hypothesized that the rate-limiting step maybe chemisorption involving valence forces due to sharing or electron exchange between adsorbents and adsorbates (Ghemit, R et al.,2017). Several authors have shown successful applications of the PSO model representing the experiment Kinetic data for drug adsorption to various adsorbents (Fallou, H. et al., 2016; Antunes, M et al., 2012; Oliveira, T. D et al., 2017; Salihi, E. Ç., Mahramanlıoğlu, M., 2014).

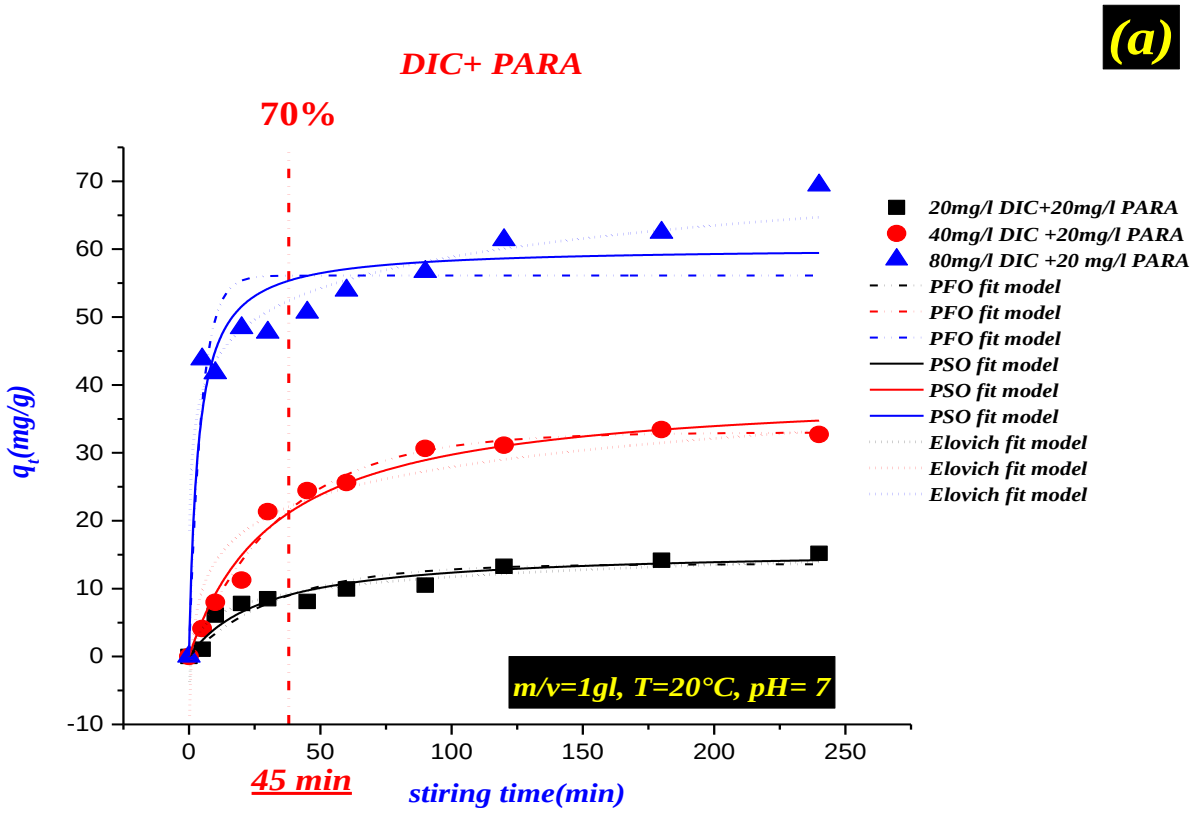


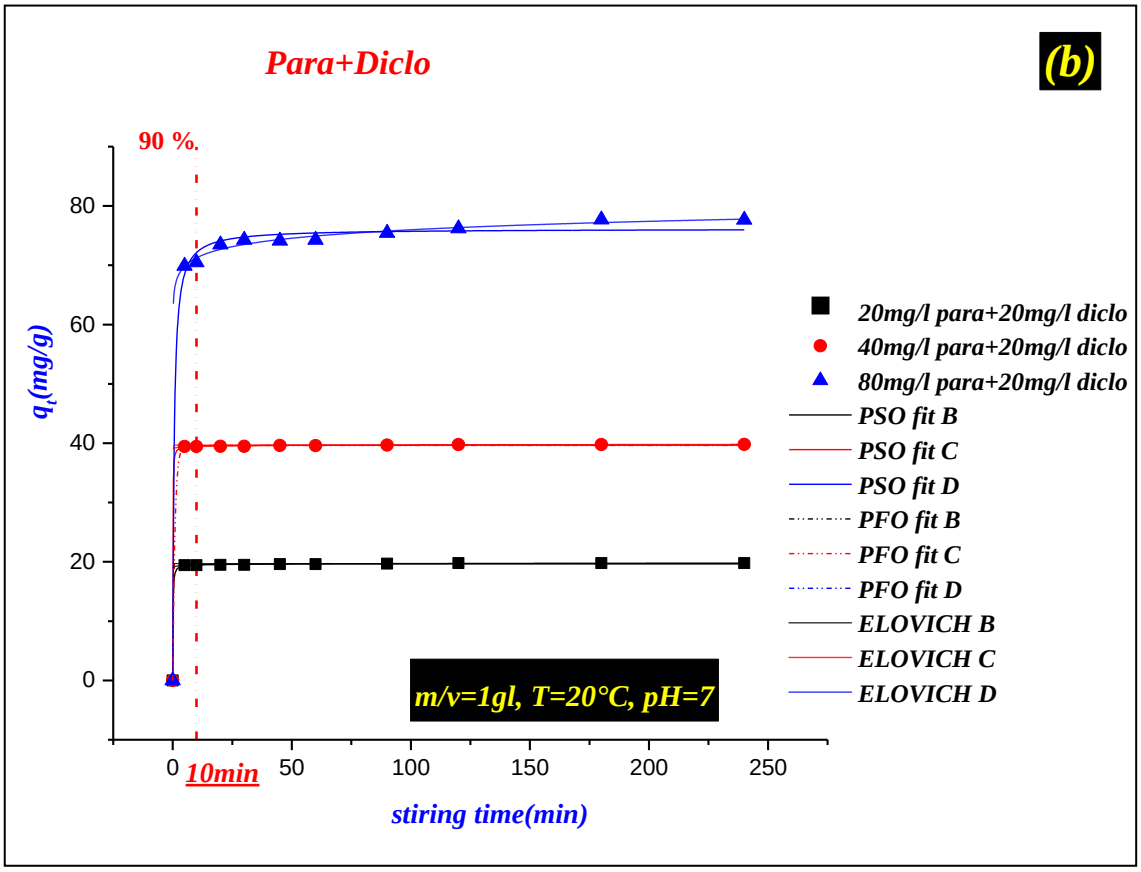


**Figure IV. 11**: (a) and (b) Variation of adsorption capacity for PARA and DIC with time *(m/V=1, T=293k, pH=7)*

**Table IV. 2:** PFO and PSO correlated data calculated by experimental data of Binary system.

| Kenitic models | | PFO | | | PSO | | | Elovich | | |
|---|---|---|---|---|---|---|---|---|---|---|
| Parametrs | C (mg. $l^{-1}$) | K1 ($min^{-1}$) | Qe ($mg.g^{-1}$) | $R^2$ | K2 ($g.mg^{1}.min^{-1}$) | Qe ($mg.g^{-1}$) | $R^2$ | A mg/ (g. min)$^{-1}$) | B ($g.mg^{-1}$) | $R^2$ |
| PARA | 20 | 0,92516 | 19,62432 | 0,99953 | 0,58527 | 19,68124 | 0,99973 | 19,19507 | 0,10737 | 0,99994 |
| | 40 | 1,06797 | 39,62401 | 0,99988 | 0,59239 | 39,68072 | 0,99993 | 39,19507 | 0,10737 | 0,99999 |
| | 80 | 0,51534 | 74,96838 | 0,99191 | 0,02367 | 76,14597 | 0,99695 | 66,51364 | 2,05485 | 0,99941 |
| DIC | 20 | 0,04859 | 16,46504 | 0,95917 | 0,00362 | 18,42463 | 0,97393 | 0,48964 | 3,28393 | 0,95923 |
| | 40 | 0,0278 | 33,01164 | **0,98652** | 7,66203E-4 | 39,53898 | 0,97626 | 1E-14 | 6,06296 | 0,89813 |
| | 80 | 0,21644 | 56,11054 | 0,8313 | 0,00489 | 60,29347 | 0,90558 | 28,12432 | 6,67595 | 0,97542 |

### IV. 3. 3. Analytical methods

The concentration of pharmaceuticals and adsorbate probes in synthetic urine were measured on a UV visible spectrophotometer (Optizen 2120 UV model) using a 1 cm quartz cuvette. A calibration curve (0, 3, 5, 10, 15, 20, 30 and 50 mg. $L^{-1}$) was developed for each adsorbate individually

### IV. 3. 4. Thermodynamic study

The influence of temperature on the adsorption of DIC and PARA in binary systems was studied at different temperatures (293, 303 and 313K). The adsorption capacity at equilibrium decreases dramatically with increasing temperature, indicating the exothermic nature of the process. According to the results shown in Table 3, increasing temperature decreased the amount of DIC adsorbed on PS700 at steady state. Similar results were reported by (Cuerda-Correa, E. M et al., 2010; Antunes, M et al., 2012). Evaluation of the effect of temperature on the adsorption of DIC and PARA by PS700 in the binary system these authors attribute the decrease in adsorption capacity he attributed to two factors. It is the solubility of the drug in water and the energy exchange that occurs during the process.

Thus, the increased temperature probably caused an increase in the solubility of DIC and PARA, impeding their adsorption as the drugs have a greater affinity for the solvent than PS700. The attractive forces between DIC, PARA and PS700 decreased with increasing temperature because the movement of dissolved species increased with increasing temperature and their interaction with PS700 decreased.

Furthermore, it confirmed that the adsorption capacity decreases with increasing temperature, as the adsorption process is exothermic and equilibrium occurs when heat released into the system. Shift in the opposite direction of the reaction. Moreover, ΔH ads are less than 40 kJ mol. $1^{-1}$ indicating a physic-sorption process (Önal, Y et al., 2007). Moreover, the change in ΔS ads of the process was positive, indicating that the randomness of the solid-solution interface decreased when DCF was adsorbed on grape bagasse (Özcan, A. S et al., 2004)

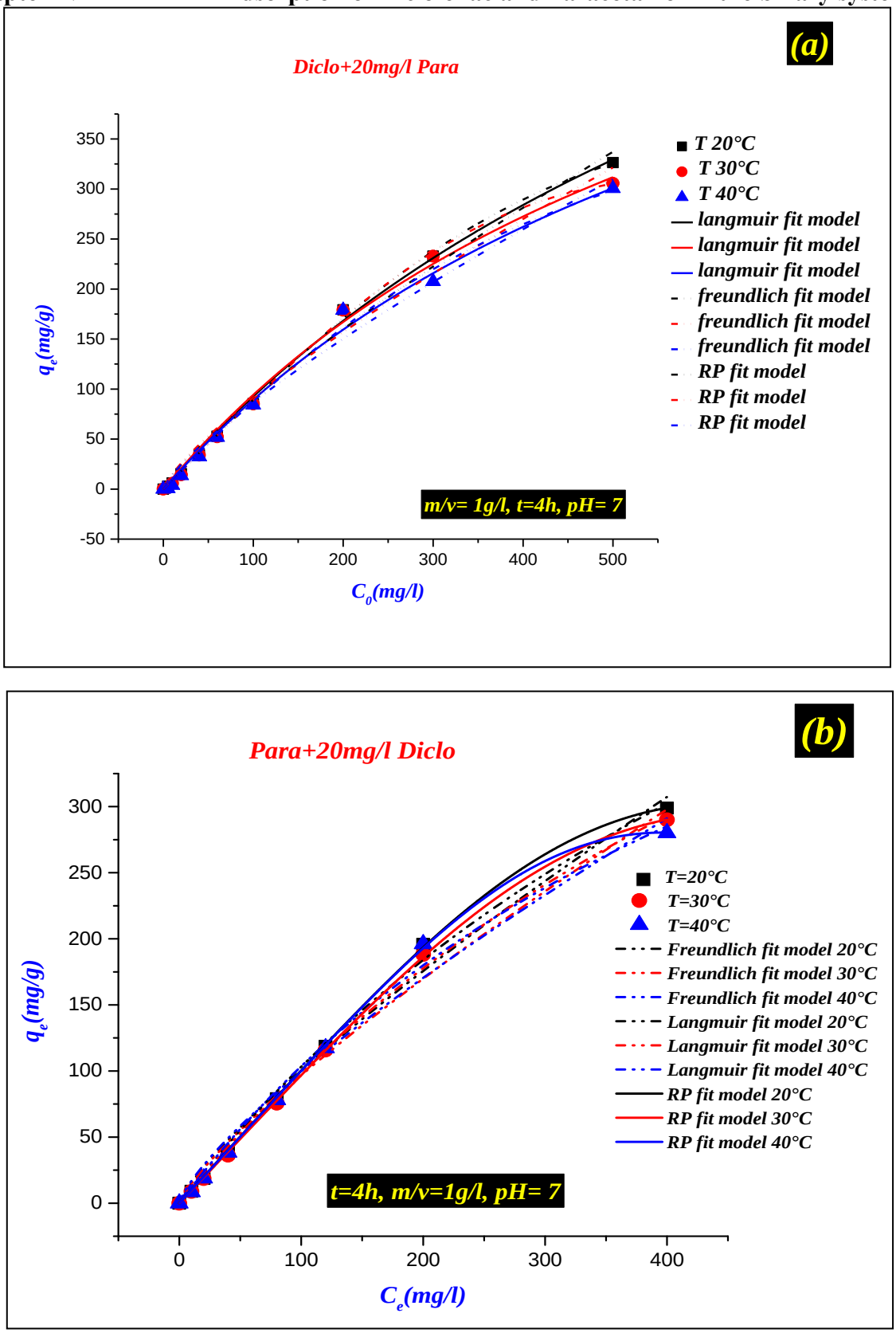


**Figure IV. 12: (**a) and (b) are isothermal fittings for DIC and PARA adsorption in the binary system at different temperatures on PS700 ($m/V$ = 0.1 g/L, pH = 7.0, $t$ = 4 h)

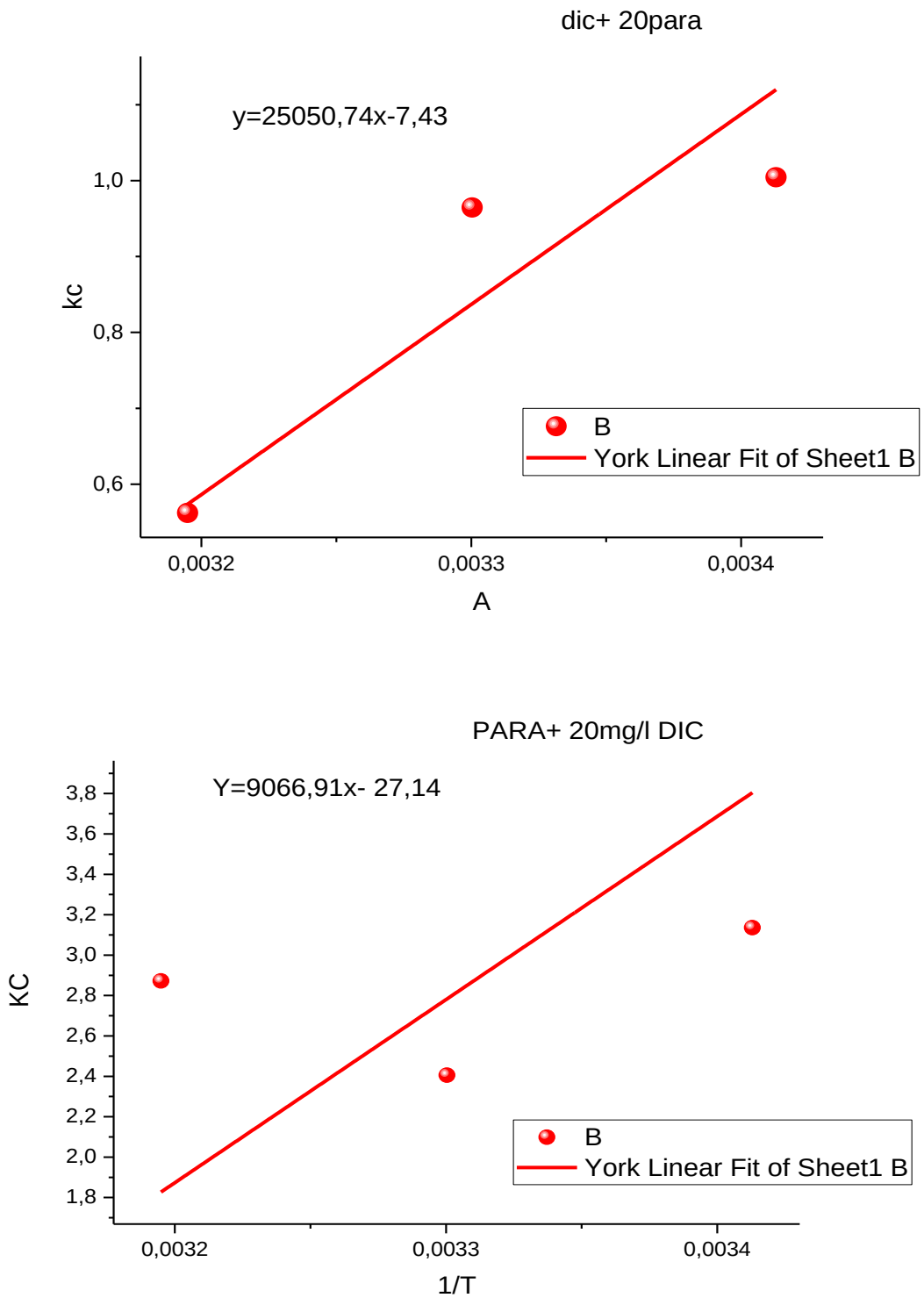


**Figure IV. 11**: Van't Hof plots for adsorption of DIC and PARA onto PS700 (Van't Hof plots (Lima, E.C et al, 2019)

**Table IV. 3:** Thermodynamic parameters for PARA and DIC adsorption onto PS700 adsorbent

| Binary system | T | 1/T ($10^{-3}$) | LN KC | ΔS(j/mol) | ΔH(kj/mol) | ΔG(kj/mol) |
|---|---|---|---|---|---|---|
| | 293 | 3,41297 | | | | -38.932 |
| DIC | 303 | 3,30033 | y=2505,74x-7,43 | 61,773 | -20.832 | -39.549 |
| | 313 | 3,19489 | | | | -40.167 |
| | 293 | 3,41297 | | | | -88.449 |
| PARA | 303 | 3,30033 | y=9066,91x-27,14 | 225,641 | -22.336 | -92.962 |
| | 313 | 3,19489 | | | | -92.962 |

### IV. 2. 2. Adsorption mechanism

Several authors have suggested that the interactions between molecular adsorbents and the surface of carbonaceous materials are electron donor acceptor (EDA) interactions (π-π- EDA and n-π EDA); hydrogen bonding interactions reported that the interaction is classified as a π-hydrogen bond. Can, hydrophobic interaction, molecular attraction between molecules at solid-liquid interface (Cazetta, A. L et al., 2016; Wang, J et al., 2015 ; Álvarez- Torrellas, S et al., 2016 ; Wu, P et al., 2019).

### IV. 3. 5. Desorption/regeneration analysis

The regeneration of sorbents studied after studying the equilibrium state. Where added 500 mg PS-biochar to a solution PARA (40 mg. $L^{-1}$) and DIC (20 mg. $L^{-1}$), after which it stirred for 4 hours. The loaded PS-biochar collected, dried, and used for the next cycle after each adsorption test. After the adsorption cycles and when the removal of (40 mg. $L^{-1}$ of PARA and 20 mg. $L^{-1}$ of DIC) decreased by less than 50%, the collected PS-biochar immersed in 50 mL of NaOH solution 0.1 M for 4 h, and then washed with distilled water. Finally, the washed adsorbent dried and

used for regeneration tests. The percentage removal (%) of (40 mg. $L^{-1}$ of PARA and 20 mg. $L^{-1}$ of DIC) at equilibrium was calculated as:

$$\text{Re}moval\,(\%) = \left[(C_0 - C_e)/C_0\right] \times 100 \qquad \text{(IV. 6)}$$

Due to stringent ecological and economic sustainability requirements, the evaluation of sorbent regeneration is of great importance for practical application (PARA + DIC) Evaluation of Adsorption Regeneration Performance Figure IV 12 shows a 4 cycle's adsorption experiment on PS700 and the results. This work confirmed that the (PARA + DIC) adsorption has excellent regeneration performance. This effectively educes the overall cost of the sorbent.

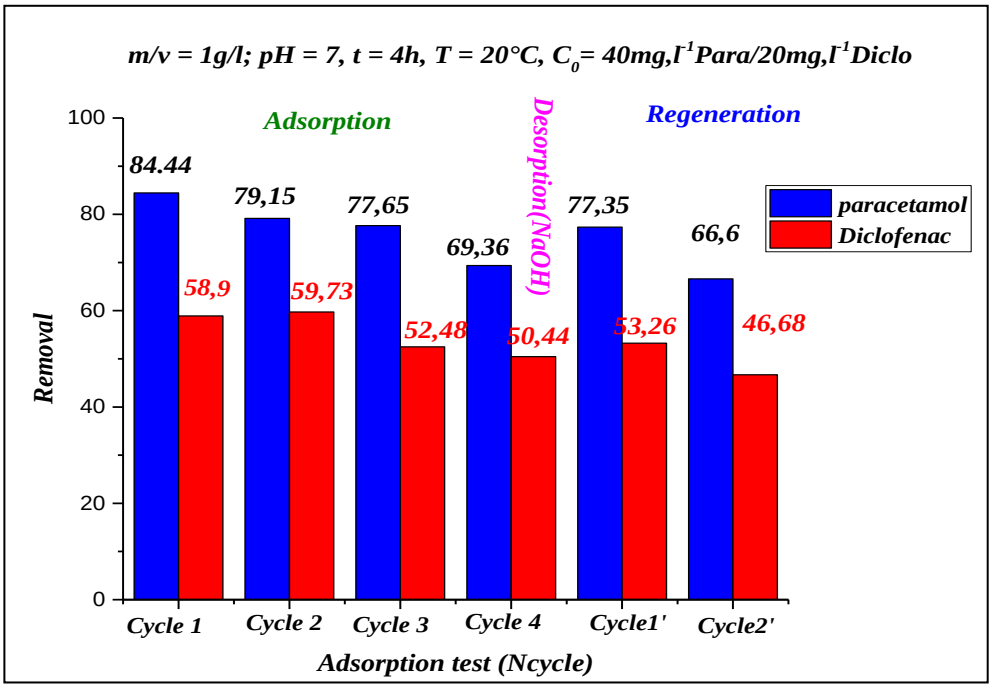


**Figure IV. 12:** Reuse and regeneration tests for the prepared PS-biochar (PARA+ DIC) in the binary system

## Conclusion

PS700 showed a relatively higher adsorption capacity for DIC than for PARA. Nonlinear Temkin and Langmuir isotherm models adequately described the equilibrium sorption data. Although the adsorption kinetics followed his PSO kinetics, thermodynamic studies revealed that the adsorption process was spontaneous and exothermic. The adsorption values for both sulfonamides indicated

that the adsorption mechanism was physical in nature. Hydrogen bonding, cationic cross-linking, and negative charge-assisted dH-bonding have been identified as possible mechanisms for the adsorption of DIC and PARA on PS700.

# General Conclusion

# General Conclusion

In conclusion, we have succeeded to fabricate a good activated biochar from pepper stems (PS700), which has excellent physico-chemical properties such as: porosity with a specific surface ($S_{BET}$ = 727.5 m2/g), and a high total pore volume ($V_{Total}$ = 0.36 cm3/g), the mesoporous material ($V_{Mesopore}$ = 56.4%) the external surface and the average pore diameter were 217.3 $m^2$. $g^{-1}$ and 1.97 nm, respectively, and a high total pore volume ($V_{Total}$ = 0.36 $cm^3$/g), the mesoporous material ($V_{Mesopore}$ = 56.4%) the outer surface and the average pore diameter were 217, 3 $m^2$. $g^{-1}$ and 1.97 nm, respectively. The pore morphology is heterogeneous, cylindrical (tunnels), and the composition of PS700 contains the majority of carbon and oxygen, with high carbon content (77.15%), therefore classified as a biochar with mesoporous type pores, and indicates the non-crystalline structure.

The biochar had a large specific surface area ($S_{BET}$ = 727.5 m2/g) and a high total pore volume ($V_{Total}$ = 0.36 cm3/g), the mesoporous material ($V_{Mesopore}$ = 56.4%) the external surface and the average pore diameter was 217.3 $m^2$. $g^{-1}$ and 1.97 nm, respectively. The morphological properties clearly show that the PS700 sample has heterogeneous tunnel-shaped pores. The EDS result of the elemental composition of the prepared PS700 indicates that C and O are the major elements in the composition of the PS700. The high carbon content (77.15%) shows that PS700 is a carbon-rich adsorbent, so it is classified as a mesoporous carbonaceous biochar and indicates the non-crystalline structure.

The adsorption parameters of the isotherm of were calculated from a nonlinear optimization method and the results show that $q_e$= f (C e) resembles the L-type (high affinity) isotherm. Isotherms showed by the Langmuir ($R^2$ = 0.982), Redlich-Peterson ($R^2$ = 0.988) and Liu ($R^2$ = 0.986) models, against the Freundlich model ($R^2$ = 0.946). Langmuir suggests that IBP molecules were adsorbed in monolayer and multilayer. Moreover, Langmuir's equation shows that the maximum adsorption capacity is ($Q_{0max}$) is 569.6 mg/g. For the PSO ($R^2$ = 0.980, $\chi^2$ = 0.589) and Avrami ($R^2$ = 0.987, $\chi^2$ = 2.629) models better describe the kinetic data than the PFO and intra-particle diffusion model, based on the correlation coefficient ($R^2$).

Biochar (PS700) is applied in two systems, single and (binary) adsorption system, to have effective behavior on adsorption process:

## General Conclusion

For a single system the adsorption study carried out by the adsorbent (PARA and DIC) on the adsorbent PS700 to have the behavior of adsorption, the phenomenon of adsorption can be easily influenced by modifying the pH of the solution (3– 11) and adding NaCl (0.05–1.0 M), reaching a rapid steady state (~120 min). DIC, according to calculated parameters Isothermal data are more adequately described by Langmuir ($R^2$ = 0.928, $R^2$= 0.925, $R^2$ = 0.909) and Redlich-Peterson ($R^2$ = 0.917, $R^2$= 0.915, $R^2$ = 0.896) and Temkin ($R^2$ = 0.895; $R^2$ = 0.903; $R^2$ = 0.897) than the Freundlich model ($R^2$ = 0.898, $R^2$ = 0.893, $R^2$ = 0.883) at different temperatures (293, 303 and 313k), respectively. The maximum adsorption capacity was found (400.16 mg/g; 397.40 mg/g and 382.46 mg/g) at different temperatures (293, 303 and 313k), respectively.

Adsorbent isotherms are better described by Langmuir ($R^2$=0.928, $R^2$= 0.925, $R^2$= 0.909) and Temkin ($R^2$ = 0.959; $R^2$= 0.971; $R^2$= 0.942) than by Freundlich ($R^2$ = 0.898, $R^2$ = 0.893, $R^2$ = 0.883) and Redlich-Peterson ($R^2$ = 0.917, $R^2$ = 0.915, $R^2$ = 0.896) at different temperatures (293, 303 and 313k), respectively. Was shown, Maximum biochar adsorption capacity for PARA, DIC and IBP (411.99 mg/g and 400.16 mg/g), respectively at 293k. The thermodynamic parameter signals were negative ΔG° and ΔH° values, but positive ΔS° values. The adsorption mechanism consists of pore filling, hydrogen bonding, n-π and π-π.

In the binary system, The adsorption equilibrium data of DIC and PARA onto PS700: the effects of different concentrations of the adsorption DIC (0- 400 mg $L^{-1}$) on the presence PARA (20 mg. $L^{-1}$) When the concentration of PARA was (20 mg $L^{-1}$), the adsorption amount of PARA decreased from (400,16 mg. $g^{-1}$ to 158,96 mg $g^{-1}$), with DIC concentration increasing from (0 to 400 mg $L^{-1}$) at 293k. Reduced adsorption of DIC caused by the presence of PARA may be due to the PARA occupied part of the active sites**.**

- ✓ The effects of different concentrations of PARA (0- 400 mg. $L^{-1}$) on the adsorption of DIC (20 mg. $L^{-1}$), When the concentration of PARA was 20 mg. $L^{-1}$, the adsorption amount of PARA decreased from (411, 99 mg. $g^{-1}$ to 320, 72 mg. $g^{-1}$) with DIC concentration increasing from (0 mg L−1 to 400 mg $L^{-1}$) at 293k.

- ✓ The effects of different times on the adsorption of DIC in the presence PARA (20 mg. $L^{-1}$, 40 mg. $L^{-1}$, 80 mg. $L^{-1}$) by PS700 as a function of time (0- 240 min) in a binary system DIC showed a rapid increase in compound adsorption kinetics to saturation with in 45min 70%. Moreover, the effects of different times on the adsorption of PARA in the presence DIC (20

mg. $L^{-1,}$ 40 mg. $L^{-1}$, 80 mg. $L^{-1}$) by PS700 as a function of time (0- 240 min) in a binary system PARA showed a rapid increase in compound adsorption kinetics to saturation within10 min 90%**.**

- ✓ The model parameters for the adsorption of DIC and PARA on PS700, PSO ($R^2$ = 0,973, $R^2$ = 0,976, $R^2$ = 0,905) and Elovich ($R^2$ = 0,959, $R^2$ = 0,898, $R^2$ = 0,975) models in the concentration 20, 40, and 80 mg/l better describe the kinetic data than the PFO model, based on the correlation coefficient $R^2$. The calculated value of the adsorption capacity ($q_{ecal}$ = 18,42 mg. $g^{-1}$, $q_{ecal}$ = 39,53mg. $g^{-1}$, $q_{ecal}$ =60,29 mg. $g^{-1}$). PS700 showed higher PARA removal efficiency compared to DIC. From the results, it can be inferred that the pseudo-second- ordre –model can better represent the adsorption process of PS700 than the first-order pseudo-model and Elovich model due to the higher $R^2$ value.

# Bibliographic references

# References


Afolabi, I. C., Popoola, S. I., Bello, O. S., (2020). Modeling pseudo-second-order kinetics of orange peel-paracetamol adsorption process using artificial neural network, Chemom. Intell. Lab. Syst. 203, https://doi.org/10.1016/j.chemolab.2020.104053

Ahmad, M; Rajapaksha, A. U; Lim, J. E; Zhang, M; Bolan, N; Mohan, D; Vithanage, M; Lee, S. S; Ok, Yong Sik (2014). Biochar as a sorbent for contaminant management in soil and water: A review. Chemosphere, 99, 19-33 http://dx.doi.org/10.1016/j.chemosphere.2013.10.071

Ahmed, M. J., Hameed, B. H. (2018). Removal of emerging pharmaceutical contaminants by adsorption in a fixed bed column: A review, Ecotoxicol. Environ. Saf. 149 257–266, https://doi.org/10.1016/j.ecoenv.2017.12.012

Alaerts, L., Maes, M., Giebeler, L., Jacobs, P. A., Martens, J. A., Denayer, J. F. M., De Vos, D. E., (2008). *Selective Adsorption and Separation ofortho-Substituted Alkylaromatics with the Microporous Aluminum Terephthalate MIL-53. Journal of the American Chemical Society, 130(43), 14170–14178.* https://doi:10.1021/ja802761z

Ali, I., Burakov, A. E., Melezhik, A. V., Babkin, A. V., Burakova, I. V., Neskomornaya, M. E. A., Kuznetsov, D. V., (2019). *Removal of Copper (II) and Zinc (II) Ions in Water on a Newly Synthesized Polyhydroquinone /Graphene Nanocomposite Material: Kinetics, Thermodynamics and Mechanism. Chemistry Select, 4(43), 12708–12718.* https://doi:10.1002/slct.201902657

Allen. S. J., Mckay. G., Khander.Y. H., Douez, O., Ehret, X et Kaczmaryk, A., (2011). Equilibrum adsorption for basic dyes into lignite. Chemical Technology and Biotechnology, 45, 291-302.

Álvarez-Torrellas, S., Rodríguez, A., Ovejero, G., García, J., (2016). Comparative adsorption performance of ibuprofen and tetracycline from aqueous solution by carbonaceous materials, Chem. Eng. J. 283 936–947, https://doi.org/10.1016/j.cej. 2015.08.023

Amimer, G et Kedadouche, S; (2015). Elimination de polluants d'origine pharmaceutique par adsorption sur une hydroxyapatite préparée à partir d'os bovin

Amimer, G ; Kedadouche, S ; (2016). Adsorption seuls et en mélange de polluants d'origine pharmaceutique sur des adsorbants préparés à partir d'un déchet textile. Mémoire de master. Université A. MIRA-BEJAIA Faculté de Technologie Département de Génie des Procédés.

Antunes, M., Esteves, V. I., Guégan, R., Crespo, J. S., Fernandes, A. N., Giovanela, M., (2012). Removal of diclofenac sodium from aqueous solution by isabel grape bagasse. J. Chem. Eng. 192, 114–121.https://doi:10.1016/j.cej.2012.03.062

Arias, M., Barral, M. T., Da Silva–Carvalhal, J., Mejuto, J. C., & Rubinos, D., (2004). *Interaction of Hg(II) with kaolin-humic acid complexes. Clay Minerals, 39(01), 35–45.* https://doi:10.1180/000985543910118

Aussenac-Gilles, N., Biébow, B., & Szulman, S., (2000). *Revisiting Ontology Design: A Method Based on Corpus Analysis. Lecture Notes in Computer Science, 172–188.* https://doi:10.1007/3-540-39967-4_13

Azri, N., Fadel, A., Ouakouak, A., Chebbi, R ., Hecini, L., Achmad S., Raj Boopathy, (2022)Development of a novel and efficient biochar produced from pepper stem for effective ibuprofen removal. Bioresource Technology.,DOI: 10.1016/j.biortech.2022.126685

Bagheri, A., Abu-Danso, E., Iqbal, J., Bhatnagar, A., (2020). Modified biochar from Moringa seed powder for the removal of diclofenac from aqueous solution, Environ. Sci. Pollut. Res. 27 ,7318–7327.

Barbosa, M. O., Moreira, N. F. F., Ribeiro, A. R., Pereira, M. F. R., Silva, A. M.T., (2016). Occurrence and removal of organic micropollutants: An overview of the watch list of EU Decision 2015/495. Water Res. 94, 257–279. https://doi.org/10.1016/j.watres.2016.02.047

Barczak, M., Wierzbicka, M., Borowski, P., (2018). Sorption of diclofenac onto functionalized mesoporous silicas: experimental and theoretical investigations. Microporous Mesoporous Mater. 264, 254–264.https://doi:10.1016/j.micromeso.2018.01.013

Baudu, M., Le Cloirec, P., & Martin, G., (1989). *Modélisations des isothermes d'adsorption sur charbon actif de composés aromatiques en solution aqueuse. The Chemical Engineering Journal, 41(2), 81–89.* http://doi:10.1016/0300-9467(89)80075-9

Baylan, N., Meriçboyu, A. E., (2016). Adsorption of lead and copper on bentonite and grapeseed activated carbon in single-and binary-ion systems. Separ. Sci. Technol. 51, 2360–2368.https://doi:10.1080/01496395.2016.1212888

Benjedim, S.; Romero-Cano, L. A.; Pérez-Cadenas, A. F.; Bautista-Toledo, M. I.; Lotfi, E.; Carrasco-Marín, F., (2020). Removal of emerging pollutants present in water using an E-coli biofilm supported onto activated carbons prepared from argan wastes: Adsorption studies in batch and fixed bed. *Sci. Total Environ., 720*, 137491

Bing, L., Junjun, M., Lincheng, Z., Yong, Q., (2017). Magnetic microsphere to remove tetracycline from water: adsorption, $H_2O_2$ oxidation and regeneration. Chemical Engineering Journal; 330: 191-201.https://doi:10.1016/j.cej.2017.07.054

Bouchelkia, N., (2015). Etude de l'élimination du Plomb, du Zinc et du cadmium par adsorption sur un charbon actif préparé à base des noyaux de jujube. Mémoire de magister. L'université de Bejaia, Faculté : Technologie Département ; Génie des procédés.

Boukhalfa, N., (2014). Synthèses et caractérisations des hydroxydes doubles lamellaires à différents rapports molaires et de montmorillonite organophile : Elimination du diclofénac, Mémoire de magister. Présenté à la faculté de technologie département de génie des procédés.

Bound, J. P., Voulvoulis, N., (2005). Household disposal of pharmaceuticals as a pathway for aquatic contamination in the United Kingdom. Environ. Health Perspect. 113, 1705–1711. https://doi.org/10.1289/ehp.8315

Brewer, C. E., Chuang, V. J., Masiello, C. A., Gonnermann, H., Gao, X., Dugan, B., Davies, C. A., (2014). *New approaches to measuring biochar density and porosity. Biomass and Bioenergy, 66, 176 185.* https://doi:10.1016/j.biombioe.2014.03.059 10.

Calisto, V., Ferreira, C. I.A., Oliveira, J., Otero, M., Esteves, V. I., (2015). Adsorptive removal of pharmaceuticals from water by commercial and waste-based carbons, J. Environ. Manage. 152 83–90.

Calvet, R., (2003). Le sol propriétés et fonction –tome1 : Constitution, structure phénomènes aux interfaces. Edition France Agricole.

Cazetta, A. L., Martins, A. C., Pezoti, O., Bedin, K. C., Beltrame, K. K. Beltrame, Asefa, T., Almeida, V. C., (2016). Synthesis and application of N-S-doped mesoporous carbon obtained from nanocasting method using bone char as heteroatom precursor and template, Chem. Eng. J. 300 54–63.http://dx.doi.org/10.1016/j.cej.2016.04.124

Cenens, J., (1988). *Visible Spectroscopy of Methylene Blue on Hectorite, Laponite B, and Barasym in Aqueous Suspension. Clays and Clay Minerals, 36(3), 214–224.* https://doi:10.1346/ccmn.1988.0360302

Chahinez, H. O., Abdelkader, O., Leila, Y., Tran, H. N., (2020). One-stage preparation of palm petiole-derived biochar: Characterization and application for adsorption of crystal violet dye in water. Environ. Technol. Innov. 19, 100872

Chakraborty, P., Banerjee, S., Kumar, S., Sadhukhan, S., Halder, G., (2018). Elucidation of ibuprofen uptake capability of raw and steam activated biochar of Aegle marmelos shell: Isotherm, kinetics, thermodynamics and cost estimation, Process Saf. Environ. Prot. 118 10–23.

Chakraborty, P., Show, S., Banerjee, S., Halder, G., (2018). Journal of Environmental Chemical Engineering Mechanistic insight into sorptive elimination of ibuprofen employing bi-directional activated biochar from sugarcane bagasse : Performance evaluation and cost estimation. J. Environ. Chem. Eng. 6, 5287–5300. https://doi.org/10.1016/j.jece.2018.08.017

Changmai, M., Banerjee, P., Nahar, K., Purkait, M. K., (2018). A novel adsorbent from carrot, tomato and polyethylene terephthalate waste as a potential adsorbent for Co (II) from aqueous solution: Kinetic and equilibrium studies. J. Environ. Chem. Eng. 6, 246–257. https://doi.org/10.1016/j.jece.2017.12.009

Chauhan, M., Saini, V. K., Suthar, S., (2020). Ti-pillared montmorillonite clay for adsorptive removal of amoxicillin, imipramine, diclofenac-sodium, and paracetamol from water, J. Hazard. Mater. 399, https://doi.org/10.1016/j.jhazmat.2020.122832

Cherraye, R., (2012). Préparation par voie chimique d'un charbon actif à partir des déchets de café (Effet de taux d'adjuvant), Mémoire Master Académique, Université Kasdi Merbah-Ouargla.

Cuerda-Correa, E. M., Domínguez-Vargas, J. R., Olivares-Marín, F. J., de Heredia, J.B., (2010). On the use of carbon blacks as potencial low-cost adsorbents for the removal of non-steroidal anti-inflammatory drugs from river waters, J. Hazard. Mater. 177 1046–1053.

Cunha, Mariene R.; Lima, Eder C.; Lima, Diana R.; da Silva, Raphaelle S.; Thue, Pascal S.; Seliem, Moaaz K.; Sher, Farooq; dos Reis, Glaydson S.; H Larsson, Sylvia (2020). Removal of captopril pharmaceutical from synthetic pharmaceutical-industry wastewaters: use of activated carbon derived from Butiacatarinensis. Journal of Environmental Chemical Engineering, 104506– https://doi:10.1016/j.jece.2020.104506

Cuthbert, R. J., Taggart, M. A., Saini, M., Sharma, A., Das, A., Kulkarni, M. D., Deori, P., Ranade, S., Shringarpure, R. N., Galligan, T. H., & Green, R. E., (2016). Continuing mortality of vultures in India associated with illegal veterinary use of diclofenac and a potential threat from nimesulide. Oryx, 50(1), 104–112. https://doi.org/10.1017/S003060531500037X

Dai, Y., Li, J., Shan, D., (2020). Adsorption of tetracycline in aqueous solution by biochar derived from waste Auriculariaauricula dregs. Chemosphere; 238: 124432.https://doi:10.1016/j.chemosphere.2019.12

Daughton, C. G., Ternes, T. A., (1999). Pharmaceuticals and personal care products in the environment: agents of subtle change, Environ. Heal. Perspect. Bullet. 111 757 – 774.

Dhiman, N., Sharma. N., (2019). Removal of pharmaceutical drugs from binary mixtures by use of ZnO nanoparticles: (Competitive adsorption of drugs), Environ. Technol. Innov. 15, https://doi.org/10.1016/j.eti.2019.100392

Djebri, N., Boutahala, M., Chelali, N. E., Boukhalfa, N., (2017). Adsorption of bisphenol A and 2, 4, 5-trichlorophenol onto organo-acid-activated bentonite from aqueous solutions in single and binary systems. Desalination and water treatment 66, 383–393.

Dominique, W., Emmanuel, N., E., Hubert. D., Jean-Stéphane, P., Marie Hélène, M., Gérard T., Xavier, L., (2011). *Etude d'un procédé hybride couplantadsorption sur zéolithes et oxydation par l'ozone. Application au traitement d'effluents aqueux industriels. Toulouse : Ecole Nationale Supérieure de Chimie de Rennes* 96-103.

Douez, O., Ehret X. et Kaczmaryk A., (2011) Réseau régional de suivi de la qualité des nappes en 2010. Rapport BRGM RP - CPER 559942- FR, 97 p., 72 ill.

Du, Y., Zhang, X., Shu, L., Feng, Y., Lv, C., Liu, H., Xu, F., Wang, Q., (2020). Safety evaluation and ibuprofen removal via an Alternanthera philoxeroides -based biochar.

Emmett, P. H., Kummer, J. T., (1943). Kinetics of ammonia synthesis. Industrial and Engineering Chemistry, 35, 677-683.

Fallou, H., Cimetière, N., Giraudet, S., Wolbert, D., Le Cloirec, P., (2016). Adsorption of pharmaceuticals onto activated carbon fiber cloths-Modeling and extrapolation of adsorption isotherms at very low concentrations. J. Environ. Manag. 166, 544–555.https://doi:10.1016/j.jenvman.2015.10.056

Feng, J., Qiao, K., Pei, L., Lv, J., & Xie, S., (2015). *Using activated carbon prepared from Typha orientalis Presl to remove phenol from aqueous solutions. Ecological Engineering, 84, 209–217.* https://doi:10.1016/j.ecoleng.2015.09.028

Fent, K et al., (2006). Ecotoxicology of human pharmaceuticals. Aquatic toxicology, 76, pp. 122- 59. https://doi:10.1016/j.aquatox.2005.09.009 10.

Fick, J., Söderström, H., Lindberg, R. H., Phan, C., Tysklind, M., Larsson, D. G. J., (2009). Contamination of surface, ground and drinking water from pharmaceutical production. Environ. Toxicol. Chem. 28, 2522. https://doi:10.1897/09-073.1

Foroutan, R., Mohammadi, R., Adeleye, A. S., Farjadfard, S., Esvandi, Z., Arfaeinia, H., (2019). Efficient arsenic (V) removal from contaminated water using natural clay and clay composite adsorbents. Environ. Sci. Pollut. Res. 1–15. https://doi.org/https://doi.org/10.1007/s11356-019-06070-5

Freundlich, H. M. F., (1906). Over the Adsorption in Solution. Physical Chemistry, 57, 385-471.

Frohlich, A. C., Foletto, E. L., Dotto. G. L., (2019). Preparation and characterization of $NiFe_2O_4$/activated carbon composite as potential magnetic adsorbent for removal of ibuprofen and ketoprofen pharmaceuticals from aqueous solutions, J. Cleaner Prod. 229 828–837.

Fu, C; Zhang, H; Xia, M; Lei, W; Wang, F., (2020). The single/co-adsorption characteristics and microscopic adsorption mechanism of biochar-montmorillonite composite adsorbent for pharmaceutical emerging organic contaminant atenolol and lead ions. Ecotoxicology and Environmental Safety, 187, 109763–. https://doi:10.1016/j.ecoenv.2019.109763

Fujiwara. K., Ramesh. A., Maki. T., Hasegawa. H., & Ueda, K., (2007). *Adsorption of platinum (IV), palladium (II) and gold (III) from aqueous solutions onto l-lysine modified crosslinked chitosan resin. Journal of Hazardous Materials, 146(1-2), 39–50.* https://doi:10.1016/j.jhazmat.2006.11.049

Galligan. T. H., Amano. T., Prakash. V. M., Kulkarni. M., Shringarpure. R., Prakash. N., Ranade. S., Green. R. E., Cuthbert. R. J., (2014). Have population declines in Egyptian Vulture and Red-headed Vulture in India slowed since the 2006 ban on veterinary diclofenac. Bird Conservation International, 24 (3), 272–281. https://doi.org/10.1017/S0959270913000580

García-Mateos, F. J., Ruiz-Rosas, R., Marqués, M. D., L. M., Cotoruelo, J., Rodríguez-Mirasol, T. Cordero., (2015). Removal of paracetamol on biomass-derived activated carbon: modeling the fixed bed breakthrough curves using batch adsorption experiments, *Chemical Engineering Journal*, doi: http://dx.doi.org/10.1016/j.cej.2015.04.144

Ghemit, R., Boutahala, M., Kahoul, A., (2017). Removal of diclofenac from water with calcined ZnAlFe-$CO_3$ layered double hydroxides: effect of contact time, concentration, pH and temperature. Desal. Water Treat. 83, 75–85.

Ghemit, R., Makhloufi, A., Djebri, N., Flilissa, A., Zerroual, L., & Boutahala, M (2019). *Adsorptive removal of diclofenac and ibuprofen from aqueous solution by organobentonites: Study in single and binary systems. Groundwater for Sustainable Development, 8, 520–529* https://doi.org/10.1016/j.gsd.2019.02.004

Ghenima, A., Kedadouche, S., (2016). Adsorption seuls et en mélange de polluants d'origine pharmaceutique sur des adsorbants préparés à partir d'un déchet textile. Mémoire de master. Université A. MIRA-BEJAIA Faculté de Technologie Département de Génie des Procédés.

Giles, C. H., Smith, D., Huitson, A., (1974). A general treatment and classification of the solute adsorption isotherm. I. Theoretical. J. Colloid Interface Sci. 47, 755–765. https://doi.org/10.1016/0021-9797(74)90252-5

Gómez, A., Badawi, A. L. M., Bedia, A. J., Belver. C., (2021). Simultaneous adsorption of acetaminophen, diclofenac and tetracycline by organo-sepiolite: Experiments and statistical physics modelling, Chem. Eng. J. 404 126601. https://doi.org/10.1016/jcej.2020.126601

Grabi, H., Derridj, F., Lemlikchi, W., Guénin, E., (2021). Studies of the potential of a native

natural biosorbent for the elimination of an anionic textile dye Cibacron Blue in aqueous solution Fourier Transform InfraRed spectroscopy French Association for Standardization 1–13. https://doi:10.1038/s41598-021-88657-y

Graouer- Bacart, M., Sayen, S., Guillon, E., (2016). Adsorption and co-adsorption of diclofenac and Cu (II) on calcareous soils, Ecotoxicol. Environ. Saf., 124 386–392. https://doi:10.1016/j.ecoenv.2015.11.010

Guedidi, H., Lakehal, I., Reinert, L., Lévêque, J.M., Bellakhal, N., Duclaux, L., (2020). Removal of ionic liquids and ibuprofen by adsorption on a microporous activated carbon: Kinetics, isotherms, and pore sites. Arab. J. Chem. 13, 258–270. https://doi.org/10.1016/j.arabjc.2017.04.006

Guedidi, H., Reinert, L., Soneda, Y., Bellakhal, N., Duclaux, L., (2014). Adsorption of ibuprofen from aqueous solution on chemically surface-modified activated carbon cloths. Arab. J. Chem. https://doi.org/10.1016/j.arabjc.2014.03.007

Hall, K. R., Eagleton, L. C., Acrivos, A., Vermeulen, T., (1966). Pore and solid diffusion kinetics in fixed bed adsorption under constant pattern conditions. Ind. Eng. Chem. Fundam. 5, 212–223.

Hamdoudi, N., Smaili, F., (2016). Etude expérimentale de l'élimination du bleu de méthylène de l'eau par adsorption sur des déchets naturels (déchets de palmiers dattier) http://doi:10.1016/s0043-1354(99)00232-8

Ho, Y., (2000). *The kinetics of sorption of divalent metal ions onto sphagnum moss peat. Water Research, 34(3), 735–742.* https://doi:10.1016/s0043-1354(99)00232-8

Hu, B., Tang, Y., Wang, X., Wu, L., Nong, J., Yang, X., & Guo, J., (2021). *Cobalt-gadolinium modified biochar as an adsorbent for antibiotics in single and binary systems. Microchemical Journal, 166, 106235.*https://doi:10.1016/j.microc.2021.106235

Iovino, P., Canzano, S., Capasso, S., Erto, A., Musmarra, D., (2015). A modeling analysis for the assessment of ibuprofen adsorption mechanism onto activated carbons. Chem. Eng. J. 277, 360–367. https://doi.org/10.1016/j.cej.2015.04.097

Jemutai-Kimosop, S., Orata, F; Shikuku, V. O.; Okello, Veronica, A.; Getenga, Zachary, M. (2019). Insights on adsorption of carbamazepine onto iron oxide modified diatomaceous earth:

Kinetics, isotherms, thermodynamics, and mechanisms. Environmental Research, (), 108898–.https://doi.org/10.1016/j.envres.2019.108898

Johnson, A. C., Jürgens, M. D., Williams, R. J., Kümmerer, K., Kortenkamp, A., & Sumpter. J. P., (2008). *Do cytotoxic chemotherapy drugs discharged into rivers pose a risk to the environment and human health? An overview and UK case study. Journal of Hydrology, 348(1-2), 167–175.* https://doi:10.1016/j.jhydrol.2007.09.054

Jung, C., Boateng, L. K., Flora, J. R. V, Oh, J., Braswell, M.C., Son, A., Yoon, Y., (2015). Competitive adsorption of selected non-steroidal anti-inflammatory drugs on activated biochars : Experimental and molecular modeling study. Chem. Eng. J. 264, 1–9. https://doi.org/10.1016/j.cej.2014.11.076

Jung, K. W., Lee, S. Y., Lee, Y. J., (2018). *Facile one-pot hydrothermal synthesis of cubic spinel-type manganese ferrite/biochar composites for environmental remediation of heavy metals from aqueous solutions. Bioresource Technology, 261, 1–9.* https://doi:10.1016/j.biortech.2018.04.003

Karami, A., Sabouni, R., Ghommem, M., (2020). Experimental investigation of competitive co-adsorption of naproxen and diclofenac from water by an aluminum-based metalorganic framework, J. Mol. Liq. 305, https://doi.org/10.1016/j.molliq.2020.112808

Kavitha. D, Namasivayam. C. (2007) Experimental and kinetic studies on methylene blue adsorption by coir pith carbon. Bioresource Technology, 98, 14-21. https://doi:10.1016/j.biortech.2005.12.00

Keiluweit, M., Nico, P. S., Johnson. M. G. and Kleber. M., (2010). Dynamic Molecular Structure of Plant Biomass-Derived Black Carbon (Biochar), Environ. Sci. Technol., 44, 1247–1253.

Keskin, S., van Heest, T. M., & Sholl, D. S., (2010). *Can Metal-Organic Framework Materials Play a Useful Role in Large-Scale Carbon Dioxide Separations? ChemSusChem, 3(8), 879–891.* https://doi:10.1002/cssc.201000114

Kreuzinger et al., (2004). Ecotoxicology of human pharmaceuticals. Aquatic toxicology, 76, pp. 122-59.

Kurniawan. T. A., Chan, G. Y. S., Lo, W.-H., & Babel, S., (2006). *Physico–chemical treatment techniques for wastewater laden with heavy metals. Chemical Engineering Journal, 118(1-2), 8398.* https://doi:10.1016/j.cej.2006.01.015 10.

Langmuir, I., (1918). *THE ADSORPTION OF GASES ON PLANE SURFACES OF GLASS, MICA AND PLATINUM. Journal of the American Chemical Society, 40(9), 1361–1403.* https://doi:10.1021/ja02242a004

Larsson, D. G. J., (2014). Pollution from drug manufacturing: review and perspectives. Philos. Trans. R. Soc. Lond. B Biol. Sci. 369, 20130571. https://doi:10.1098/rstb.2013.0571

Li, Z., Gomez-Avil ´ ´ es, A., Sellaoui. L., Bedia, J., Bonilla- Petriciolet, A., Belver, C., (2019). Adsorption of ibuprofen on organo-sepiolite and on zeolite/sepiolite heterostructure: Synthesis, characterization and statistical physics modeling, Chem. Eng. J. 371 868 875, https://doi.org/10.1016/j.cej.2019.04.138.

Lima, É. C., Adebayo, M. A., Machado, F. M., (2015). Kinetic and equilibrium models of adsorption, Carbon Nanostructures. https://doi.org/10.1007/978-3-319-18875-1_3

Lima, E. C., Hosseini-Bandegharaei, A., Moreno-Piraján, J. C., Anastopoulos, I., (2019).A critical review of the estimation of the thermodynamic parameters on adsorption equilibria. Wrong use of equilibrium constant in the Van't Hoof equation for calculation of thermodynamic parameters of adsorption, J. Mol. Liq. 273 425–434. https://doi:10.1016/j.molliq.2018.10.048.

Lima, E. C., Gomes, A. A., Tran, H. N., (2020). Comparison of the nonlinear and linear forms of the van't Hoff equation for calculation f adsorption thermodynamic parameters (ΔS◦ and ΔH◦), J. Mol. Liq. 311 113315, https://doi.org/10.1016/j.molliq.2020.113315

Liu, H; Xu, G; Li. G., (2021). Preparation of porous biochar based on pharmaceutical sludge activated by NaOH and its application in the adsorption of tetracycline. Journal of Colloid and Interface Science, 587, 271–278. https://doi:10.1016/j.jcis.2020.12.014

Liu, Y., Eubank, J. F., Cairns, A. J., Eckert, J., Kravtsov, V. C., Luebke, R., & Eddaoudi. M., (2007). *Assembly of Metal–Organic Frameworks (MOFs) Based on Indium-Trimer Building Blocks: A Porous MOF with soc Topology and High*

*Hydrogen Storage. Angewandte Chemie International Edition, 46(18), 3278–3283.* https://doi:10.1002/anie.200604306

Liu, Z., Singer, S., Tong, Y., Kimbell. L., Anderson. E., Hughes. M., McNamara. P., (2018). *Characteristics and applications of biochars derived from wastewater solids. Renewable and Sustainable Energy Reviews, 90, 650 664.* https://doi:10.1016/j.rser.2018.02.040

Llado, J., Lao-Luque, C., Ruiz, B., Fuente, E., Sol ´ e-Sardans, ´ M., Dorado, A.D., (2015). Role of activated carbon properties in atrazine and paracetamol adsorption equilibrium and kinetics, *Process Safety and Environment Protection*, http://dx.doi.org/10.1016/j.psep.2015.02.013

Llado, J., Lao-Luque, C., Ruiz, B., Fuente, E., Sol ´ e-Sardans, ´ M., Dorado, A.D., Role of activated carbon properties in atrazine and paracetamol adsorption equilibrium and kinetics, *Process Safety and Environment Protection* (2015), http://dx.doi.org/10.1016/j.psep.2015.02.013

Llinàs, A. et al., (2007). Diclofenac solubility: independent determination of the intrinsic solubility of three crystal forms. Journal of medicinal chemistry, 50(5), pp. 979– 83.

Lu, X., Shao, Y., Gao, N., Chen, J., Zhang, Y., Wang, Q., & Lu, Y., (2016). Adsorption and removal of clofibric acid and diclofenac from water with MIEX resin. Chemosphere, 161, 400 411. https://doi:10.1016/j.chemosphere.2016.07.025 10.

Lung, I., Soran, M., Stegarescu, A., Opris, O., Gutoiu, S., Leostean, C., Lazar, M.D., Kacso, I., Silipas, T., Porav, A.S., (2021). Evaluation of CNT-COOH/MnO2/$Fe_3O_4$ nanocomposite for ibuprofen and paracetamol removal from aqueous solutions, J. Hazard. Mater. 403, https://doi.org/10.1016/j. jhazmat.2020

Luo, Y., Guo, W., Ngo, H. H., Long Duc, N., Hai, F. I., Zhang. J., Liang, S., & Wang, X. C., (2014). A review on the occurrence of micro pollutants in the aquatic environment and their fate and removal during wastewater treatment. The Science of the Total Environment, 473-474, 619–641. https://doi.org/10.1016/j.scitotenv.2013.12.065

Ma, J., Lei, Y., Khan, M. A, Wang, F., Chu, Y., Lei, W et al., (2019). Adsorption properties, kinetics & thermodynamics of tetracycline on carboxy methyl-chitosan reformed montmorillonite. Int J BiolMacromol; 124: 557-567.

Manceau, A., Marcus, M. A., Tamura, N., (2002). *Quantitative Speciation of Heavy Metals in Soils and Sediments by Synchrotron X-ray Techniques. Reviews in Mineralogy and Geochemistry, 49(1), 341–428.* https://doi:10.2138/gsrmg.49.1.341

Mansouri, H., Carmona, R.J., Gomis-berenguer, A., Souissi-, S., Ouederni, A., Ania, C.O., (2014). Competitive adsorption of ibuprofen and amoxicillin mixtures from aqueous solution on activated carbons. J. Colloid Interface Sci. https://doi.org/10.1016/j.jcis.2014.12.020

Marrakchi, F., Ahmed, M. J., Khanday, W. A., Asif, M., Hameed, B. H., (2017). Mesoporous activated carbon prepared from chitosan flakes via single- step sodium hydroxide activation for the adsorption of methylene blue, Int. J. Biol. Macromol. 98 233–239.

Mboula. V. M., (2012) Devenir de polluants émergents lors d'un traitement photochimique ou photocatylitique sous irradiation solaire, Thèse de Doctorat, Université de Nantes Angers.

Mechati, F., Bouchelta, C., Medjram, M. S., Benrabaa, R., & Ammouchi, N., (2015). *Effect of hard and soft structure of different biomasses on the porosity development of activated carbon prepared under $N_2$ /microwave radiations. Journal of Environmental Chemical Engineering, 3(3), 1928–1938.* https://doi:10.1016/j.jece.2015.07.007

Mestre, A. S., Pires, J., Nogueira, J. M. F., Carvalho, A. P., (2007). Activated carbons for the adsorption of ibuprofen 45, 1979–1988. https://doi.org/10.1016/j.carbon.2007.06.005

Mestre, A.S., Pires, J., Nogueira, J.M.F., Parra, J.B., Carvalho, A.P., Ania, C.O., (2009). Bioresource Technology Waste-derived activated carbons for removal of ibuprofen from solution : Role of surface chemistry and pore structure. Bioresour. Technol. 100, 1720–1726. https://doi.org/10.1016/j.biortech.2008.09.039

Meyer, E. E., Rosenberg, K. J. and Israelachvili, J., (2017). Recent progress in understanding hydrophobic interactions, Proc. Natl. Acad. Sci. U. S. A., 103, 15739–15746.compounds, Environ. Sci. Technol., 51, 8893–8908.

Meyer, S., Glaser, B., Quicker, P., (2011). *Technical, Economical, and Climate-Related Aspects of Biochar Production Technologies: A Literature Review. Environmental Science & Technology, 45(22), 9473–9483.* https://doi:10.1021/es201792c

Mohseni- B, A., Eslami, A., Kazemian, H., Zarrabi, M., T. J., (2020). A high density 3-aminopropyl triethoxysilane grafted pumice-derived silica aerogel as an efficient adsorbent for

ibuprofen: characterization and optimization of the adsorption data using response surface methodology, Environ. Technol. Innov. 18 100642, *https://doi.org/10.1016/j.eti.2020.100642*.

Mondal, S., Bobde, K., Aikat, K., Halder, G., (2016). Biosorptive uptake of ibuprofen by steam activated biochar derived from mung bean husk : Equilibrium , kinetics , thermodynamics , modeling and eco-toxicological studies. J. Environ. Manage. 182, 581–594. https://doi.org/10.1016/j.jenvman.2016.08.018

Mondal, S., Patel, S., Majumder, S. K., (2020). Naproxen removal capacity enhancement by transforming the activated carbon into a blended composite material, Water Air Soil Pollut.

Nakayama, T., Tran, T, Tuyet., H., Harada, K., Warisaya, M., Asayama, M., Hinenoya, A., Lee, J. W., Tran Minh, P., Ueda, S., Sumimura, Y., Hirata, K., Nguyen Thanh, P., Yamamoto, Y., (2017). Water metagenomic analysis reveals low bacterial diversity and the presence of antimicrobial residues and resistance genes in a river containing wastewater from backyard aquacultures in the Mekong Delta, Vietnam. Environ. Pollut. 222, 294–306.

Nguyen, D. T., Tran, H. N., Juang, R.-S., Dat, N. D., Tomul, F., Ivanets, A., … Chao, H.-P. (2020)**.** *Adsorption process and mechanism of acetaminophen onto commercial activated carbon. Journal of Environmental Chemical Engineering, 104408.* https://doi:10.1016/j.jece.2020.104408

Nguyen, H., Wang, Y., You, S., Chao, H., (2017). Insights into the mechanism of cationic dye adsorption on activated charcoal : The importance of □ – □ interactions. Process Saf. Environ. Prot. 107, 168–180. https://doi.org/10.1016/j.psep.2017.02.010

Ocampo-Perez, R., Aguilar-Madera, C. G., Díaz-Blancas, V., (2017). 3D modeling of overall adsorption rate of acetaminophen on activated carbon pellets, Chem. Eng. J. 321 510–520. https://doi:10.1016/j.cej.2017.03.137

Ocampo-Perez, R., Padilla-Ortega, E., Medellin-Castillo, N. A., Coronado-Oyarvide, P., Aguilar-Madera, C.G., Segovia-Sandoval, S.J., Flores-Ramírez, R., Parra-Marfil, A., (2019). Synthesis of biochar from chili seeds and its application to remove ibuprofen from water. Equilibrium and 3D modeling. Sci. Total Environ. 655, 1397–1408. https://doi.org/10.1016/j.scitotenv.2018.11.283

Oliveira, T. D., Guégan, R., Thiebault, T., Milbeau, C. L., Muller, F., Teixeiraa, V., Giovanela, M., Boussafira, M., (2017). Adsorption of diclofenac onto organoclays: effects of surfactant and environmental (pH and temperature) conditions. J. Hazard Mater. 323, 558–566.https://doi:10.1016/j.jhazmat.2016.05.001

Önal. Y, Akmil- Basar. C, Ç. Sar1c1-Özdemir, (2007) Elucidation of the naproxen sodium adsorption onto activated carbon prepared from waste apricot: kinetic, equilibrium and thermodynamic characterization, J. Hazard. Mater. 148 727–734.

Ouyang, J., Zhou, L., Liu, Z., Heng, J. Y. Y., & Chen, W., (2020). *Biomass-derived activated carbons for the removal of pharmaceutical mircopollutants from wastewater: A review. Separation and Purification Technology, 253, 117536.* https://doi:10.1016/j.seppur.2020.117536 10.

Özcan, A. S., Özcan, A., (2004) Adsorption of acid dyes from aqueous solutions onto acid-activated bentonite, J. Colloid Interf. Sci. 276 39–46.

P. Wu., Z. Cai., H. Jin., Y. Tang., (2019). Adsorption mechanisms of five bisphenol analogues on PVC microplastics, Sci. Total Environ. 650 671–678, https://doi.org/10.1016/j.scitotenv.2018.09.049.

Pap, N., Fidelis, M., Azevedo, L., do Carmo, M. A. V., Wang, D., Mocan, A., Granato, D., (2021). *Berry polyphenols and human health: evidence of antioxidant, anti-inflammatory, microbiota modulation, and cell-protecting effects. Current Opinion in Food Science, 42, 167–186.* https://doi:10.1016/j.cofs.2021.06.003

Pauletto, P. S., Lütke, S. F., Dotto, G. L., & Salau, N. P. G., (2021). *Adsorption mechanisms of single and simultaneous removal of pharmaceutical compounds onto activated carbon: Isotherm and thermodynamic modeling. Journal of Molecular Liquids, 336, 116203.* https://doi:10.1016/j.molliq.2021.116203

Pauletto. P. S, Lütke. S. F, G. L. Dotto, N. P. G. Salau, (2020). Forecasting the multicomponent adsorption of nimesulide and paracetamol through artificial neural network, Chemical Engineering Journal https://doi.org/10.1016/j.cej.2020.127527

Pena-Guzm ˜ ´ an, C., Ulloa-S´ anchez, S., Mora, K., Helena-Bustos, R., E., Lopez-Barrera, Alvarez, J., Rodrigues-Pinzon, M.., (2019). Emerging pollutants in the urban water cycle in Latin America: a review of the current literature, J. Environ. Manage. 237 408– 423, *https://doi.org/10.1016/j.jenvman.2019.02.100*.

Pignatello, J. J., Mitch, W. A., & Xu, W., (2017*). Activity and Reactivity of Pyrogenic Carbonaceous Matter Toward Organic Compounds. Environmental Science & Technology, 51(16), 8893–8908.* https://doi:10.1021/acs.est.7b01088

Quesada, H. B., Baptista, A. T. A., Cusioli, L. F. Seibert, D., Bezerra, C. O. Bergamasco, R., (2019). Surface water pollution by pharmaceuticals and an alternative of removal by low cost adsorbents: A review, Chemosphere 222 766–780, https://doi.org/10.1016/j.chemosphere.2019.02.009

Quintana, J., Weiss, S., Reemtsma, T., (2005). Pathways and metabolites of microbial degradation of selected acidic pharmaceutical and their occurrence in municipal wastewater treated by a membrane bioreactor. Water Research, 39(12), 2654 2664. https://doi:10.1016/j.watres.2005.04.068 10.

Rad, L. R., Haririan, I., Divsar, F., (2014). Comparison of adsorption and photo-Fenton processes for phenol and paracetamol removing from aqueous solutions: single and binary systems, *Spectrochimica Acta PartA: Molecular and Biomolecular Spectroscopy* doi: http://dx.doi.org/10.1016/j.saa.2014.09.052

Rafatullah, M., Sulaiman, O., Hashim, R., & Ahmad, A., (2010). *Adsorption of methylene blue on low-cost adsorbents: A review. Journal of Hazardous Materials, 177(1-3), 70–80.* https://doi:10.1016/j.jhazmat.2009.12.047

Rangabhashiyam, S., Balasubramanian, P., (2019). *The potential of lignocellulosic biomass precursors for biochar production: Performance, mechanism and wastewater application—A review. Industrial Crops and Products, 128, 405–423.* https://doi:10.1016/j.indcrop.2018.11.041

Rocha, L. S., Pereira, D., Sousa, E., Otero, M., Esteves, V. I., Calisto, V., (2020). Recent advances on the development and application of magnetic activated carbon and char for the removal of pharmaceutical compounds from waters: A review, Sci. Total Environ. 718, https://doi.org/10.1016/j.scitotenv.2020.

Rouahna, N., Barkat, D., Ouakouak, A., Srasra, E., (2018). Synthesis and characterization of Mg-Al layered double hydroxide intercalated with D2EHPA: Application for copper ions removal from aqueous solution. J. Environ. Chem. Eng. 6, 1226–1232. https://doi.org/10.1016/j.jece.2018.01.036

Salihi, E.Ç., Mahramanlıoğlu, M., (2014). Equilibrium and kinetic adsorption of drugs on bentonite: presence of surface active agents effect. Appl. Clay Sci. 101, 381–389.https://doi:10.1016/j.clay.2014.06.015

Sarkar, M., Acharya, P. K., & Bhattacharya, B., (2003). *Modeling the adsorption kinetics of some priority organic pollutants in water from diffusion and activation energy parameters. Journal of Colloid and Interface Science, 266(1), 28–32.* https://doi:10.1016/s0021-9797(03)00551-4

SEDDIK K, B. (2015). Élimination d'Antibiotiques Des Eaux Épurées De La STEP de Tiaret. Mémoire de Magister. Université d'Oran : Faculté de chimie Département de chimie organique industrielle 251P.

Sharma, A. K., Saini, M., Singh, S. D., Prakash, V., Das, A., Dasan, R. B., Pandey, S., Bohara, D., Galligan, T. H., Green, R. E., Knopp, D., & Cuthbert, R. J., (2014). Diclofenac is toxic to the Steppe Eagle Aquila nipalensis: Widening the diversity of raptors threatened by NSAID misuse in South Asia. Bird Conservation International, 24(3), 282–286. https://doi.org/10.1017/S0959270913000609

Sharma, P., Hussain, N., Borah, D. J., Das, M. R., (2013). Kinetics and adsorption behavior of the methyl blue at the graphene oxide/reduced graphene oxide nano sheet-water interface: A comparative study, J. Chem. Eng. Data. 58 3477–3488. https://doi:10.1021/je400743r.

Shikuku, V. O., Zanella, Renato., Kowenje, C. O., Donato, F. F., Bandeira, N. M. G., Prestes, O. D., (2018). Single and binary adsorption of sulfonamide antibiotics onto iron-modified clay: linear and nonlinear isotherms, kinetics, thermodynamics, and mechanistic studies. Applied Water Science, 8(6), 175– https://doi.org/10.1007/s13201-018-0825-4

Shirani, Z., Song, H., Bhatnagar, A., (2020). *Efficient removal of diclofenac and cephalexin from aqueous solution using Anthriscus sylvestris-derived activated biochar. Science of The Total Environment, 140789* https://doi.org/10.1016/j.scitotenv.2020.140789

Słomkiewicz, P., Kolbus, A., Jedynak, K., Szczepanik, B., Nina, R., (2019). Ordered

Mesoporous Carbons for Adsorption of Aqueous Solutions 1–21.

Spessato, L., Bedin, K. C., Cazetta, A. L., Souza, I. P. A. F., Duarte, V. A., Crespo, L. H. S., Silva, M. C., Pontes, R. M., Almeida, V. C., (2019). KOH-super activated carbon from biomass waste: Insights into the paracetamol adsorption mechanism and thermal regeneration cycles, J. Hazard. Mater. 371 499–505, *https://doi.org/10.1016/j.jhazmat.2019.02.102*

Sun, H., Hockaday, W. C., Masiello, C. A., Zygourakis, K. (2012). *Multiple Controls on the Chemical and Physical Structure of Biochars. Industrial & Engineering Chemistry Research, 51(9), 3587–3597.* https://doi:10.1021/ie201309r

Tang, J., Lv, H., Gong, Y., Huang, Y., (2015). Preparation and characterization of a novel graphene/biochar composite for aqueous phenanthrene and mercury removal. Bioresour. Technol. 196, 355–363. https://doi.org/10.1016/j.biortech.2015.07.047

Thakur, A., Sharma, N., Mann, A., (2020). Removal of ofloxacin hydrochloride and paracetamol from aqueous solutions: Binary mixtures and competitive adsorption, Mater. Today 28 1514–1519, https://doi.org/10.1016/j.matpr.2020.04.833

Thomas, K. V., Dye, C., Schlabach, M., Langford, K. H., (2007). *Source to sink tracking of selected human pharmaceuticals from two Oslo city hospitals and a wastewater treatment works. Journal of Environmental Monitoring, 9(12), 1410.* https://doi:10.1039/b709745j

THOMAS, T., (2015) L'adsorption des produits pharmaceutiques par interactions organominérales. Processus et applications environnementales. Thèse de doctorat SciencesdelaTerre.Universitéd'Orléans, 323P.

Tong, Y., McNamara, P. J., & Mayer, B. K., (2019). *Adsorption of organic micropollutants onto biochar: a review of relevant kinetics, mechanisms and equilibrium. Environmental Science: Water Research & Technology.* https://doi:10.1039/c8ew00938d

Tran, H. N., Tomul, F., Nguyen, H. T. H., D. T. Nguyen, E. C. Lima, G. T. Le, C. Chang, V. Massindi, S. H. Woo, (2020). Innovative spherical biochar for pharmaceutical removal from water: Insight into adsorption mechanism, J. Hazard. Mater. 122255. https://doi.org/10.1016/j.jhazmat.2020.122255.

Tran, H. N., You, S. J., Chao, H. P., (2016). Thermodynamic parameters of cadmium adsorption onto orange peel calculated from various methods: A comparison study, J. Environ. Chem. Eng. 4 2671–2682. https://doi.org/10.1016/j.jece.2016.05.009

Tran, H. N., You, S., Hosseini-B, A., Chao, H. P., (2017). Mistakes and inconsistencies regarding adsorption of contaminants from aqueous solutions: A critical review. Water Res. 120, 88–116. https://doi.org/10.1016/j.watres.2017.04.014

Uchimiya, M., (2014). *Influence of pH, Ionic Strength, and Multidentate Ligand on the Interaction of Cd <sup>II</sup> with Biochars. ACS Sustainable Chemistry & Engineering, 2(8), 2019–2027.* https://doi:10.1021/sc5002269

Velma, B. K. Y., Mohamed, Z., Sérgio, B. O., Satu, O., (2021). *Hydrochar-derived adsorbent for the removal of diclofenac from aqueous solution. Nanotechnology for Environmental Engineering.* https://doi.org/10.1007/s41204-020-00099-5

Verlicchi, P., Al Aukidy, M., Zambello, E., (2012). Occurrence of pharmaceutical compounds in urban wastewater: removal, mass load and environmental risk after a secondary treatment – a review. Sci. Total. Environ. 429, 123–155.https://doi:10.1016/j.scitotenv.2012.04.0

Wang, J., Chen, B., (2015). Adsorption and co adsorption of organic pollutants and a heavy metal by graphene oxide and reduced graphene materials, Chem. Eng. J. 281 379–388, https://doi.org/10.1016/j.cej.2015.06.102.

Weber, W. J., Morris, J. C., (1963). Kinetics of adsorption on carbon from solution. Sanitary Engineering Division American Society, 89, 31-60.

Weber. J. W., (1972). Physicochemical process for water quality control. Wiley interscience, New York.

Xu, M. J., Huang, H. T, Li, N., Li, F., Wang, D. H, Luo, Q., (2019). Occurrence and ecological risk of pharmaceuticals and personal care products (PPCPs) and pesticides in typical surface watersheds, China. Ecotoxicol Environ Saf 175:289–298

Xu, Y., Liu, T. J., Zhang, Y., Ge, F., Steel, R. M., Sun, L. Y., (2017). Advances in technologies for pharmaceuticals and personal care products removal. Journal of Materials Chemistry A, 5(24), 12001–12014. https://doi.org/10.1039/C7TA03698A

Yan L, Liu Y, Zhang Y, Liu S, Wang C, Chen W, et al. (2020). ZnCl2 modified biochar derived from aerobic granular sludge for developed microporosity and enhanced adsorption to tetracycline. Bioresource Technology 2020; 297: 122381.https://doi:10.1016/j.biortech.2019.122381

Yang G, Gao Q, Yang S, Yin S, Cai X, Yu X, et al. (2020). Strong adsorption of tetracycline hydrochloride on magnetic carbon-coated cobalt oxide nanoparticles. Chemosphere; 239: 124831.https://doi:10.1016/j.chemosphere.2019.124831

Yang, Y., Ok, Y. S., Kim, K. H., Kwon, E. E., Tsang, Y. F., (2017). Occurrences and removal of pharmaceuticals and personal care products (PPCPs) in drinking water and water/sewage treatment plants: A review. The Science of the Total Environment, 596-597, 303–320. Https://doi.org/10.1016/j.scitotenv.2017.04.102

Yuan-da. D; Zhang, X; Shu, L; Feng, Y; Lv, C; Liu, H; Xu, F; Wang, Q; Zhao, C; Kong, Q., (2020). *Safety evaluation and ibuprofen removal via an Alternanthera philoxeroides-based biochar. Environmental Science and Pollution Research,* https://doi.org/10.1007/s13399-020-00922-8

Yusoff, N. A., Ngadi, N., Alias, H., Jusoh, M., (2017). Chemically treated chicken bone waste as an efficient adsorbent for removal of acetaminophen. *Chem. Eng. Trans.*, *56*, 925–930

Zhang P, Li Y, Cao Y, Han L. (2019). Characteristics of tetracycline adsorption by cow manure biochar prepared at different pyrolysis temperatures. Bioresource Technology; 285: 121348.https://doi:10.1016/j.biortech.2019.12134

Zhang, J., Liu, J., Liu, R., (2015). Effects of pyrolysis temperature and heating time on biochar obtained from the pyrolysis of straw and lingo sulfonate. Bioresour. Technol. 176, 288–291. https://doi:10.1016/j.biortech.2014.11.011

Zhang, W., Li, Y., Wang, C., Wang, P., Hou, J., Yu, Z., Niu, L., Wang, L., Wang, J., (2016). Modeling the biodegradation of bacterial community assembly linked antibiotics in river sediment using a deterministic stochastic combined model. Environ. Sci. Technol. 50, 8788–8798.

Zhu, D., Pignatello, J. J., (2005). *Characterization of Aromatic Compound Sorptive Interactions with Black Carbon (Charcoal) Assisted by Graphite as a Model. Environmental Science & Technology, 39(7), 2033–2041.* https://doi:10.1021/es0491376

Zur, J., Wojcieszynska, D., Hupert-Kocurek, K., Marchlewicz, A., Guzik, U., (2018). Paracetamol toxicity and microbial utilization. Pseudomonas moorei $KB_4$ as a case study for

exploring degradation pathway, Chemosphere 206 192–202, https://doi.org/10.1016/j.chemosphere.2018.04.179.